ORNL 120
MASTER COPY

EXTERNAL TRANSMITTAL AUTHORIZED
Distribution Limited to Recipients Indicated
ORNL
Central Files Number
59-10-77

CHEMICAL TECHNOLOGY DIVISION

UNIT OPERATIONS SECTION

MONTHLY PROGRESS REPORT

OCTOBER 1959

NOTICE

[redacted]

Full public release
David R. Hamrin
11/11/11

OAK RIDGE NATIONAL LABORATORY
operated by
UNION CARBIDE CORPORATION
for the
U.S. ATOMIC ENERGY COMMISSION

EXTERNAL TRANSMITTAL AUTHORIZED-
Distribution Limited to Recipients Indicated

ORNL CF 59-10-77

UNIT OPERATIONS SECTION MONTHLY PROGRESS REPORT

October 1959

CHEMICAL TECHNOLOGY DIVISION

J. C. Bresee
J. O. Blomeke
P. A. Haas
R. W. Horton
A. D. Ryon
C. D. Watson
M. E. Whatley

Date Issued

FEB 3 1960

OAK RIDGE NATIONAL LABORATORY
Oak Ridge, Tennessee
Operated By
UNION CARBIDE CORPORATION
for the
U. S. Atomic Energy Commission

ABSTRACT

The chemical kinetic effect was separated from the diffusional effect in the study of the transpiration protection of porous surfaces from corrosion by using a glass frit surface, which does not corrode, immersed in a stirred bath of dilute KCl and transpiring water through the frit. Consolidated uranium metal was recovered in three of the four final Druhm runs with yields of 3%, 56% and 90% with a maximum metal purity of 99.98% uranium. A cost estimate was prepared for a 5000 ton (U_3O_8)/year Fluorox plant. About 45 lb of flame denitrated thoria prepared as previously reported contains rounded product particles, with about 8 wt % of over 10μ dia particles. Using a loading solution 0.004 M in uranium and 0.15 M in total sulfate, an "apparent" uranium diffusion coefficient in 1200μ Dowex 21K of 1.3 x 10^{-7} sq cm/sec was measured. A single experiment was performed confirming the feasibility of steam stripping for removing HNO_3 from concentrated solutions of SS, Th and U. In one run using boiling 4 M H_2SO_4 as the dissolvent, 17.67 kg of stainless steel plate was completely dissolved in 2.75 hrs resulting in a reaction rate of 2.43 mg/sq cm-min and an average product loading of 75.2 g SS/liter as compared to a reaction rate of 1.85 mg/cm-min and product loading of approximately 60 g SS/liter when using 6 M H_2SO_4 at comparable operating conditions. Cake washing experiments made on siliceous solids centrifuged from Darex (APPR) solvent extraction feed solutions, in 5-in. and 12-in. centrifuges, demonstrated that the weight of uranium retained in the centrifuge after n batch washes can be predicted by the simple dilution-decantation formula $Y_n/Y_o = (1-F)^{n+1}$. Assembly of the SRE decladding machine was completed. In studies on the flow capacity and stage efficiency of pulsed columns as a function of operating variables and cartridge design with a typical flowsheet for Yankee Atomic fuel, the flow capacity of a compound extraction-scrub column with a sieve-plate cartridge (0.125-in. holes, 23% free area, 2-in. spacing) was limited by flooding in the scrub section. Two additional batch waste calcination tests were performed with Darex waste in an 8-in. dia by 48-in. long pot to assess the effects of higher feed rates on calciner operability and product characteristics.

CONTENTS

		Page
	Abstract	2
	Previous Reports in This Series for the Year 1959	4
	Summary	5
1.0	Chemical Engineering Research	10
2.0	Druhm	18
3.0	Fission Product Recovery By Solvent Extraction	28
4.0	Fluorox	32
5.0	Fuel Cycle Development	47
6.0	HR Thorium Blanket Studies	48
7.0	Ion Exchange	50
8.0	Power Reactor Fuel Processing	53
9.0	Solvent Extraction Studies	86
10.0	Volatility	97

Previous Reports in This Series for the Year 1959

January	ORNL CF 59-1-74
February	ORNL CF 59-2-45
March	ORNL CF 59-3-61
April	ORNL CF 59-4-47
May	ORNL CF 59-5-47
June	ORNL CF 59-6-63
July	ORNL CF 59-7-58
August	ORNL CF 59-8-76
September	ORNL CF 59-9-69

Previous reports in this series are listed in the June 1959 report, CF 59-6-63.

SUMMARY

1.0 CHEMICAL ENGINEERING RESEARCH

Transpiration Protection

The chemical kinetic effect was separated from the diffusional effect in the study of the transpiration protection of porous surfaces from corrosion by using a glass frit surface, which does not corrode, immersed in a stirred bath of dilute KCl and transpiring water through the frit. The concentration difference was measured by silver-silver chloride electrodes placed at the surface and in the bulk of the solution. It was found that the concentration difference decreased with the speed of the rotating disc which stirred the bath; that the distance between the porous surface and the rotating disc had little effect on the concentration difference; and the concentration difference increased rapidly with transpiration velocity up to velocities of 4 to 6 cm/min, after which the wall concentration became constant. This critical transpiration velocity was relatively independent of the other variables.

Further quantitative conclusions were hampered by the difficulty of preparing electrode-frit assemblies reproducibly. Supposedly identical assemblies have given, in the worst case, concentration differences under identical conditions that differed by a factor of 20. The ratio of concentration differences for any two assemblies remained constant over the range of variables studied. The cause of the difference is believed to be the very great sensitivity of the exact location of the electrode surface relative to the surface of the frit.

2.0 DRUHM

Four semi-continuous reduction runs were made in the 6-in. reactor with 1/4-in. thick graphite liners backed-up with 1/2-in. thick MgO crucibles. Inconel UF_6 nozzles with internal He cooling were used. Consolidated uranium metal was recovered by three runs with yields of 3%, 56% and 90% with a maximum metal purity of 99.98% uranium. The UF_6 nozzles were still operative with only slight damage to the nozzle tips and the graphite liners resisted corrosive attack in two of the four runs.

3.0 FISSION PRODUCT RECOVERY

High Speed Contactor Development

A high speed contactor, known as the "Stacked Clone Contactor," is under development which has demonstrated high capacity and high efficiency. It is a stacked arrangement of hydroclones driven by pumps which move mostly the heavy (aqueous) phase from the overflow back to the feed port of the same clone. The underflow port of each clone is closely connected to the

overflow port of the one below, and the phases pass countercurrently to each other through the underflow port by the induced underflow effect. Because of the nature of the induced underflow effect, the net flow of phases from stage to stage is insensitive to the circulation rate within the stages, and the control of this contactor is in all respects equivalent to the control of pulsed or packed columns.

A contactor of five stages was constructed, each consisting of a 0.75-in. hydroclone 4-in. long and a pump, with a 200 ml holdup per stage (mostly pump volume). For flow rate ratios (aqueous to organic) from 1 to 2 the contactor flooding point was more than a liter per minute total throughput. For an aqueous rate of 600 ml/min and an organic solvent rate of 500 ml/min, the organic solvent holdup per stage was 44 ml (or 22%).

4.0 FLUOROX

A cost estimate was prepared for a 5000 ton (U_3O_8)/year Fluorox plant. The total fixed cost of the plant is $3,904,000 and the manufacturing cost for UF_6 preparation from UF_4 is $0.288 per pound of uranium processed.

5.0 FUEL CYCLE DEVELOPMENT

A program was started to develop complete power reactor fuel cycles with the initial emphasis on remote fabrication for recycle of thorium-U^{233} to heterogeneous reactors.

6.0 HR THORIUM BLANKET STUDIES

About 45 lb of flame denitration product prepared as previously reported contains rounded product particles, with about 8 wt % of over 10μ dia particles. The + 10μ particles will be removed by hydroclone classification prior to toroid and loop tests.

7.0 ION EXCHANGE

Using a loading solution 0.004 M in uranium and 0.15 M in total sulfate, an "apparent" uranium diffusion coefficient in 1200μ Dowex 21K of 1.3×10^{-7} sq cm/sec was measured. This value is the same which has been measured for essentially all solutions studied. The uranium self-diffusion coefficient in resin equilibrated with an identical solution was $3.2 \pm 1.2 \times 10^{-8}$ sq cm/sec, which is less than that predicted by considering the loading process to involve only counter diffusion of $UO_2(SO_4)_2^{=}$ and $SO_4^{=}$ ions.

8.0 POWER REACTOR FUEL PROCESSING

8.1 Darex

Two runs dissolving 93.5% ThO_2-UO_2 pellets (Davison, 93% theoretical density, H_2 fired) were made in a 1-in. diameter semi-continuous dissolver. In run Th-1 Thorex dissolvent (13.3 M HNO_3, 0.07 M $Al(NO_3)_3$, 0.04 NaF) was used and in run SS-1 adjusted Darex declad solution (9.84 M HNO_3, 53 g SS/liter, 0.04 M NaF, trace chloride) was used as dissolvent. In the first run the pellets rested on the bottom of the dissolver while in run SS-1 they were suspended 2-1/4-in. above the bottom. In both runs 16 pellets were charged to the dissolver which weighed 74 g with a total area of 45.9 sq cm. In run Th-1 69.4% (by weight) of the pellets dissolved in 19-1/2 hrs at an average dissolvent feed rate of 0.507 cc/min, yielding 592 cc of product with an average loading of 73 g Th/liter. In run SS-1 97.3% dissolved in 18 hrs at an average feed rate of 0.376 cc/min yielding 408 cc of product with an average loading of 148 g Th/liter.

A single experiment was performed proving the feasibility of steam stripping for removing HNO_3 from concentrated solutions of SS, Th and U. A 1225 cc batch of solution (131 g Th/liter, 50 g SS/liter, 8 M HNO_3 and trace chloride) was concentrated to 455 cc and then steam stripped to 0.15 M HNO_3 using 350 cc of water. The maximum solution temperature reached was 131°C compared with 143°C required in straight batch distillation.

Instantaneous dissolution rates of high density (ρ = 9.5) ThO_2-4% $UO_{2.3}$ pellets in fluoride-catalyzed nitric acid have been found to be highly erratic and dependent on the color produced on the surface of the pellet. In boiling 13 M HNO_3, 0.03 M fluoride, 0.1 M Al^{+++}, pellets which maintained a black surface dissolved at a rate of 0.4-0.6 mg/sq cm-min. Pellets whose surface turned partially or completely yellow in color (while remaining black beneath the surface) dissolved at rates from 1-6 mg/sq cm-min. The same phenomenon was noted in acids of different compositions.

8.2 Sulfex

Two semi-continuous Sulfex dissolution runs were made dissolving dummy stainless steel plate-type elements in 6 M H_2SO_4. Dissolvent flow rates of 1.91 and 2.40 liters/min resulted in reaction rates of 2.49 and 3.16 mg/sq cm-min, based on initial area and total dissolution.

The results of such dissolutions show a straight line relationship between reaction rate and dissolvent flow rate (expressed as F/S) over the range F = 0-2.4 liter/min. The slope of this line, which is the product loading, is 58 mg/cu cm. Consequently approximately the same product loading was obtained regardless of dissolvent flow rate, the only variable being dissolution time as determined by dissolvent feed rate.

In an attempt to obtain a higher product loading (~80 g SS/liter) two semi-continuous runs were made in which the dissolvent flow rate was varied with time, and one run was made following a combination semi-continuous and batch dissolution procedure. The product loading averaged 60-65 g SS/liter for each of these runs.

In one run using boiling 4 M H_2SO_4 as the dissolvent, 17.67 kg of stainless steel plate was completely dissolved in 2.75 hrs resulting in a reaction rate of 2.43 mg/sq cm-min and an average product loading of 75.2 g SS/liter as compared to a reaction rate of 1.85 mg/cm-min and product loading of approximately 60 g SS/liter when using 6 M H_2SO_4 at comparable operating conditions.

8.3 Feed Clarification

Cake washing experiments made on siliceous solids centrifuged from Darex (APPR) solvent extraction feed solutions, in 5-in. and 12-in. centrifuges, demonstrated that the weight of uranium retained in the centrifuge after n batch washes can be predicted by the simple dilution-decantation formula $Y_n/Y_o = (1-F)^{n+1}$.

In the same experiments, 1/4-3/8-in. thick siliceous cake deposited at 800 gees on the wall of the 12-in. centrifuge was effectively dislodged and slurried with the wash by mechanically braking the bowl from 2180 rpm to rest in 3-5 seconds.

8.4 Mechanical Processing

SRE Decladding - Assembly of the SRE decladding machine was completed. Several prototype fuel elements were successfully declad under mineral oil by mechanically removing the spacer wire, end caps, hydraulically expanding the 10 mil wall stainless steel clad and ejecting the uranium slugs. A movie was made of the complete operation, including recanning the slugs in aluminum cans.

SRE Canner - A food-canning machine was altered and its remote operation was demonstrated for recanning uranium slugs in aluminum for storage and subsequent dissolution.

SRE Slug Washer - Tests in a high pressure resistant vessel showed that (1) the slug holder basket will rotate from ~1000 to 2450 rpm at 30 to 40 psig steam pressure consuming steam at ~22 gal/hr and (2) a 3.27 sq ft tube heat exchanger is adequate for condensing the steam.

Abrasive Sawing - Fabrication of a pedestal type multi-purpose saw was completed by the Ty-Sa-Man Machine Co., Knoxville, Tennessee. Delivery is awaiting acceptance tests to be performed upon receipt of a special hydraulic fluid.

Shearing - A ventilated enclosure was installed around the 125 ton Manco shear for shearing 336 kg UO_2 for leaching tests in the 24 kg intermediate-size glass leacher.

Leaching - A preliminary leaching run was made in the 24 kg size UO_2 batch equipment leaching 4.5 kg of UO_2 from 1-in. sheared lengths of 0.4-in. dia stainless steel-clad UO_2. Efficient removal of nitrogen oxides was observed with only one fine spray fog nozzle in the off-gas system immediately following the leacher. There appeared to be excellent liquid circulation by natural convection. The sampling system performed satisfactorily, taking five samples simultaneously from various positions in the leacher.

8.5 Radiation Damage

Irradiation of greases, oils and hydraulic fluids by a cobalt-60 source to determine acceptable materials for use in the segmenting facility showed that two greases (1) type APL from the Shell Oil Co., and (2) Bemol No. 3 (MoS_2) from Bemol, Inc. exhibited the best resistance when inspected after 6×10^8r, γ. Four other lubricants were less promising; UCON Hydrolube AC, an ethylene glycol with polyglycol thickner for use as a fire-resistant hydraulic fluid, failed at 4×10^8r.

9.0 SOLVENT EXTRACTION STUDIES

In studies on the flow capacity and stage efficiency of pulsed columns as a function of operating variables and cartridge design with a typical flowsheet for Yankee Atomic fuel, the flow capacity of a compound extraction-scrub column with a sieve-plate cartridge (0.125-in. holes, 23% free area, 2-in. spacing) was limited by flooding in the scrub section. The maximum throughput was 700 gal/hr sq ft for operation with the aqueous phase continuous and 300 with the organic phase continuous. At greater flow rates (maximum 1200 gal/hr sq ft), operation was stable with an aqueous-continuous dispersion in the scrub section while the extraction section remained organic-continuous. The maximum flow capacity of a strip column with a sieve-plate cartridge was 1100 gal/hr sq ft aqueous-continuous and 300 organic-continuous. Operation with the organic phase continuous was characterized by relatively poor dispersion, with most of the aqueous phase flowing as a film down the column wall and center support rod.

10.0 VOLATILITY

The formation of solids under expected hydrofluorination conditions (total metallic impurities in feed salt <0.14 wt %) was studied during run N-4. It was observed that approximately 70% of the major impurity, Sn, was removed from the salt by entrainment to the off-gas and deposition on surfaces of the hydrofluorinator covered by salt.

11.0 WASTE PROCESSING

Two additional calcination tests were performed with Darex waste in an 8-in. dia by 48-in. long pot to assess the effects of higher feed rates on calciner operability and product characteristics. Increasing the feed rate from 5.6 to 10.6 liter/hr increased the ratio of non-condensible off-gas to feed from 4.6 to 7.1 cu ft/liter and resulted in less iron carried by entrainment into the condensate (0.012% vs. 0.073%). The bulk density of the final cake obtained at 10.6 liter/hr feed rate was 0.8 g/cc with a nitrate content of 0.005%, while the cake produced at the lower feed rate had a bulk density of 0.64 and a nitrate content of 0.11%.

Preliminary tests with a distillation tower operating with water at total reflux yielded decontamination factors near 1700 when an aerosol containing Cr-51 tracer was passed through the column.

1.0 CHEMICAL RESEARCH ENGINEERING

M. E. Whatley

Transpirational corrosion protection is a possible means of protecting an enclosing surface from corrosion by an agressive fluid by mechanically transpiring through a porous surface a diluent or non-aggresive fluid, thereby maintaining a much reduced corrosion potential in the boundary layer next to the surface.

The present investigation involves a study of ion transport, under flowing transpirational conditions, independantly of corrosion kinetics. A technique has been developed using the concentration cell potential of the cell Ag, AgCl/KCl aq·(C_{Bulk})/KCl aq·(C_{wall})/AgCl, Ag to measure C_w, the concentration at a point on the porous wall under bulk flow with transpiration through the wall.

Transpirational Studies - W. M. Woods, G. Jones, Jr.

Slab geometry water transpiration experiments were made using 2.86 cm dia coarse and medium porosity glass frits 0.4 cm to 3.75 cm from the stirrer disc. The frits had an Ag, AgCl electrode mounted in the surface. The reference electrode was Ag, AgCl in 0.05 M KCl connected to the 0.1 M KCl bulk solution through a capillary salt bridge.

Potential measurements indicated that the wall dilution factor, C_w/C_B, at all disc speeds from 0 - 475 rpm decreased very rapidly as q, the transpirational velocity, was increased from 0 to 4 to 6 cm/min and then became nearly constant with further increases in q. The limiting value of C_w/C_B (at transpirational velocities 4 to 6 cm/min or higher) increased with agitator disc speed. The spacing between the frit and the disc had little effect on C_w/C_B.

The absolute effect of the independant variables, particularly the effect of frit porosity, on C_w/C_B was obscured by a lack of reproducibility among various supposedly identical electrode frit assemblies which showed a variation among themselves under identical condition of 20 to 1 in limiting C_w/C_B. However, on the average, the coarse porosity frit gave lower limiting values of C_w/C_B than did the medium frit. The reproducibility of a given assembly "against itself" was good.

Transpiration Experiments. The experimental apparatus which has been described* consisted of a 12 liter battery jar stirred by a smooth 12-in. dia Plexiglass disc. The frit containing the wall Ag, AgCl electrode was positioned parallel to and above the stirrer disc. The transpirant was distilled water and the bulk solution was 0.1 M KCl. The bulk solution was replenished with measured volumes of 1.0 M KCl to correct for dilution by the transpirant so that the bulk concentration, C_B, was maintained at

* April Unit Operations Monthly Progress Report, CF 59-4-47.

0.1 M ± 0.01 M KCl.

The potentials between the wall electrode in the surface of the frit and the reference electrode in 0.05 M KCl were read with a Kiethley electrometer having a d.c. input impedance of 10^{14} ohms. The output of the amplifier of which was recorded on a Brown potentiometer. Figure 1.1 shows a typical chart taken from the Brown. The time average potential was read from the chart after the average became steady. The concentration of KCl at the wall electrode was calculated from the cell potential using the Nernst equation for a concentration cell with transference.*

Experimental Results. In general, it was found that the wall dilution factor, C_w/C_B, the ratio of measured concentration at the porous wall electrode to bulk concentration (in these experiments 0.1 M), decreased very rapidly as q, the transpiration velocity normal to the porous surface, was increased until, at some critical value of q the wall dilution factor became essentially constant. Figure 1.2 shows a typical plot of C_w/C_B vs q with the stirring disc rotation rate as a parameter.

Table 1.1 presents the $(C_w/C_B)_{min}$ and $q_{critical}$ for three different medium porosity frit-electrode assemblies measured at four disc rotation rates from 175 to 475 rpm and at frit to disc spacings from 0.75 to 3.4 cm. The values entered in the table were read from semi-log plots of C_w/C_B vs q similar to Figure 1.2. The starred values indicate results secured from a particular glass frit after one electrode had been removed and replaced by another. Table 1.2 presents $(C_w/C_B)_{min}$ and $q_{critical}$ in the same manner for three coarse frits.

Reproducibility of Results with a Given Assembly. The reproducibility of data with a given frit-electrode assembly is shown by changes in $(C_w/C_B)_{min}$ at the 1.5 cm disc spacing in Tables 1.1 and 1.2. The properties of the medium assembly 1 were reproducible in separate experiments within about 30%. Assembly 2 showed variations as much as a factor of 4. These larger variations might be expected because the absolute level of concentration measured was one or two orders of magnitude lower and the relation between cell potential and concentration is logarithmic. It is also possible that some movement of the electrode surface relative to the frit may have occurred during the experiments.

Reproducibility of Results with Different Assemblies. Three different frit-electrode assemblies in each porosity were tested. These assemblies were made up by the same procedure and were intended to be as similar as possible. The $(C_w/C_B)_{min}$ and $q_{critical}$ values are shown under "Frit-Electrode Assembly Number" in Table 1.1. Similar comparison for the three coarse porosity frits are shown in Table 1.2. It is apparent that different assemblies do not give reproducible results, there being a 100 fold difference, for example, between the results for medium assemblies 1 and 2. It is interesting to note that the results with medium assemblies 2 and 3 checked very

* Samuel Glasstone, "Elements of Physical Chemistry," Second Printing, p.465 D. Van Nostrand Co., New York, (1946).

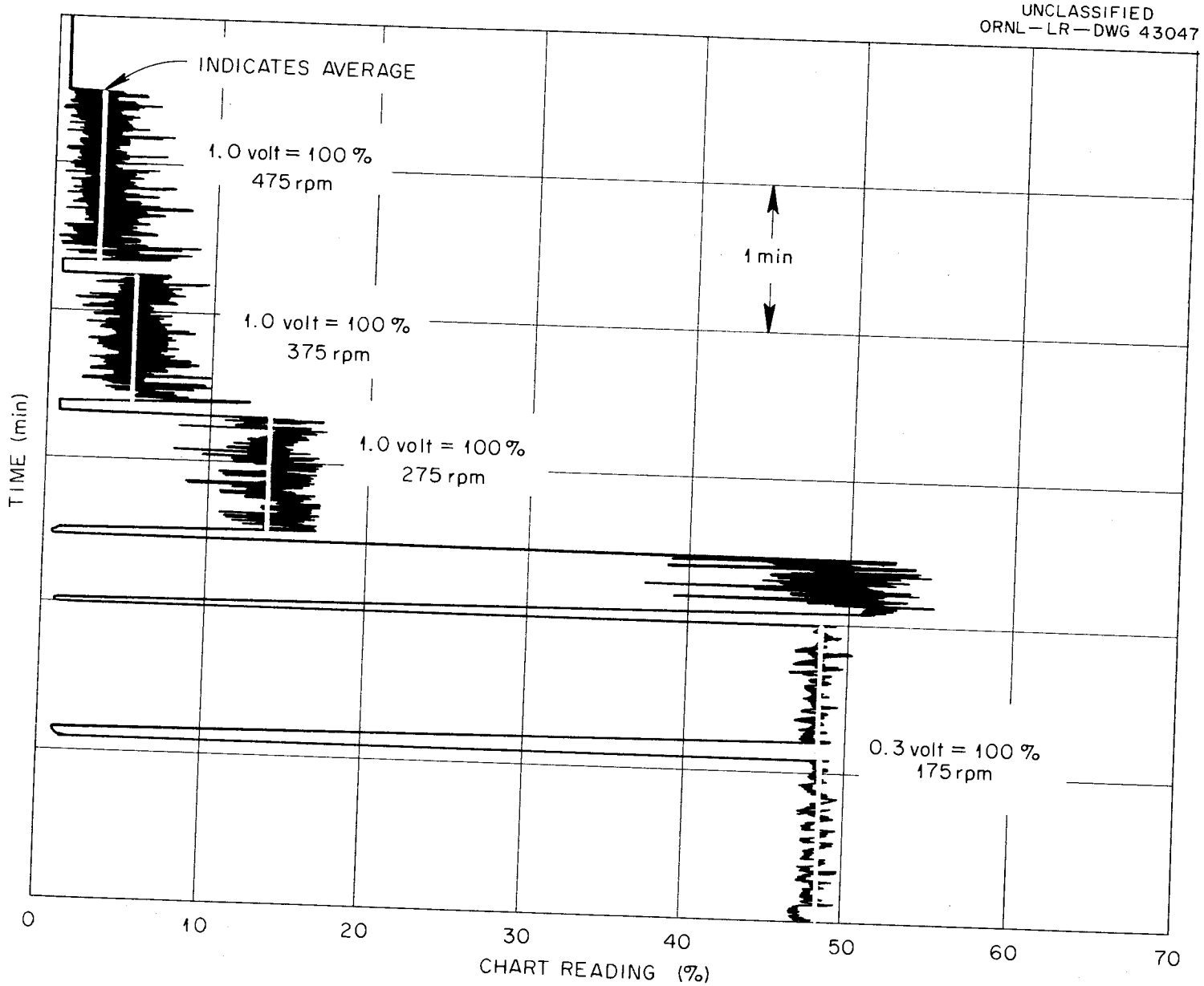

Fig. 1.1 Typical Brown Potentiometer Chart Run B-17 Coarse Frit Assembly 3
Transpiration Velocity 2.4 cm/min

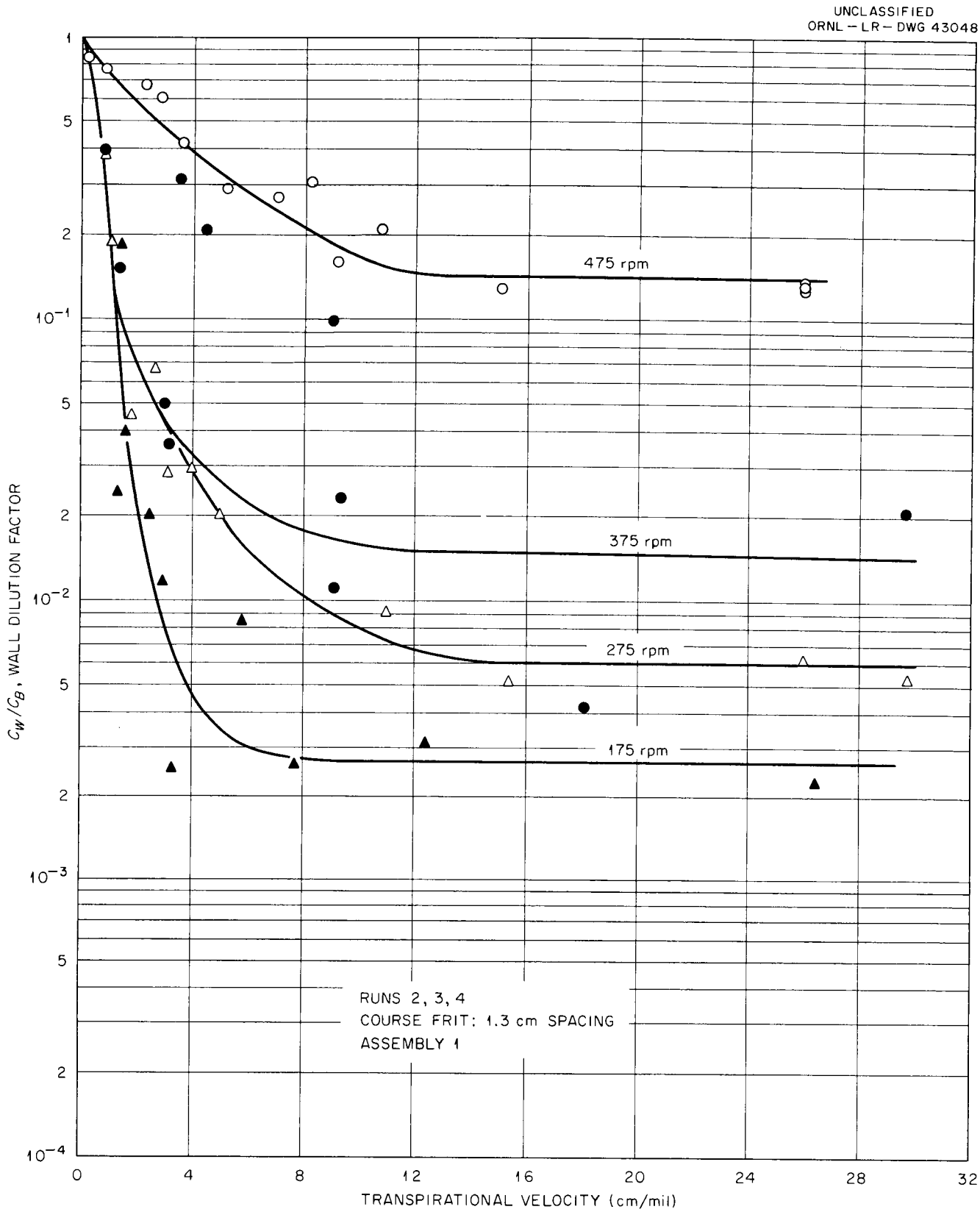

Fig. 1.2. Wall Dilution Factor vs Transpiration Velocity at Various Stirrer Speeds.

Table 1.1. Results for Medium Porosity Frits

Line	rpm	Disc Spacing	Minimum Wall Dilution Factor $(C_w/C_B)_{min}$, Dimensionless Assembly Number 1	2	3	Critical Transpiration Velocity, $q_{crit.}$ cm/min Assembly Number 1	2	3
1	175	0.75		0.0025			4.0	
2		1.5	0.1	0.004		12	8.0	
3		1.5	0.15	0.0016	0.0021	5	2.0	2.8
4		1.5*			0.04*			2.2*
5		2.0		0.0019			2.0	
6		3.4		0.0015			2.5	
7	275	0.75		0.0016			3.5	
8		1.5	0.2	0.004		12	8.0	
9		1.5	0.19	0.0011	0.0014	14	4.0	2.9
10		1.5*			0.04*			2.0*
11		2.0		0.0012			3.6	
12		3.4		0.0010			3.0	
13	375	0.75		0.0019			4.5	
14		1.5	0.5	0.011		12	8.0	
15		1.5	0.4	0.003	0.01	10	4.5	5.0
16		1.5*			0.11*			2.9*
17		2.0		0.003			4.3	
18		3.4		0.004			4.0	
19	475	0.75		0.05			3.1	
20		1.5	0.8	0.07		12	8.0	
21		1.5	0.9	0.045	0.1	14	3.0	4.5
22		1.5*			0.35*			2.0*
23		2.0		0.5			2.5	
24		3.4		0.5			3.0	

* Electrode removed and replaced.

Table 1.2. Results for Coarse Frits

		Minimum Wall Dilution Factor $(C_W/C_B)_{min}$ Dimensionless Assembly Number			Critical Transpiration Velocity, $q_{crit.}$ cm/min Assembly Number		
rpm	Disc	1	2	3	1	2	3
175	0.4			0.0015			4.0
	0.6		0.042			2.0	
	1.0		0.058			4.0	
	1.5	0.005	0.02	0.0010	7.0	2.5	5.0
	1.6		0.045	0.001		2.5	6.0
	1.5*			0.005*			2.0*
	3.0		0.02			2.0	
	3.75			0.0010			3.0
275	0.4			0.0015			3.0
	0.6		0.018			5.0	
	1.0		0.031			3.8	
	1.5	0.003	0.018	0.001	12	5.0	3.0
	1.6		0.011	0.001		5.0	2.5
	1.5*			0.0055*			7.0*
	3.0		0.040			4.0	
	3.75			0.001			3.0
375	0.4			0.0019			5.0
	0.6		0.015			6.0	
	1.0		0.02			7.0	
	1.5	0.09	0.015	0.002	9	4.0	6.0
	1.6		0.012	0.003		6.1	5.0
	1.5*			0.008			9.0*
	3.0		0.018			6.5	
	3.75			0.018			4.0
475	0.4			0.0085			5.0
	0.6		0.012			17	
	1.0		0.022			16	
	1.5	0.12	0.011	0.008	10	12	7.0
	1.6		0.024	0.0085		14	15
	1.5*			0.024*			10
	3.0		0.04			13	
	3.75			0.01			6.0

* Electrode removed and replaced.

well at 175 and 275 rpm, but deviated at 375 and 475 rpm. Similar comparisons can be drawn among the three coarse assemblies.

The starred values in Tables 1.1 and 1.2 are for a particular glass frit (in both cases No. 3). The original assemblies for which data are shown in the same columns were taken apart, and new electrodes were installed in the same glass frits. Comparison of the starred values of $(C_w/C_B)_{min}$ with the non-starred values taken for the same rpm and disc spacing shows a material difference.

These results may be interpreted in several ways. The most plausible explanation is that the assembly procedure was not sufficiently precise to place the active surface of the electrode always in the same position relative to the porous surface. The higher measurements of $(C_w/C_B)_{min}$ would then result because they are not true wall concentration ratios but are concentrations at some point in the boundary layer a small distance from the wall.

Effect of Stirrer Disc Speed. Tables 1.1 and 1.2 show a marked increase of $(C_w/C_B)_{min}$ in every case with increased stirrer rpm. Figure 1.2 illustrates this effect, although absolute values are not possible because of the lack of reproducibility of different assemblies.

Effect of Frit to Stirrer Disc Spacing. Tables 1.1 and 1.2 indicate generally that disc spacing has relatively little effect on $(C_B/C_w)_{min}$. Figure 1.3 shows this phenomenon graphically. This result is somewhat surprising. However, a possible explanation is that the degree and scale of turbulence in the bulk solution is a function of disc rpm only (diameter, baffling and other geometric factors being relatively fixed), and that the general bulk turbulence persisted into the zone of measurement because insufficient smoothing distance was provided.

Effect of Frit Porosity. The non-reproducibility of the frit assemblies obscures the effect of frit porosity. However, a comparison of Tables 1.1 and 1.2 show lower values of $(C_w/C_B)_{min}$, on the average, for the coarse frit.

Effect of the Variables on $q_{critical}$. Table 1.1 shows that for a medium porosity frit, $q_{critical}$, the transpiration velocity at which the rate of change of C_w/C_B with q decreases markedly, falls in the narrow range of 2.0 to 8.0 cm/min, for assemblies No. 2 and 3. The results from assembly No. 1 were in a range of 5 to 12 cm/min for $q_{critical}$. It will be noted that assembly No. 1 also shows high values of $(C_w/C_B)_{min}$, which may indicate that the electrode surface was not at the wall but penetrated a small distance into the boundary layer.

In any event, $q_{critical}$ for each assembly changed very little with the independant variables of disc speed and spacing. Table 1.2 shows a somewhat similar pattern for the coarse frits, except at 475 rpm. Even considering that only relative comparisons may be made, optimum reduction in wall dilution factor, and by inference, in corrosion rate, will probably be secured at transpiration velocities in the range of 2.0 to 15 cm/min.

UNCLASSIFIED
ORNL-LR-DWG 43049

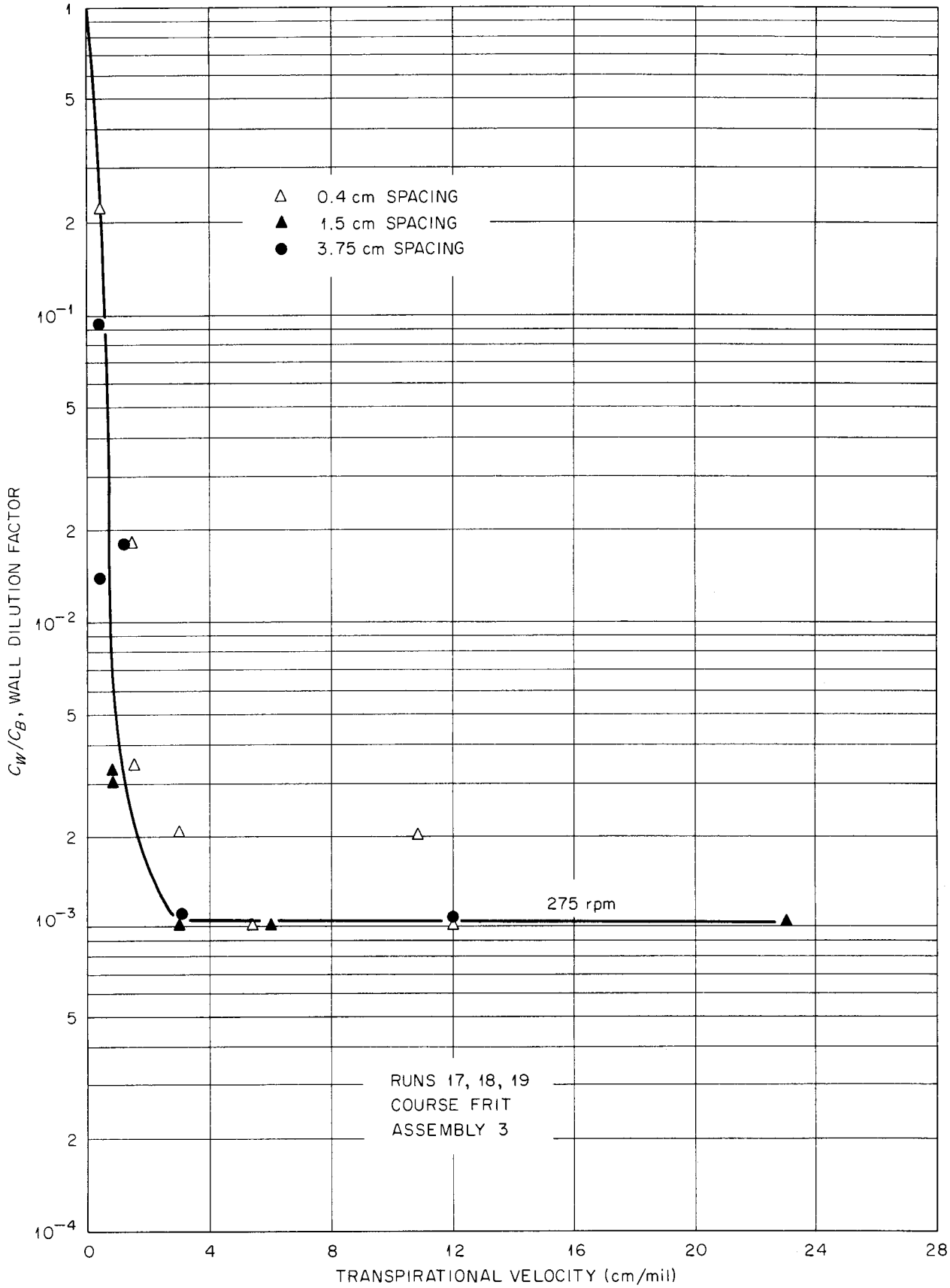

Fig. 1.3. Wall Dilution Factor vs Transpiration Velocity at Various Disk Spacings.

2.0 DRUHM

P. A. Haas

The direct reduction of uranium hexafluoride to uranium metal by use of sodium ($UF_6 + 6Na = U + 6NaF$) is being investigated. A continuous reaction study is being made with the emphasis on reactor design and materials of construction.

Semi-Continuous Reduction Study - C. D. Scott, W. G. Sisson

Four semi-continuous reduction runs, D-42, D-43, D-44 and D-45, were made in the DRUHM experimental facility described in the Unit Operations September 1959 monthly progress report. The purposes of these runs were to test the design of the reactant nozzles and reactor off-gas line and to determine the feasibility of using graphite as a liner material of construction. Uranium metal recovery was also determined when operating conditions resulted in metal consolidation.

2.1 Reactor Assembly. The reactor assemblies used in D-42 through D-45 were similar to that used in run D-40. The reaction zone liner was graphite with 1/4-in. thick walls. In these runs the graphite liner was enclosed by a MgO crucible with 1/2-in. thick walls (Figure 2.1) to confine reaction products in case of graphite failure and to act as a thermal barrier between the reaction zone and the reactor walls. There was approximately a 1/2-in. clearance between the MgO crucible and the 6-in. Inconel reactor wall (Figure 2.2).

The reaction zone was enclosed at the top by a 1/4-in. thick graphite cover and was insulated by a 1/4-in. MgO cover and 2-1/2-in. of K-30 firebrick (Figure 2.3). The sodium entrance line and the 3/4-in. dia off-gas line extended through the graphite cover into the reaction zone about 1/4-in. while the UF_6 nozzle extended to the middle of the magnesia cover with entrance ports in the magnesia and graphite covers. This placement of the UF_6 nozzle gave high-temperature insulation to the nozzle tip and removed the entire nozzle from the reaction zone environment.

Three thermowells were provided at various heights in the reactor: one just above the K-30 firebrick, one just above the graphite cover, and one 2 in. below the UF_6 nozzle just outside the MgO crucible. The reactor was also provided with a helium purge line at the top flange to confine reactants and products to the reaction zone and off-gas (Figure 2.4). The total weight of the assembled reactor was about 100 lbs.

2.2 Operating Procedure. The operating procedures used in these runs were similar to those used in previous runs. (1) The reactor was heated by induction to above 1130°C, (2) The liquid sodium was metered into the reactor at about 10 g/min while maintaining a He purge through the UF_6 nozzle and into the top of the reactor and a flow of cooling gas through the UF_6 nozzle, (3) The UF_6 flow was started after which the He purge

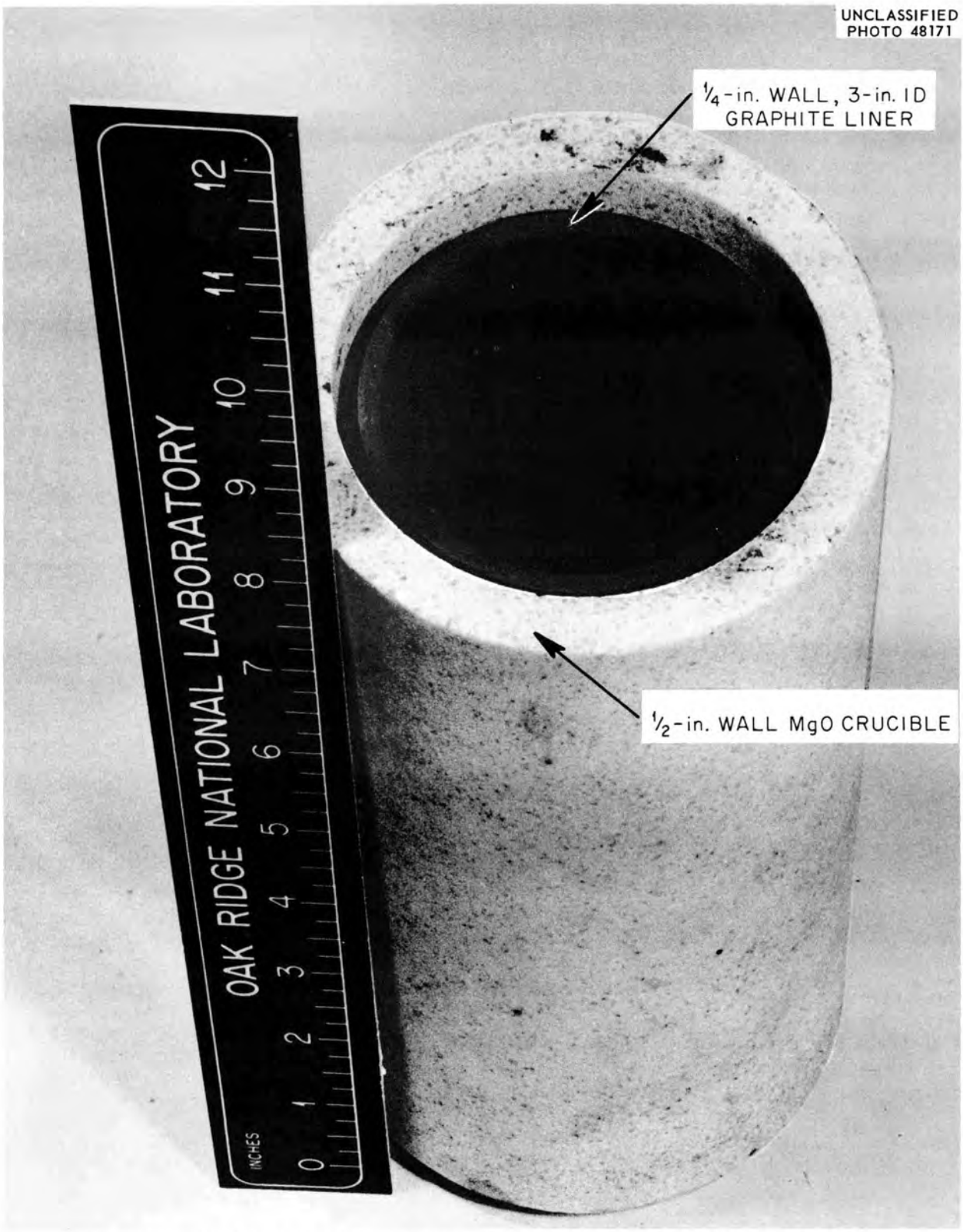

Fig. 2.1 Graphite Liner Enclosed by MgO Crucible for DRUHM Reactor.

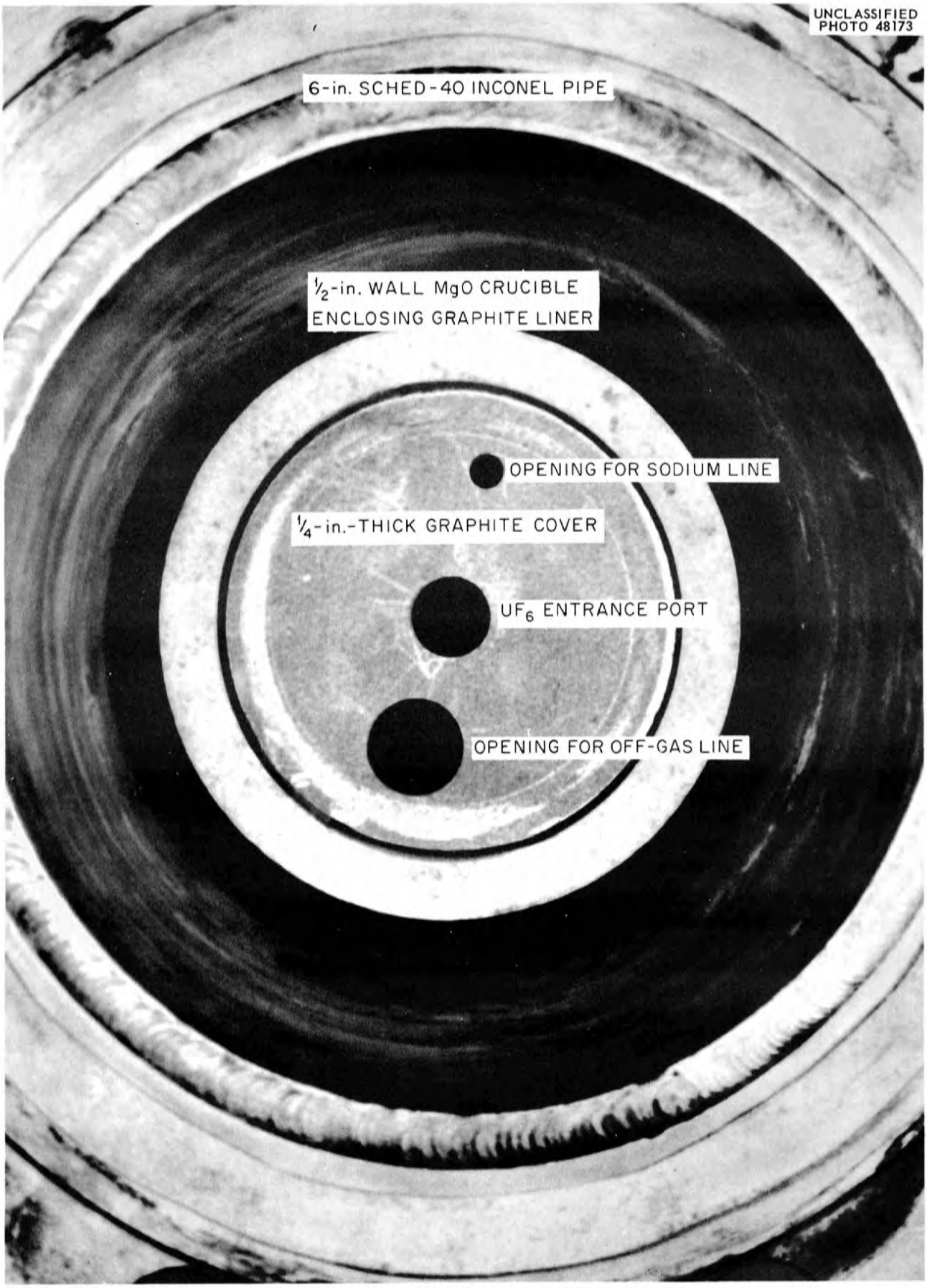

Fig. 2.2 Placement of MgO Crucible and Graphite Liner in the 6-in.-Dia DRUHM Reactor.

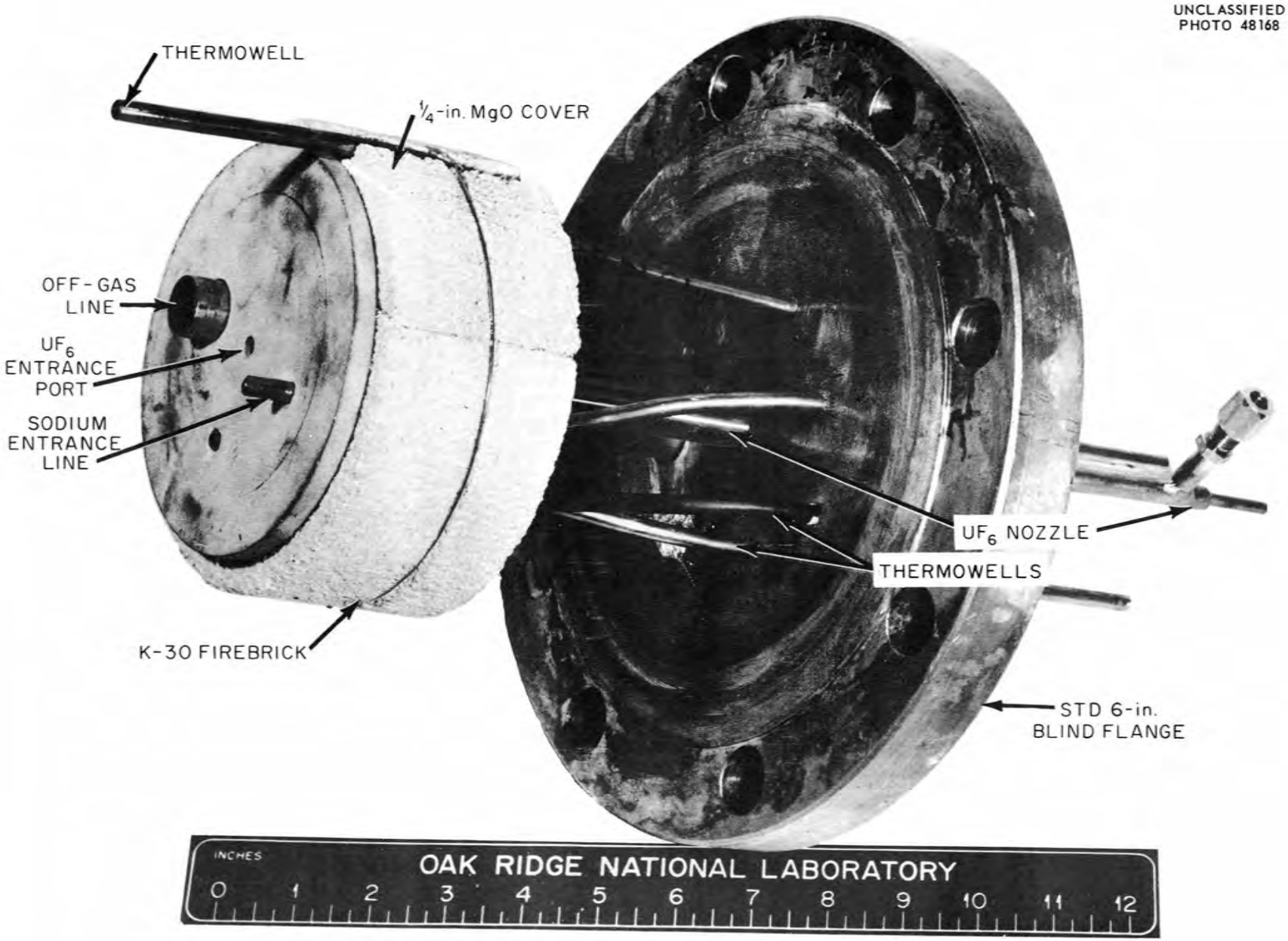

Fig. 2.3 Top Flange Arrangement For DRUHM 6-in.-Dia Reactor.

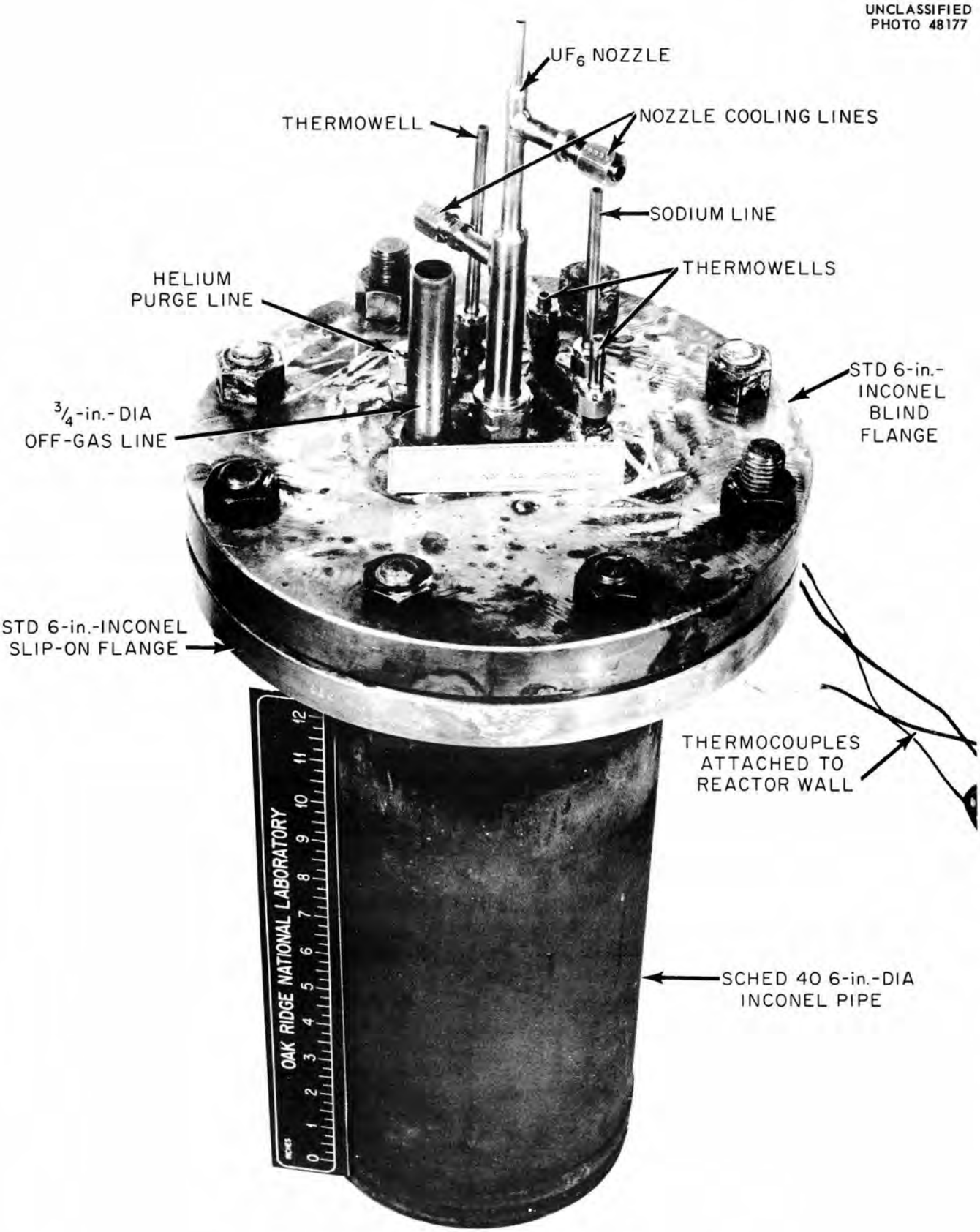

Fig. 2.4 Assembled DRUHM 6-in. Reactor.

through the UF_6 nozzle was stopped, (4) Both reactant flow rates were increased until the internal temperature was above 1200°C always maintaining at least 100% excess sodium. Finally the system was to be run at approximately steady state until at least 2000 g of UF_6 had been introduced.

2.3 Experimental Results. Run D-42 was made at an average UF_6 rate of 43.0 g/min and less than stoichiometric sodium. The run lasted for 21.5 minutes, and termination was due to a plug in the off-gas line. The sodium was metered into a boiler for vaporization prior to its introduction to the reactor. Because of an obstruction in the sodium line, the boiler operated at a high pressure, allowing an accumulation of sodium and less than a stoichiometric amount of sodium entering the reactor.

There was no visible damage to either the graphite liner or MgO crucible and only slight damage to the tip of the UF_6 nozzle (Table 2.1). No metal was recovered but a large quantity of crystalline material, probably slag and UF_4, was collected in the graphite liner. The maximum internal temperature measured was 1140°C.

Run D-43 was made with an average UF_6 rate of 28.7 g/min and 130% excess sodium introduced through a boiler operated at 1025°C. The sodium boiler operated irregularily with alternate build-up of sodium inventory and sudden release of the entire sodium volume. Thus, during part of the run there was a high excess of sodium and during the other part the sodium rate was less than stoichiometric. Run termination after 30 minutes of operation was due to plugging of the off-gas line.

There was slight damage to the UF_6 nozzle tip, no visible damage to the graphite liner, and product penetration of the MgO crucible with apparent surface attack by UF_6. The maximum inside temperature was 1178°C.

The product in the graphite liner was composed of two layers, (1) a dark crystalline material with included metal "beads" and (2) an irregular metal button on the bottom of the liner which was porous and contained included slag. Total metal recovery of 303 g was 55.5% of the amount of uranium added as UF_6.

In run D-44 a 3/4-in. off-gas line was used instead of the 1/2-in. line and the sodium was introduced to the reactor as a liquid. A total of 2438 g of UF_6 was introduced to the reactor in 19.5 minutes. The UF_6 flow rate was very erratic and was 2 or 3 times greater than the amount anticipated. The probable cause of the high, erratic flow rate was the presence of liquid UF_6 in the metering system. As a result of this high rate, the sodium introduced was less than stoichiometric. Run termination after 19.5 minutes of operation was due to failure of the UF_6 metering system.

There was no damage to the UF_6 nozzle, but there was a small crack in the bottom of the graphite liner and a large amount of product penetration in the MgO. A small, well-consolidated metal button, 49 g, was recovered adhering to the underside of the graphite. This button contained 3% of the uranium in the UF_6 feed. The maximum temperature measured inside the reactor opposite the reaction zone was 1265°C.

Table 2.1. Experimental Results for Four DRUHM Runs

Run No.	Length of run, min	Average UF_6 flow rate g/min	Sodium Excess, %	Maximum Inside Temp., °C	Recovery of Uranium as metal: Weight, g	Recovery of Uranium as metal: % of Theoretical	Reason for run Termination	Condition of Reactor Components after the Run: UF_6 nozzle	Condition of Reactor Components after the Run: Liners
D-42	21.5	43.0	less than Stoichiometric	1140	0	0	Plug in off-gas line	Slight damage to nozzle tip	No damage
D-43	30.0	28.7	130	1178	315	55.5	Plug in off-gas line	Slight damage to nozzle tip	No damage to graphite, product penetration in MgO
D-44	19.5	125	less than Stoichiometric	1265	49	3.0	Malfunction in UF_6 metering system	No damage	Small crack on bottom of graphite, product penetration in MgO
D-45	16.0	12.1	180	1225	140	89.7	Reduction in UF_6 flow	No damage, U metal build-up on tip	No damage to graphite, penetration in MgO

Run D-45 was made with an average UF_6 rate of 12.1 g/min and an average sodium rate which was 180% in excess of stoichiometric. The maximum feed UF_6 rate was 40 g/min. Run termination after 16 minutes was due to an obstruction in the UF_6 meter and depletion of the UF_6 supply. The maximum internal temperature measured was 1225°C.

There was no damage to the UF_6 nozzle other than several grams of uranium metal build-up on the nozzle tip. There was no visible damage to the graphite liner (Figure 2.5). There was also no slag in the graphite which indicated complete slag penetration of the graphite. There was evidence of slag penetration of the MgO wall also but there was no uranium metal in the MgO.

A porous uranium metal button was found in the bottom of the graphite liner (Figure 2.6) which weighed 122 g after clean-up. In addition, a total of 18 g of metal was recovered from the upper graphite liner walls. Without counting the uranium metal build-up on the UF_6 nozzle, the 140 g of recovered metal represents 89.7% of the amount of uranium introduced as UF_6. Preliminary analytical results showed that the metal button was 99.98% U and the metal on the walls was 99.75% U.

2.4 Conclusions. It appears that liquid sodium feed to the reactor is adequate for DRUHM runs. Significant metal consolidation occurred when the reaction zone temperature was greater than 1200°C. The presently designed Inconel UF_6 nozzle with internal cooling has not been damaged in several runs and is probably adequate for experimental runs.

Under conditions of high temperature (>1200°C) and nominal sodium excesses (<180%), graphite is probably satisfactory as a liner material. It will contain any uranium metal which formed while allowing some or perhaps all of the slag to penetrate and escape to the outer liner.

UNCLASSIFIED
PHOTO 48218

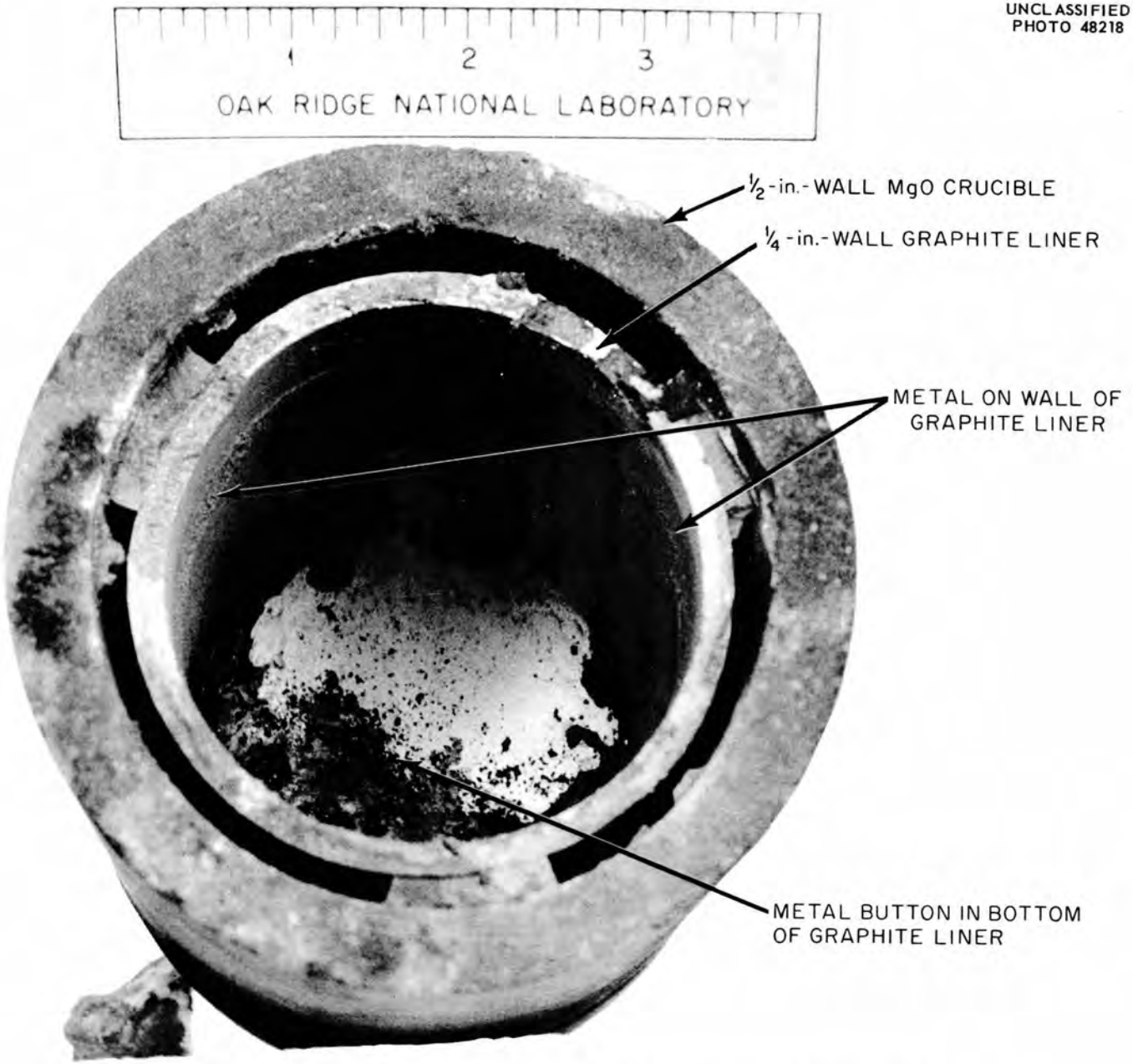

Fig. 2.5 MgO Crucible and Graphite Liner After DRUHM Run D-45.

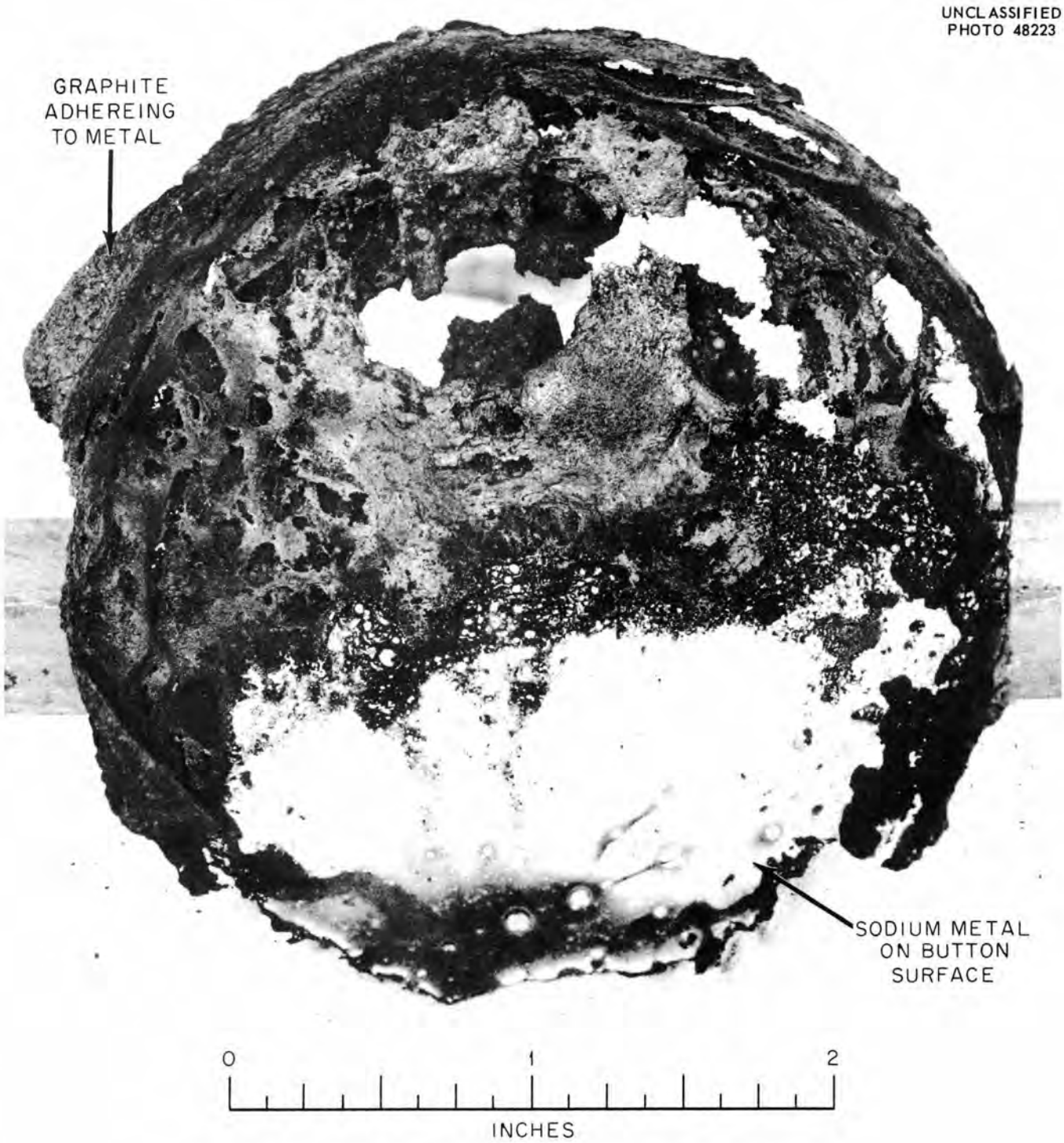

Fig. 2.6 Rough Metal Button from Run D-45 Before Clean-up.

3.0 FISSION PRODUCT RECOVERY BY SOLVENT EXTRACTION

M. E. Whatley

One of the problems that will be encountered is the use of solvent extraction for fission product recovery from aqueous raffinates is solvent radiation damage. The problem will be greater than the present problem in fuel processing since specific radio-isotopes such as strontium-90 may be dissolved in an organic solvent in high concentrations in the extract stream leaving a contactor. Using a high speed contactor is one possible solution to the problem, and the stacked clone contactor is a possible high speed contactor design.

Stacked Clone Contactor - W. E. Dunn, W. M. Woods

The stacked clone contactor is a liquid-liquid continuous countercurrent extraction apparatus which contacts and separates the phases rapidly with a high throughput to holdup ratio. A three-stage stacked clone contactor was described in Unit Operations September monthly report, CF 59-9-69.

In the contactor now under development, five Lucite hydroclones are stacked above one another. Each is provided with a pump for heavy phase recirculation to the clone. The light (organic) phase proceeds up the column through the vortex created by the hydroclones while the heavy (aqueous) phase moves down column along the walls of the hydroclones. Phase separation is achieved in a top disengaging section which is packed with pieces of polyethylene tubing to coalesce the organic solvent. The column has been run aqueous continuous with the interface in the top section.

Flooding data were obtained with kerosene as the organic phase and 0.08 M HNO_3 as the aqueous phase. These data are summarized in Figure 3.1 where the organic flooding rate is plotted against the aqueous flooding rate and in Figure 3.2, a plot of the log of the aqueous to organic flow rate ratio vs. the aqueous flooding rate.

For a constant organic flow rate the aqueous flow rate was increased until flooding occurred. At organic flow rates of 500 ml/min or less, flooding took place below the point of organic feed injection. Flooding here caused some of the solvent to be carried down the column and out through the aqueous takeoff. However, at organic flow rates greater than 500 ml/min flooding took place by a buildup of solvent in the underflow ports of the hydroclones.

Total solvent holdup in the column was measured at an organic flow rate of 500 ml/min. The results of this series of experiments are summarized in Table 3.1 where solvent holdup values are tabulated for various aqueous flow rates. The average solvent holdup per hydroclone stage was 33 ml which is 17% of the total volume of a clone stage. The procedure for holdup measurements was to operate the column at constant flow rates, shut off all streams simultaneously, and measure the resulting interface drop.

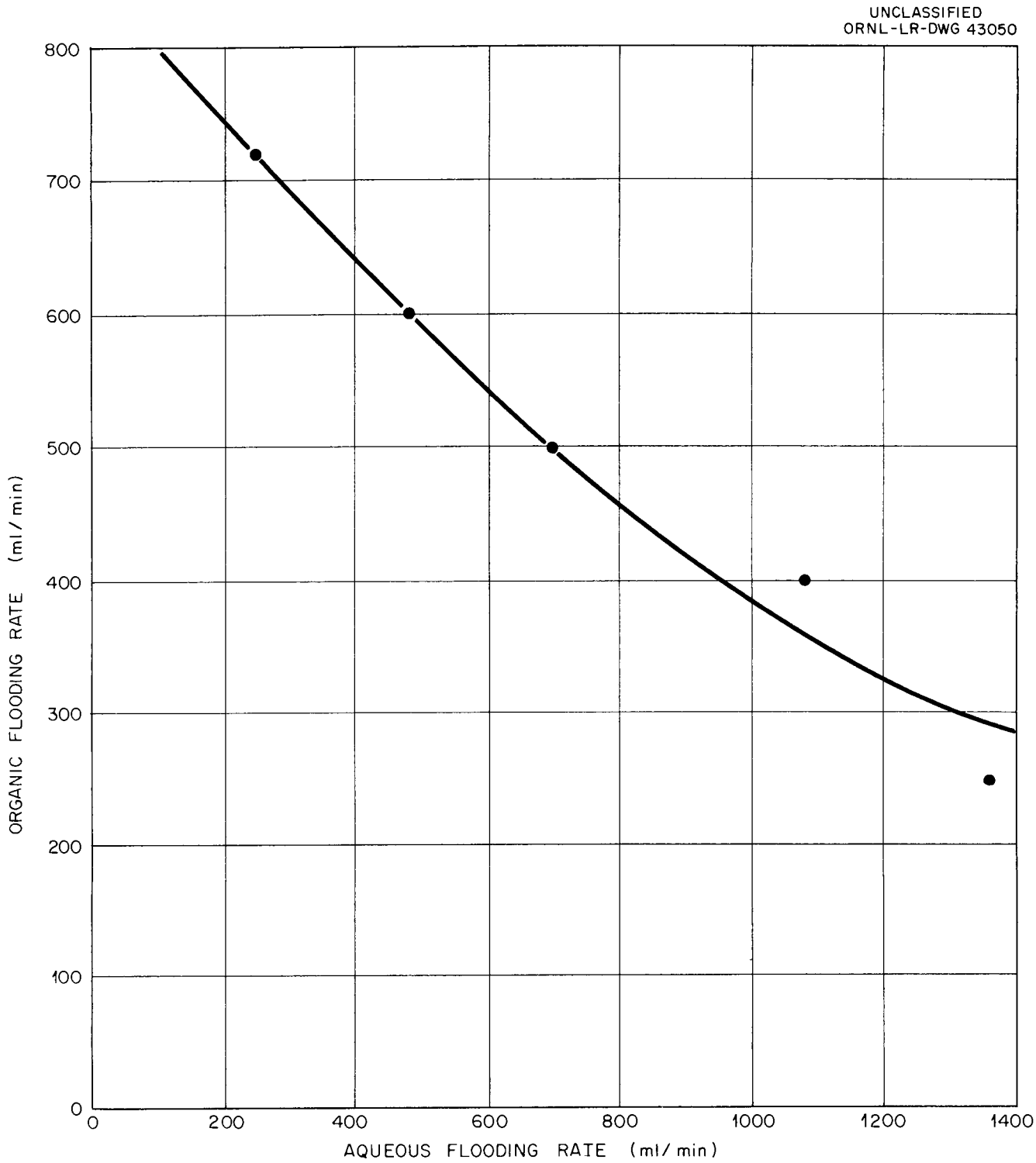

Fig. 3.1. Flooding Organic Flow Rate vs Flooding Aqueous Flow Rate for Stacked Clone Contactor.

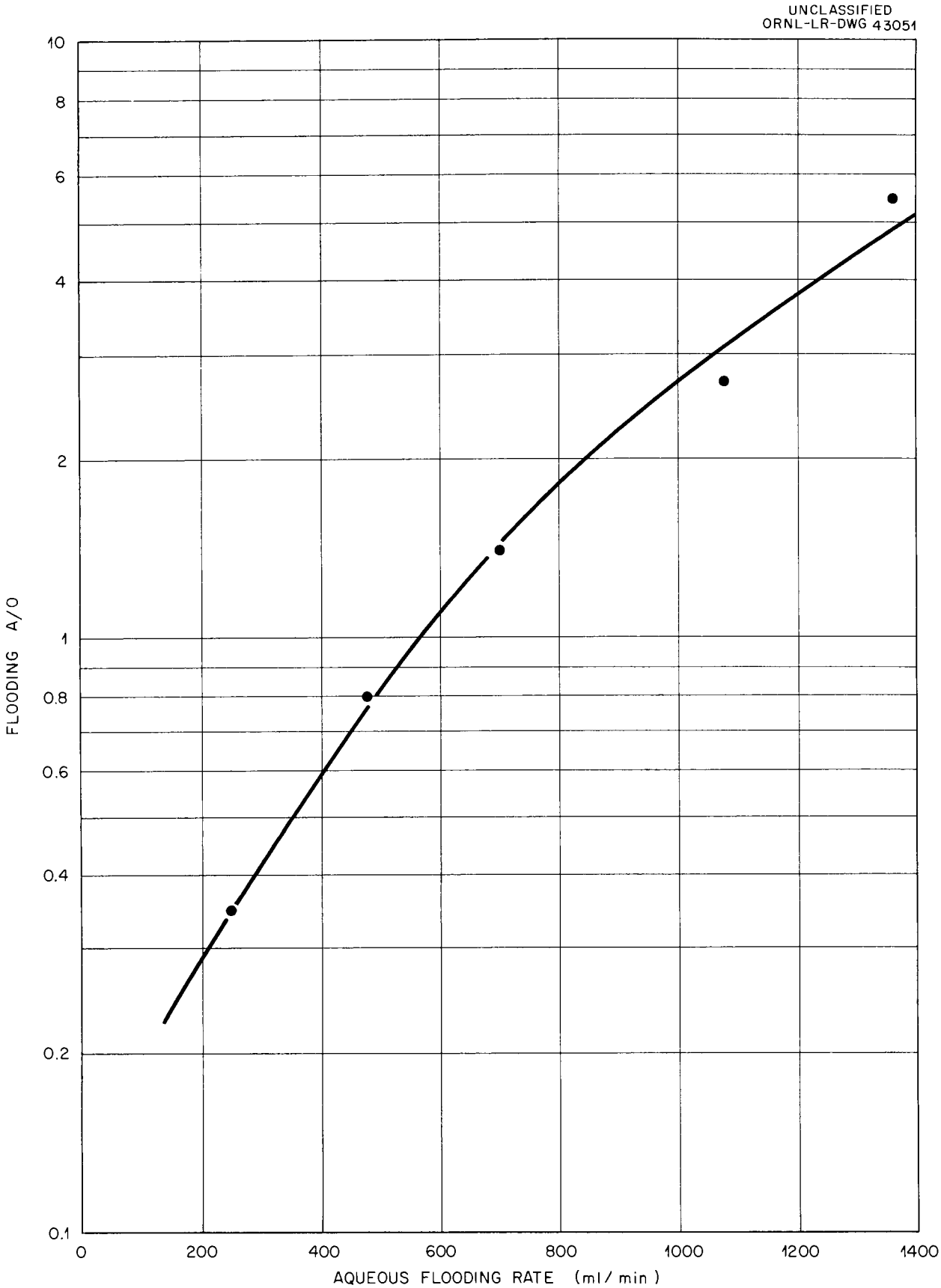

Fig. 3.2. Flooding A/O vs Flooding Aqueous Flow Rate for Stacked Clone Contactor.

Table 3.1. Organic Flow Rate - 500 ml/min

Aqueous Flow Rate-ml/min	Total Solvent Holdup-ml	Holdup in Hydroclone Stages-ml	End Section Holdup-ml
200	244	133	111
400	258	130	128
600	273	127	146

It was found that the solvent holdup was less if the organic stream was injected into the bottom hydroclone through the discharge line of the recirculation pump to that clone rather than through a standpipe located about 1-in. below the bottom hydroclone. Solvent holdup was determined when the organic inlet was through the recirculation pump to the bottom hydroclone and again when the inlet was into the top hydroclone. The difference in holdup for these two cases represents the amount of solvent present in four hydroclone stages, whereas the difference between holdup when injection is through the bottom clone and holdup in the four hydroclone stages yields a value for end section holdup.

4.0 FLUOROX

P. A. Haas

The Fluorox process is the oxidation of UF_4 with dry oxygen or air to form UF_6($2UF_4 + O_2 = UF_6 + UO_2F_2$) with subsequent recycle of the UO_2F_2 by reduction and hydrofluorination. The experimental phase of the program was completed and a final report and cost estimate are being prepared.[1,2]

Fluorox Plant Cost Estimate - C. D. Scott

The primary oxidation reaction for the Fluorox process, $2UF_4 + O_2 = UF_6 + UO_2F_2$, was studied in the laboratory and on an engineering scale while the recycle of the UO_2F_2 was studied in the laboratory. The next logical development step would be a pilot plant of the overall process. Since no further development work is anticipated on this process at ORNL, a cost estimate was prepared for a Fluorox plant utilizing all of the presently available laboratory and engineering data. Such a cost estimate would be usable in any economic study made for evaluation of this process for a future pilot plant or production facility.

The size of plant chosen for the cost estimate is equivalent to 5000 tons of U_3O_8 throughput. This size is the same as the facility bid on by private industry in the Civilian Applications Program in 1956.

4.1 Design Criteria

The cost estimate is for a fully integrated facility capable of converting feed materials-grade UF_4 to cascade-grade UF_6 (Figure 4.1). The plant consists of (1) a feed preparation section (where finely divided UF_4 can be increased in size to -20 +150 mesh fluid bed feed) which consists of a compacting machine for the initial up-grading step, a vibrating screen for recycle of fines, a granulator for producing an exceptable feed from the up-graded material and the necessary storage and solids handling facilities; (2) an oxidation reaction section where the primary Fluorox reaction ($2UF_4 + O_2 \rightarrow UO_2F_2 + UF_6$) is carried out in two 24-in. fluid beds; (3) an oxidation reactor off-gas facility which removes the UF_6 product from the off-gas by a series of two cold traps and allows an oxygen purge to the atmosphere through a fluid bed of UF_4 to prevent build-up of HF; (4) a recycle section consisting of two 24-in. fluid bed reactors for converting the by-product UO_2F_2 from the oxidation reactors to UF_4 by reduction with H_2 ($UO_2F_2 + H_2 = UO_2 + 2HF$) and hydrofluorination of the resulting UO_2($UO_2 + 4HF \rightarrow 2H_2O + UF_4$), and (5) a purification section which is a small Excer plant to be used to process a portion of the oxidation reactors by-product for removal of accumulated metal fluoride and other non-volatile impurities.

The design and operating conditions of the oxidation reactors are based on experimental information and represent apparent optimum conditions. Design of the other equipment and determination of other operating conditions are based on available experimental and operational information from similar production systems.

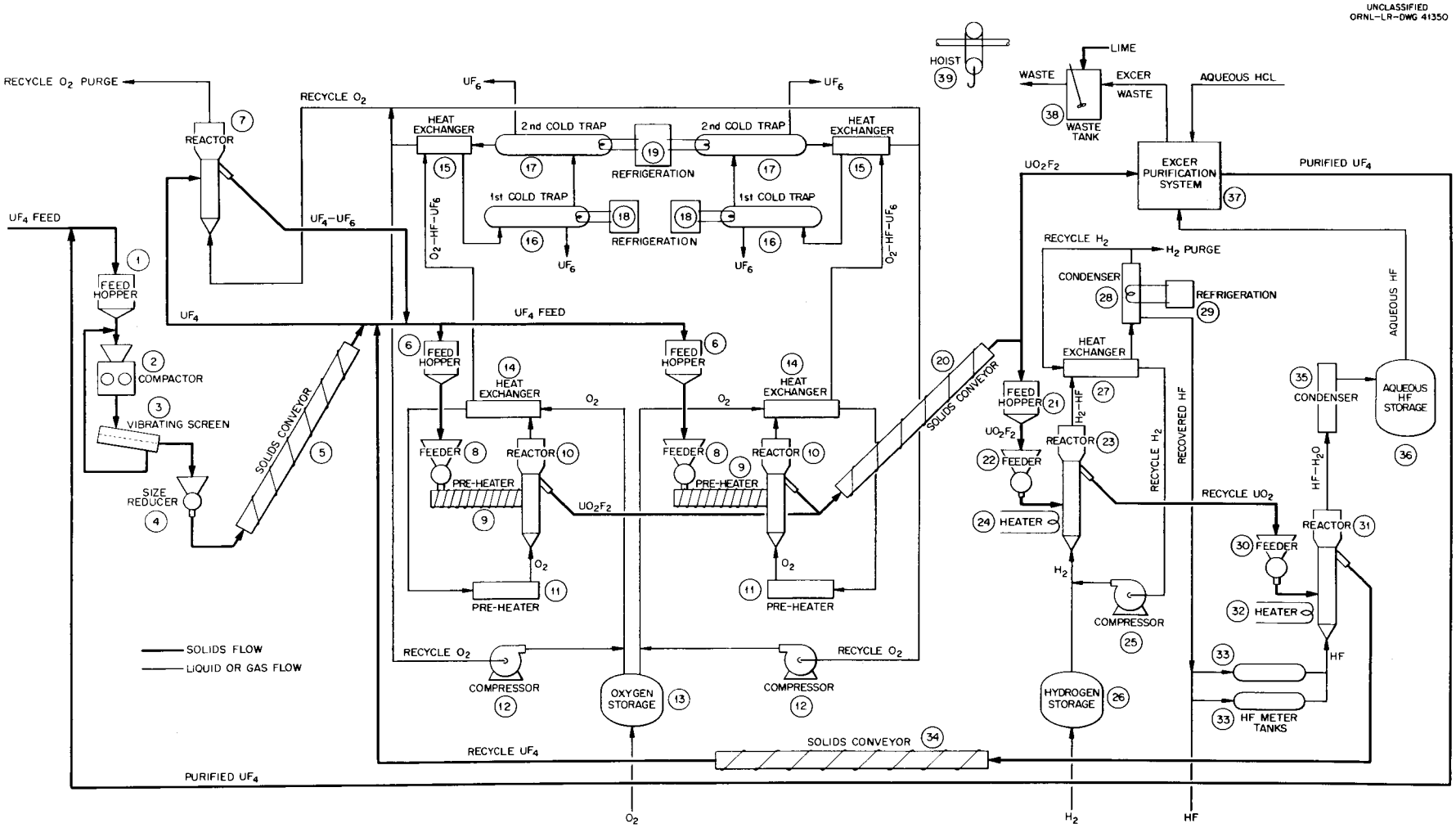

Fig. 4.1 Fluorox Process Flowsheet Showing Major Process Equipment.

Although some of the design criteria (Table 4.1) are based on available information, there are also some arbitrary choices which were made without benefit of experimental or operational data. The resulting system is operable but it is not necessarily the most economical system because of the arbitrary criteria. These arbitrary choices show that some additional experimental work would be desirable.

On the basis of the design criteria listed in Table 4.1, a chemical process flowsheet (see Figure 4.2) was developed. This flowsheet gives a complete material balance on all major process streams. Use of this information makes it possible to properly size process equipment and determine throughputs.

4.2 Cost Estimating Procedure

The plant cost estimating procedure used was presented by Aries and Newton in "Chemical Engineering Cost Estimation."(3) In this procedure, the purchased cost of major process equipment is used to determine the other components of physical plant cost by use of factors which have been empirically determined. Manufacturing costs can be estimated in a similar manner by use of costs of fixed capital, raw materials, labor and utilities.

This abbreviated cost estimating method is probably as accurate as is justified by the available experimental data. The various factors given by Aries and Newton to determine the different costs are usually given as a range of values. In general, the present cost estimate was prepared by using the maximum value of each factor; therefore, the determined costs should represent maximum values and the overall effect is a conservative estimate.

4.3 Fixed Capital Estimate

The fixed capital is primarily based on the purchased cost of major process equipment. Major process equipment was defined as any process equipment with an installed cost of $1000 or greater. There are a total of 39 pieces of major process equipment (Figure 4.2). The size and material of construction of this equipment (Table 4.2) was determined from the material balance or throughput and operating conditions. Purchased costs of the major process equipment were determined from published cost data such as equipment cost graphs, by use of sizing factors on comparable but different sized equipment and actual cost data on similar equipment now in use. The "Engineering News Record" cost index was used to equate all cost data to purchased cost in 1959.

The total purchased cost for all major process equipment is $611,400 (Table 4.2). Use of the factors given by Aries and Newton makes it possible to determine the physical plant cost, by using 43% of the purchased equipment cost for installation cost, 36% for piping, 30% for instrumentation, 8% for insulation, 15% for electrical, 65% for building, 15% for land and yard improvements, and 75% for utilities. This procedure gives a total physical plant cost of $2,366,100 (Table 4.3).

Table 4.1. Fluorox Plant Design and Cost Estimating Criteria

1. The plant size is equivalent to a capacity of 5000 tons U_3O_8/year or 4240 tons uranium/year.

2. The design operating time is 300 days per year.

3. The oxidation reactors will be two 24-in. Inconel fluid bed reactors with 0.5-in. thick walls.

4. The oxidation reactors must be replaced once each year.

5. Corrosion products contaminate the system at a rate of 0.25 ipy of corrosion in the two oxidation reactors and 25% of this amount in the recycle system.

6. The superficial gas velocity in all fluid bed reactors must be at least 0.5 ft/sec.

7. The oxidation off-gas will be 10% UF_6.

8. The oxygen recycle stream will be 1% HF, 0.02% UF_6 and the remainder O_2.

9. The UF_4 concentration in the oxidation reactor fluid bed will be 10%.

10. The oxidation reactor bed temperature will be 825°C.

11. The recycle system will consist of a reduction reactor and a hydrofluorination reactor both of which will be 24-in. dia, 1/2-in. thick Inconel.

12. Operating conditions in the reduction and hydrofluorinating systems will be similar to present comparable feed materials processes.

13. 99% of the H_2 introduced to the recycle system will be utilized in the reduction reactor by means of off-gas recycle.

14. 90% of the anhydrous HF introduced to the hydrofluorination reactor will be utilized in that reactor and the remainder will be used in the Excer facility.

15. An Excer purification system will be used to remove accumulated metal fluoride impurities from the process stream.

16. All process heaters will be electrical.

17. High purity oxygen, 99.5%, will be available at the plant site at 200 psig and at current cost.

18. Pure H_2, 99%, will be available at the plant site at 200 psig and current costs.

Table 4.1. (Continued)

19. The initial UF_4 feed will have the following composition:

UF_4	96.00%
UO_2F_2	2.50%
UO_2	1.35%
Other metal fluorides	0.05%
H_2O	0.10%

20. The solids by-product from the oxidation reactors will have the following composition:

UF_4	10.0%
UO_2F_2	88.0%
Other metal fluorides	2.0%

21. The UF_4 from the recycle system will have the following composition:

UF_4	95.00%
UO_2F_2	1.90%
UO_2	1.00%
Other metal fluorides	2.00%
H_2O	0.10%

22. The Excer purification UF_4 will have the following composition:

UF_4	97.40%
UO_2F_2	2.25%
U_3O_8	0.20%
Other metal fluorides	0.05%
H_2O	0.10%

23. All material listed as "other metal fluorides" is composed of 50% metal and 50% fluoride.

24. Specific gravity of loose solids is 3.0 and of fluidized solids is 2.0.

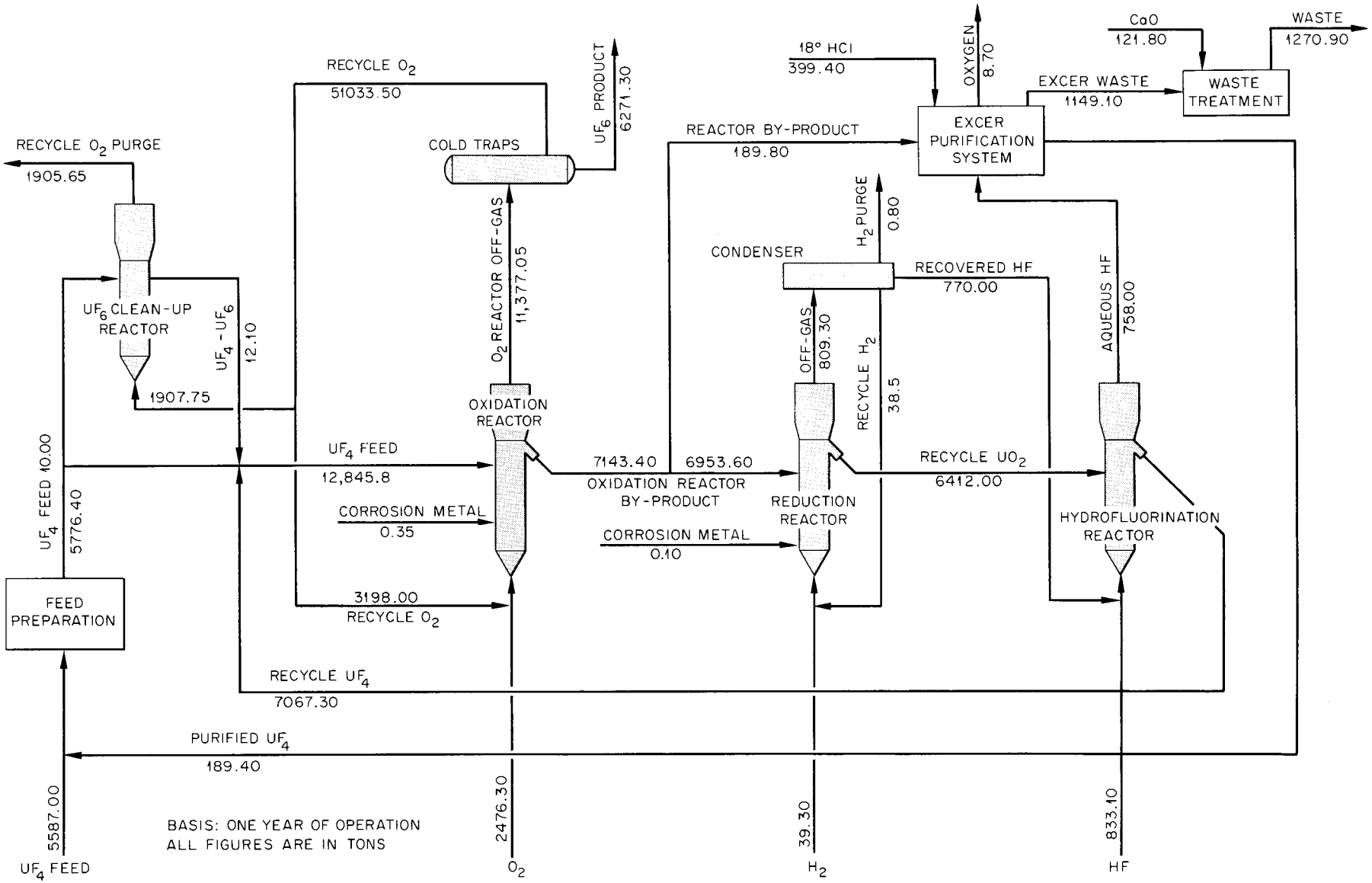

Fig. 4.2. Fluorox Process Chemical Flowsheet.

Table 4.2. Specifications and Purchase Cost of Major Process Equipment

1	2	3	4	5	6	7	8	9	10	11
Equipment No. (in Figure 2)	Description	Size	No. of Units	Material of Construction	Material Handled	Temperature, °C	Pressure, psig	Material flow rate, lb/hr	Purchased Cost, 1959	Cost Reference
1	Feed hopper	66.2 cu ft	1	SS	UF_4 feed	atm	atm	1600	$ 2800	5 p. 100
2	Solids Compactor	3200 lb/hr	1	SS	UF_4 feed	atm	atm	3200	13400	10
3	Vibrating Screen	100 mesh, 7.5 sq ft	1	SS	UF_4 feed	atm	atm	3200	1400	14 and 3, p. 58
4	Solids size reduction	50 hp	1	SS	UF_4 feed	atm	atm	1600	3900	14, p.141 and 3, p. 60
5	Solids conveyor, screw type	4-in. dia, 20 ft long	1	SS	UF_4 feed	atm	atm	1600	1500	3, p. 28
6	Feed hopper	76.2 cu ft	2	SS	UF_4 feed	atm	atm	1800	7000	3, p. 66
7	O_2 purge reactor	18-in. dia with 30-in. expanded section, and 17 sq ft filter	1	Monel	UF_4 and recycle O_2	atm	atm	UF_4-3 O_2-530	6600	4, p. 269 and 12
8	Solids feeder	2-in. screw	2	SS	UF_4 feed	atm	atm	1800	1900	13
9	Solids preheater	6-in. screw, 200,000 Btu/hr	2	Inconel	UF_4 feed	600	atm	1800	27500	3, p. 28 and 15
10	Oxidation reactor	24-in. dia with 36-in. expanded section and 48 sq ft filter	2	Inconel	O_2, UO_2F_2, UF_6, and UF_4 feed	825	5	UF_4-1800	17600	4, p. 269 and 12
11	Oxygen preheater	176,000 Btu/hr	2	Inconel	Oxygen	1100	100	790	34100	3, p. 49 and 15
12	Oxygen compressor	5000 scfh	2	SS	Oxygen	atm	0-150	450	8400	3, p. 25
13	Oxygen storage tank	5500 cu ft	1	Steel	Oxygen	atm	150	690	12900	3, p. 67

Table 4.2. (Continued)

1	2	3	4	5	6	7	8	9	10	11
14	Heat exchanger	105 sq ft	2	Inconel	O_2-UF_6	25-825	5	1600	7500	3, p. 49
15	Heat exchanger	64 sq ft	2	Copper	O_2-UF_6	-55 to 200	5	1600	5700	3, p. 49
16	Primary cold traps	10 tons UF_6	3	Monel	O_2-HF-UF_6	-17	5	UF_6-826	104600	8
17	Secondary cold traps	3 tons UF_6	3	Monel	O_2-HF-UF_6	-60	5	UF_6-44	69700	8
18	Refrigeration	7.8 tons	2			-17			22700	5, p. 105
19	Refrigeration	4 tons	1			-60			34100	5, p. 105
20	Solids conveyor, screw type	4-in. dia, 20 ft long	1	SS	UO_2F_2	200	atm	2000	1500	3, p. 28
21	Feed hopper	40 cu ft	1	SS	UO_2F_2	200	5	2000	2300	3, p. 66
22	Solids feeder	2-in. screw	1	SS	UO_2F_2	200	5	1900	1000	13
23	Reduction reactor	same as No.10	1	Inconel	UO_2F_2-UO_2	625	5	1900	8800	4, p. 269 and 12
24	Heater	223,600 Btu/hr	1			650			14300	3, p. 49 and 15
25	H_2 compressor	3500 scfh	1	Steel	H_2	atm	0-150	108	3900	3, p. 25
26	H_2 storage tank	1370 cu ft	1	Steel	H_2	atm	150	110	5200	3, p. 67
27	Heat exchanger	142 sq ft	1	Copper	H_2-HF	-55 to 400	5	240	3100	3, p. 49
28	HF condenser	67 sq ft	1	Copper	HF	-60	5	220	1500	3, p. 49
29	Refrigeration	5.5 tons	1			-60			42600	5, p. 105
30	Solids feeder	2-in. screw	1	SS	UO_2-UF_4	200	5	1700	1000	13
31	Hydrofluorination reactor	same as No. 10	1	Monel	UO_2-UF_4	575	5	1700	8800	4, p. 269 and 10
32	Heater	20,000 Btu/hr	1			600			3400	3, p. 40 and 15
33	HF meter tanks	220 gal	2	Steel	HF	100	100	230	1000	3, p. 66
34	Solids conveyor screw type	4-in. dia 50 ft long	1	SS	UF_4	atm	atm	2000	1500	3, p. 28
35	Aqueous HF condenser	700 gal/hr cooling H_2O	1	Copper	Aq. HF	100	5	210	1000	3, p. 26

Table 4.2. (Continued)

1	2	3	4	5	6	7	8	9	10	11
36	Aqueous HF hold-up tank	200 gal	1	Rubber lined steel	Aq. HF	atm	atm	210	1300	3, p. 66
37	Excer process	0.47 tons U/day	1		UO_2F_2			53	110500	11
38	Waste tank	340 gal, agitated	1	rubber lined steel	Excer waste	atm	atm	320	4400	3, p. 64
39	Hoist	15 ton capacity on monorail	1						11000	9

Total Purchased Equipment Cost $611,400

UNCLASSIFIED
ORNL-LR-DWG. 41444

TABLE 4.3. TOTAL FIXED CAPITAL

PURCHASED EQUIPMENT COST	$ 611,400
INSTALLATION (43% OF PURCHASED EQUIPMENT COST)	262,900
PIPING(36% OF PURCHASED EQUIPMENT COST)	220,100
INSTRUMENTATION (30% OF PURCHASED EQUIPMENT COST)	183,400
INSULATION (8% OF PURCHASED EQUIPMENT COST)	48,900
ELECTRICAL (15% OF PURCHASED EQUIPMENT COST)	91,700
BUILDING (65% OF PURCHASED EQUIPMENT COST)	397,400
LAND AND YARD IMPROVEMENT (15% OF PURCHASED EQUIPMENT COST)	91,700
UTILITIES (75% OF PURCHASED EQUIPMENT COST)	458,600
PHYSICAL PLANT COST	$2,366,100
ENGINEERING AND CONSTRUCTION (25% OF PHYSICAL PLANT COST	591,500
DIRECT PLANT COST	$2,957,600
CONTRACTORS FEE (7% OF DIRECT PLANT COST)	207,000
CONTINGENCY (25% OF DIRECT PLANT COST)	739,400
TOTAL FIXED CAPITAL	$3,904,000

Addition of the engineering and construction cost (25% of physical plant cost) to physical plant costs gives the direct plant cost of $2,957,600. Addition to the contractors fee (7% of direct plant cost) and contingency (25% of direct plant cost) to direct plant cost gives the total fixed capital of $3,904,000.

4.4 Manufacturing Cost Estimates

The direct manufacturing cost was determined by estimating the cost of raw materials, labor and utilities and applying factors for determining the cost of supervision (25% of labor), maintenance (6% of fixed capital) and plant supplies (15% of maintenance). Total raw materials cost for one year of operation is $517,000 (Table 4.4). The operating labor force necessary for continuous operation is 64 men (Table 4.5), and the labor cost per year at a rate of $2.50 per hour is $332,800. Utilities will cost $37,400 per year (Table 4.6). Summation of the costs of raw materials, labor, supervision, maintenance, plant supplies and utilities is the total direct manufacturing cost which is $1,239,700 per year.

Indirect manufacturing cost is based entirely on the cost of labor. This cost includes payroll overhead (15% of labor), laboratory (15% of labor) and plant overhead (75% of labor) which totals $349,400 per year.

Fixed manufacturing cost is composed of the depreciation of the total fixed capital which is 20% of fixed capital per year of $780,800, property tax of $39,000 per year (1% of fixed capital) and insurance of $39,000 per year (1% of fixed capital). Thus, the total fixed manufacturing cost is $858,800 per year. The depreciation on fixed capital of 20% per year represents a 5 year authorization period, the shortest period generally used in the chemical industry.

The total manufacturing cost is the summation of direct manufacturing cost, indirect manufacturing cost and fixed manufacturing cost. This cost is $0.288 per lb of uranium processed from UF_4 to UF_6 (Table 4.7). Costs for company administration, sales, research, finance, etc., were not estimated since the type of market is unknown and there is no general agreement among various companies for handling these functions.

4.5 References

1. Bresee, J. C., et al., "The Development of a Fluidized Bed Reactor for the Fluorox Process: Unit Operations Monthly Status Reports for the Period January through October, 1958," ORNL CF 58-11-30, Nov. 17, 1958.

2. Bresee, J. C., et al., "The Development of a Fluidized Bed Reactor for the Fluorox Process: Unit Operations Monthly Status Reports for the Period November 1958 through May 1959," ORNL CF 59-5-93, May 26, 1959.

3. Aries, R. S., and Newton, R. D., "Chemical Engineering Cost Estimation," McGraw-Hill, New York, 1955.

Table 4.4. Raw Materials Cost per Year

Material	Amount, Tons per Yr	Unit Cost	Reference for Unit cost	Total Cost per year
Oxygen	2476	$23.3/ton	4	$ 61,200
Anhydrous HF	833	0.21/lb	16, p. 75	350,000
Hydrogen	39	4.7/1000 cu ft	5	65,000
18° HCl	399	1.40/100 lb	16, p. 75	11,200
Lime	122	10/ton	16, p. 82	1,200
Other Materials:				
Excer resin				2,800
Excer cell membranes				400
2 Oxidation reactors				25,200
Total raw materials cost per year				$517,000

Table 4.5. Operating Labor Force

Operation	Number of men per shift	Number of men for 4 shifts
Feed preparation	2	8
Recycle O_2 purge reactor	1	4
Cold traps	2	8
Oxidation reactors	3	12
Reduction reactor	1	4
Hydrofluorination reactor	1	4
Excer system	2	8
Utilities	2	8
Relief and Misc.	2	8
Totals	16	64

At 2080 hours per man per year and $2.50/hr or $5200 per man per year, total yearly labor cost is $332,800.

- -

Table 4.6. Cost of Utilities per Year

Type of Utility	Amount per year	Unit cost	Total cost per year
Steam, 100 psi	6,452,000 lbs	$0.70/100 lb	$ 4,510
Electric poser	3,318,000 KWH	0.007/kwh	23,200
Cooling H_2O	5,040,000 gal	0.10/1000 gal	500
Process H_2O	11,300,000 gal	0.05/1000 gal	570
Demineralized H_2O	113,000 gal	0.15/1000 gal	20
Total process utilities			$28,800
Building and service needs (30% of process utilities)			8,600
Total cost of utilities			$37,400

UNCLASSIFIED
ORNL-LR-DWG. 41443

TABLE 4.7. MANUFACTURING COST

BASIS: 1 lb OF URANIUM PROCESSED FROM UF_4 TO UF_6

RAW MATERIALS	$ .061	
LABOR	.039	
SUPERVISION (25% OF LABOR)	.010	
MAINTENANCE (6% OF FIXED CAPITAL)	.027	
PLANT SUPPLIES (15% OF MAINTENANCE)	.004	
UTILITIES	.004	
DIRECT MANUFACTURING COST		$ .145
PAYROLL OVERHEAD (15% OF LABOR)	$ .006	
LABORATORY (15% OF LABOR)	.006	
PLANT OVERHEAD (75% OF LABOR)	.029	
INDIRECT MANUFACTURING COST		.041
DEPRECIATION (20% PER YEAR OF FIXED CAPITAL)	$ .092	
PROPERTY TAX (1% OF FIXED CAPITAL)	.005	
INSURANCE (1% OF FIXED CAPITAL)	.005	
FIXED MANUFACTURING COST		.102
MANUFACTURING COST		$ .288

4. Happel, John, "Chemical Process Economics," Wiley, New York, 1958.

5. Chilton, C. H., "Cost Data Correlated," Chemical Engineering, June 1949.

6. Van Dyke, B. H., Dougherty, W. J., "Cost of Low Temperature Processing," Chemical Engineering Progress, April 1955.

7. Fairchough, Hugh, "What Price Hydrogen?," Petroleum Refiner, September 1956.

8. Shapiro, T., Personal communication, August 11, 1959.

9. E and M Division of ORNL, personal communication, August 17, 1959.

10. Kircher, Albert, Letter to J. B. Adams from W. J. Fitzpatric Co., July 25, 1957.

11. I. R. Higgins, et al., "Development of the Excer Process. IV. Chloride System," ORNL-2490, Nov. 19, 1958.

12. Boyd, W., personal communication, Aug. 17, 1959.

13. Bulletin, "The Better Method of Feeding Dry Materials," and price list, Vibra Screw.

14. Perry, J. H., "Chemical Engineers Handbook," McGraw-Hill, New York, 1950.

15. Hancher, C. W., personal communications, August 21, 1959.

16. "Quarterly Report on Current Prices," Chemical and Engineering News, Sept. 28, 1959.

5.0 FUEL CYCLE DEVELOPMENT

P. A. Haas

A new program at ORNL was started to develop complete power reactor fuel cycles not restricted by the needs of a particular reactor program. This approach may result in more economical fuel cycles than restricted consideration of small portions of the cycles. The initial emphasis is on the U^{233}-thorium cycle because of past ORNL experience in this field and the relatively small amount of previous and present development of heterogeneous reactors using the thorium cycle.

Clad Ceramic Elements from Oxide Powders - S. D. Clinton, J. W. Snider

A program was recently initiated to study the fabrication problems which will be encountered during the recycle of uranium-233 to nuclear breeder reactors. At the present the major emphasis of the program will be directed toward the remote fabrication of mixed uranium-thorium oxides for pressurized water reactors.

An acquaintance with the present technology for fuel element fabrication was acquired from the literature on this subject and from trips to Babcock and Wilcox at Lynchburg, Virginia, and to Davison at Erwin, Tennessee. These companies operate the two major commercial facilities for producing mixed ceramic oxide fuel elements.

One of the more difficult fabrication steps is that of introducing finished oxide pellets into the metal tube or cladding. The present tolerable clearance (approximately 1 mil) between the pellet and metal clad requires grinding of the pellets to give the final dimensions. The grinding does not allow for slight imperfections in the tube diameter, and pellet binding is a frequent occurrence when filling the metal tube. The problem is further multiplied by the overall dimensions of the presently designed oxide fuel element tubes. For example, the Consolidated Edison fuel element cladding is 102-in. long, has an outside dia of 0.304-in., and has a wall thickness of 0.020-in.

Techniques for remote compacting of mixed oxide powders into tubes will be studied at ORNL in an effort to eliminate the problem of assembling pellets into a closely fitting tube or tube bundle. The initial method to be investigated for compacting the ceramic powders will be vibration. Several air driven vibrators have been ordered which cover a frequency range of 2,800 to 80,000 vibrations per minute. The maximum theoretical fuel density attainable by this technique will be greatly dependent on the oxide particle density, shape, and size distribution. Therefore, ThO_2 powders of varying properties are being obtained for the studies.

6.0 HR THORIUM BLANKET STUDIES

P. A. Haas

Methods are being developed for thoria slurry preparation as required for the aqueous homogeneous reactor program. The present emphasis is on the preparation of improved slurry materials, particularly spherical thoria particles for blanket slurries by flame denitration procedures.

Flame Calcining - C. C. Haws, Jr., K. O. Johnsson

Photomicrographs of the product material prepared in the two extended runs described last month show rounding of the particles (Figure 6.1). Particle size analysis showed that approximately 8% of the particles were larger than 10μ. The product will be size classified to remove the + 10 μ particles prior to toroid or loop testing. This concentration of large round particles may not be detrimental for reactor use; however, it is certainly preferable to have the material of comparable size to that of the standard pilot plant preparation for the first loop tests.

A series of small scale flame calcination runs has been made preparing micro-spheres of urania and a glassing agent, and thoria and a glassing agent. Essentially all previous runs have been with thoria-urania mixtures. In some of the recent runs SiO_2 was substituted for Al_2O_3 as the glassing agent. This is desirable since the thermal cross-section of SiO_2 is only half that of Al_2O_3. Also since the melting point of SiO_2 is much lower than that of Al_2O_3, a considerably smaller amount may be effective in decreasing the thoria melting point. The runs which have been made to date are listed below:

Basic Oxide	Additive
UO_2	1% Al_2O_3
UO_2	5% Al_2O_3
UO_2	1% SiO_2
UO_2	5% SiO_2
ThO_2	1% SiO_2
ThO_2-UO_x	5% SiO_2

Approximately 400 g of each of these combinations was prepared but analytical reports of the quality of the product are not available.

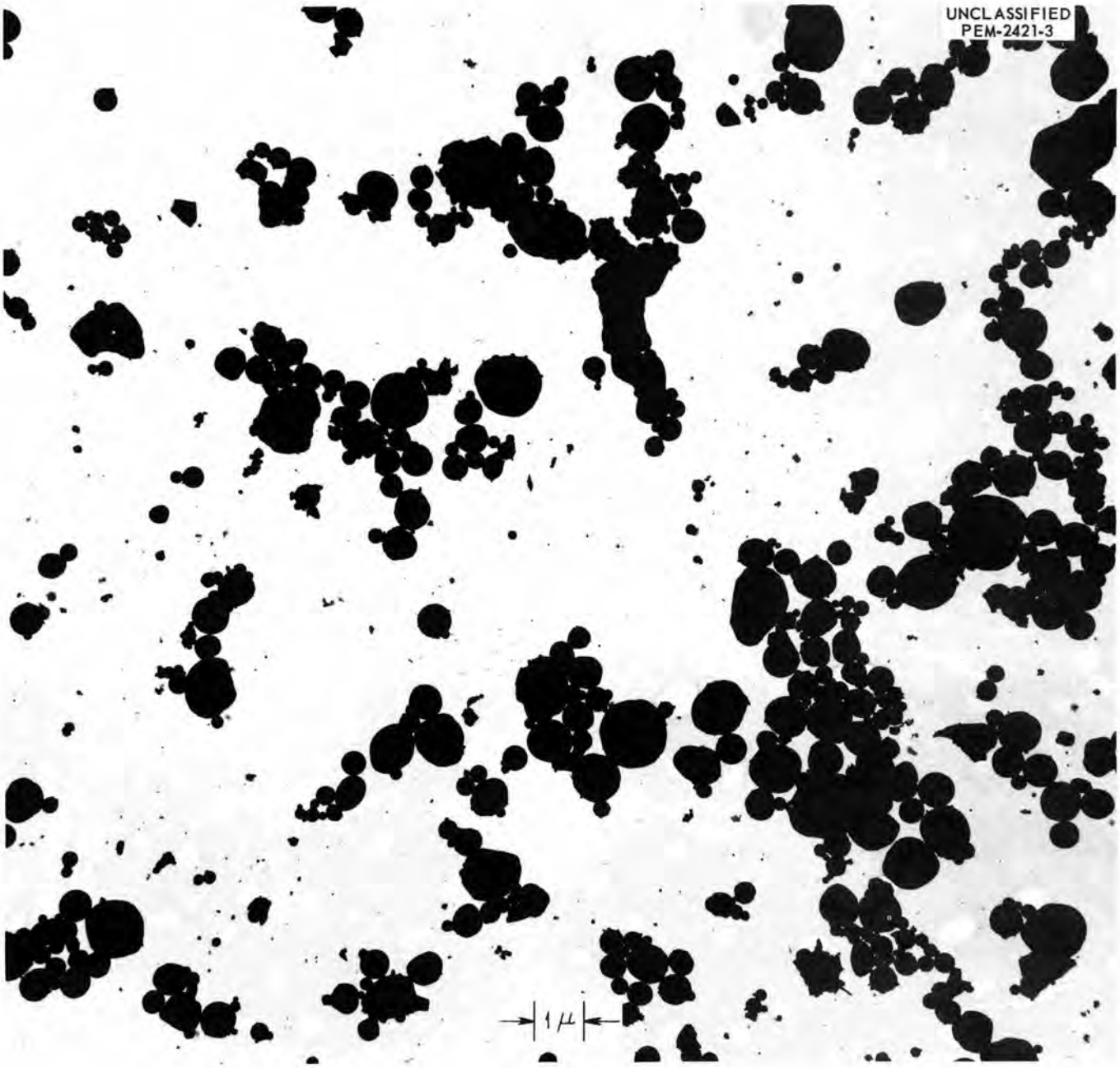

CONDITIONS

94 % ThO_2 BY WEIGHT

3.5 % UO_4 BY WEIGHT

2.5 % Al_2O_3 BY WEIGHT

TEMPERATURE OUTSIDE REFLECTOR = 1500 °C

SAMPLE NOT CLASSIFIED-SHOWN AS COLLECTED

Fig. 6.1 Flame Calcined Thorium-Uranium Oxides Containing Alumina.

7.0 ION EXCHANGE

M. E. Whatley

To make rational predictions of the operating characteristics of uranium anion exchange contactors, an understanding of the mechanism and kinetics of the exchange is necessary. Toward this objective the equilibrium sorption isotherms and rates of sorption of uranium on Dowex 21K are being determined.

Mechanism and Kinetics Studies - J. S. Watson

Further attempts were made to measure the self-diffusion coefficient of uranium in 1200μ Dowex 21K. The rate of sorption of uranium on sulfate loaded resin differs from the value predicted by the equation for simple diffusion into a sphere with a constant surface concentration. The reasons why the experimental curve should differ from the theoretical curve are (1) electrical fields are formed within the resin, (2) the uranium distribution as UO_2^{++}, UO_2SO_4, $UO_2(SO_4)_2^{=}$, and possibly $UO_2(SO_4)_3^{\equiv}$ may vary along the diffusion path, and (3) the resin diameter changes during the loading because of osmotic effects. For self-diffusion measurements, none of these effects should cause the results to deviate from the equation for simple diffusion. Data on the self-diffusion of uranium in the resin is of interest for two reasons: (1) deviations from the simple diffusion equation for a self-diffusion resin would indicate that the current experimental technique is not reducing the film resistance to a negligible value and (2) a quantitative measure of the self-diffusion coefficient is needed to check the preliminary calculation of the effect of electric fields within the resin.

The technique used to measure the self-diffusion coefficient involved equilibrating several resin beads with a U-235 solution and determining the fraction of U-235 lost as a function of time when the beads were placed in a stirred natural uranium bath with the same concentrations as the equilibration solution. The U-235 content of each bead was determined by counting it in a gamma spectrometer.

Two self-diffusion runs have been completed, and analyses of the beads from a third run have been started. The data from the first run, as reported last month, was too scattered to allow any conclusions. The solution used for the second run was 0.004 M in uranium and 0.15 M in total sulfate.

A uranium loading run was made with the same bulk solution concentrations (Figure 7.1) and gave an apparent uranium diffusion coefficient of approximately 1.3×10^{-7} sq cm/sec. This diffusivity is the same value which has been found in essentially all of the loading runs with 1200μ resin.

The second self-diffusion run gave slightly better results than the first, but the scatter was still far from satisfactory. If there was any significant film resistance, its effect was obscured by the data scatter. An evaluation of the diffusion coefficient was made for each bead. The

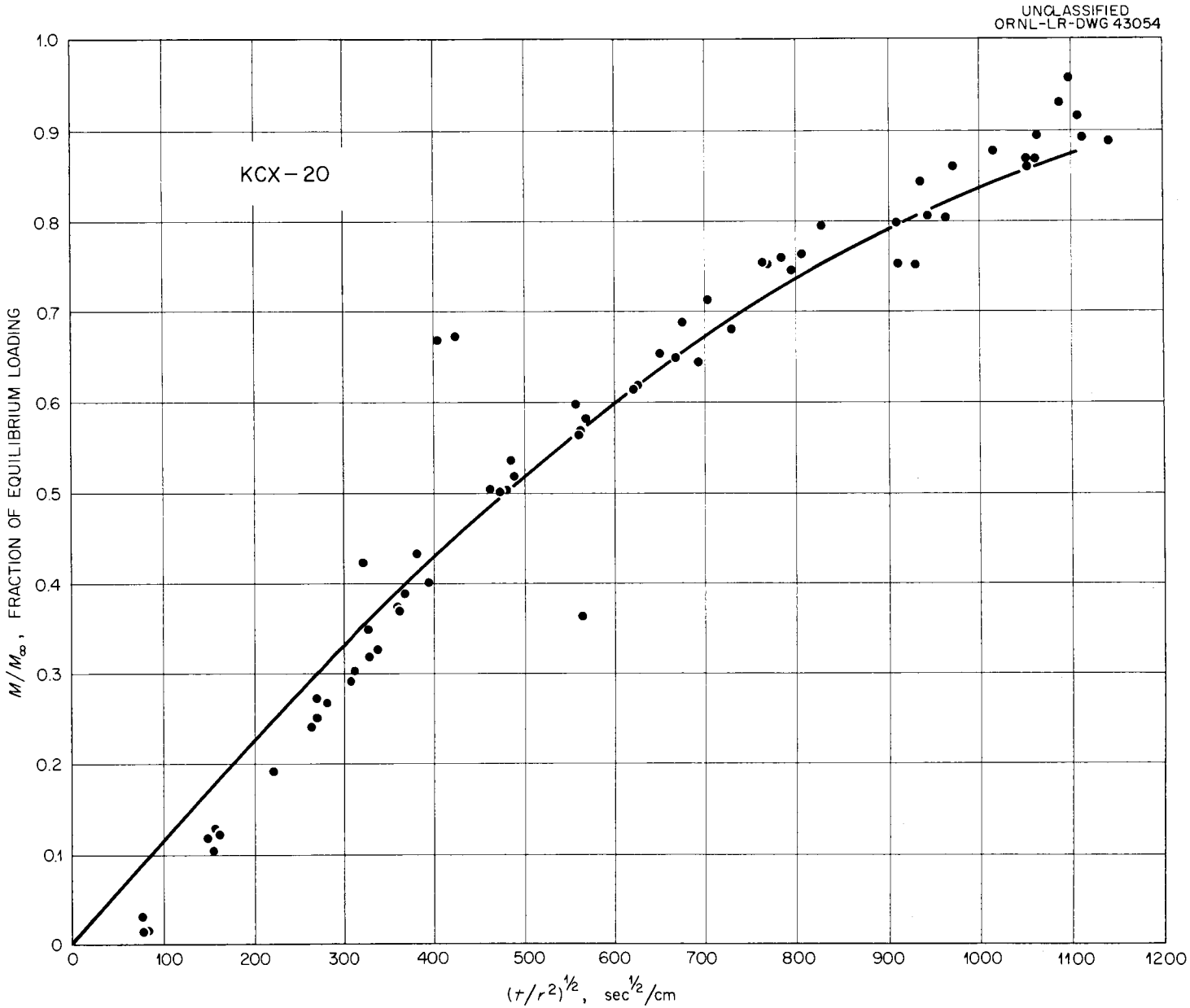

Fig. 7.1 Uranium Loading on 1200 μ Dowex 21K from a Loading Solution 0.004 M in Uranium and 0.15 M in Total Sulfate.

results from all beads were averaged to give a self-diffusion coefficient of $3.2 \pm 1.2 \times 10^{-8}$ sq cm/sec. The precision of this value will probably be improved, but it is interesting to note that this number is considerably lower than the value of 8.6×10^{-8} sq cm/sec which was predicted by the model for counter diffusion of $UO_2(SO_4)_2^{=}$ and $SO_4^{=}$ ions.

There are several reasons why the predicted and measured values of the self-diffusion coefficient may be different. It is possible that one must consider the uranium to exist as several complexes. Also even if the uranium within the resin is completely in the most complexed form, this form may be the $UO_2(SO_4)_3^{\equiv}$ rather than $UO_2(SO_4)_2^{=}$ complex. The prediction of the existance of the trisulfate complex is largely a matter of using the complex formation constants of Ahrland or Allen. Ahrland found the $UO_2(SO_4)_3^{\equiv}$ complex with a potentiometric method but failed to detect its presence spectrophotometrically. Allen found little or none of the $UO_2(SO_4)_3^{\equiv}$ specie.

8.0 POWER REACTOR FUEL PROCESSING

C. D. Watson

8.1 Darex

The purpose of the Darex process is to convert stainless steel-containing fuels into chloride-free nitrate solutions suitable for processing in existing stainless steel solvent extraction equipment. Chloride is necessary to effect dissolution of stainless steel in HNO_3 but it must be removed to avoid corrosion of process equipment.

Presently the Darex process is being applied to stainless steel clad UO_2-ThO_2 fuels such as Consolidated Edison. Two types of flowsheets are under consideration. In one, the UO_2-ThO_2 is dissolved separately in Thorex dissolvent; in the other the decladding solution, with chloride removed and fluoride added, is used to dissolve the core material. Nitric acid recovery and solvent extraction feed adjustment may be accomplished in the two separate solutions (decladding and core) or from one mixed solution. Data are being gathered for various steps in both flowsheets.

Semi-continuous Dissolution Studies - F. G. Kitts, R. C. Early

A 1-in. i.d. glass semi-continuous dissolver for UO_2-ThO_2 pellets was assembled (see Figure 8.1) and tested using Thorex dissolvent (13.3 M HNO_3, 0.07 M $Al(NO_3)_3$, 0.04 M NaF). The apparatus was then used to make two semi-continuous dissolution runs, one using Thorex solution (run Th-1), the other (run SS-1) using adjusted SS declad solution of composition 9.84 M HNO_3, 60 ppm chloride, 0.04 M NaF and 53 g SS/liter. Data from the two runs are shown in Table 8.1. Although the data for run SS-1 appear more favorable, a direct comparison of these two runs may not be made. In run Th-1 the pellets rested on the bottom of the dissolver below the heated zone while in run SS-1 the pellets were supported on a screen 2-1/4-in. above the bottom (see Figure 8.1).

At the beginning of both runs the dissolver was charged and refluxed to bring the Th concentration up to the desired level. This initial reflux period was assumed to be the time that would have been required to feed the initial charge to the dissolver at the initial feed rate. Dissolvent was then fed at set rates and the density of the product was measured at 1 hr intervals. Higher feed rates gave lower densities (indicative of lower loadings). As dissolution progressed the feed rate was lowered to maintain an arbitrarily set minimum density.

Since the dissolution rates of pellets have varied so widely and since a relatively long time is required to accomplish total dissolution, it was assumed that the density of the dissolver solution would be used to control the flow of dissolvent to the dissolver thus producing a uniformly loaded product. Future runs will be made varying the flow rate to maintain a constant density in the dissolution product. The density and loading data from run SS-1 are plotted in Figure 8.2. Although these data are exact

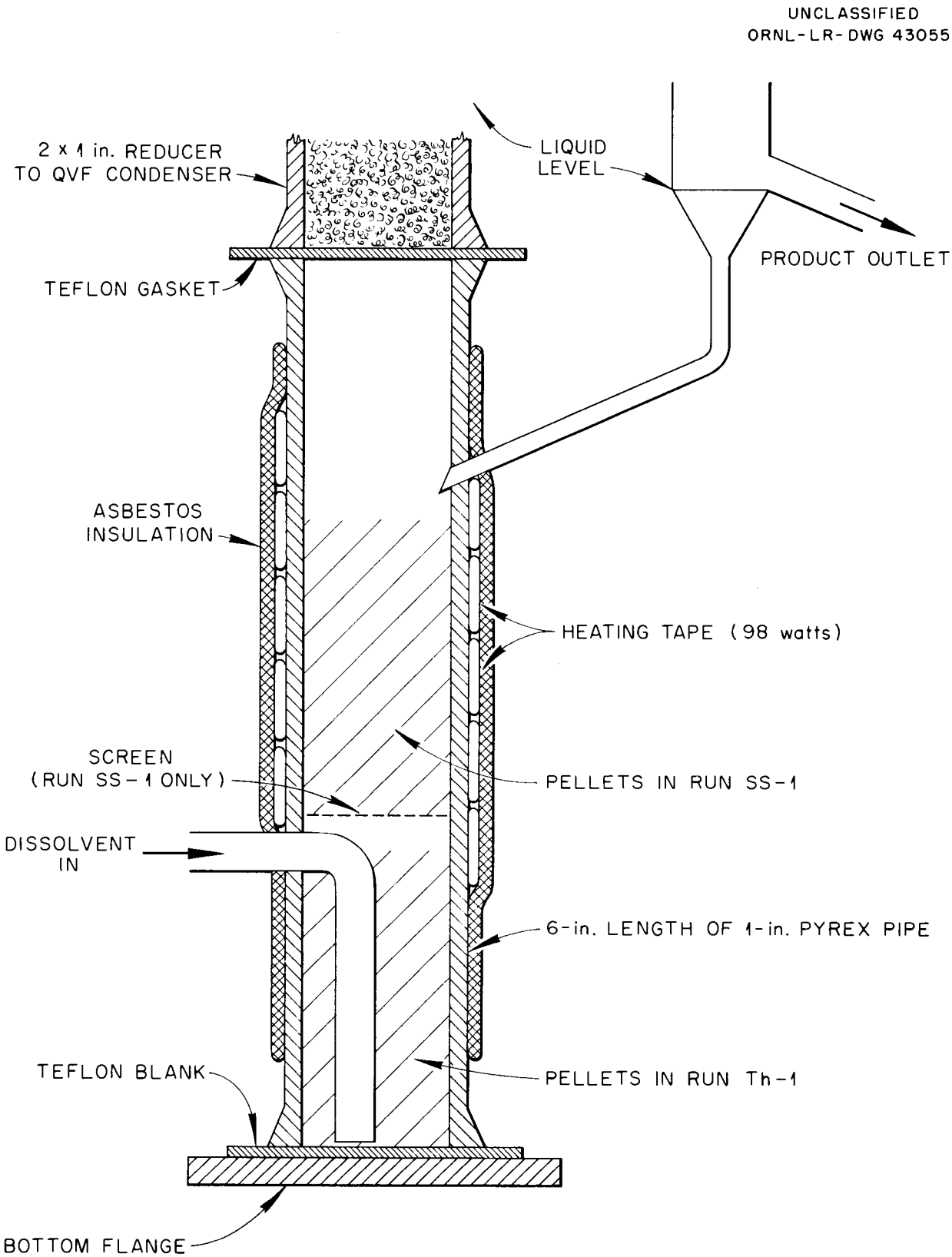

Fig. 8.1. Semi-Continuous Dissolution Apparatus.

Table 8.1. Data for Semi-Continuous Runs Th-1 and SS-1 in the 1-in. Dissolver

	Run Th-1	Run SS-1
Initial weight of pellets (g)	74	74
Initial area of pellets (sq cm)	57.3	57.3
Pellets dissolved (% by wt)	69.4	97.3
Dissolver hold-up (cc)	~90	~65
Total dissolvent + product* (cc)	592	408
Total refluxing time (hrs)	19.50	18.08
Av feed rate (cc/min)	0.507	0.376
Time dissolvent fed (hrs)	18.25	14.67
Instantaneous feed rates (cc/min)	0.684-0.261	0.505-0.208
Th dissolved (g)	43	59
Average loading (g Th/liter)	73	148
Instantaneous loadings (g Th/liter)	60-90	93-230
Av overall dissolution (mg UO_2-ThO_2/sq cm-min)		
rate (based on initial area)	0.77	1.16

* These were equal within accuracy of the measurements.

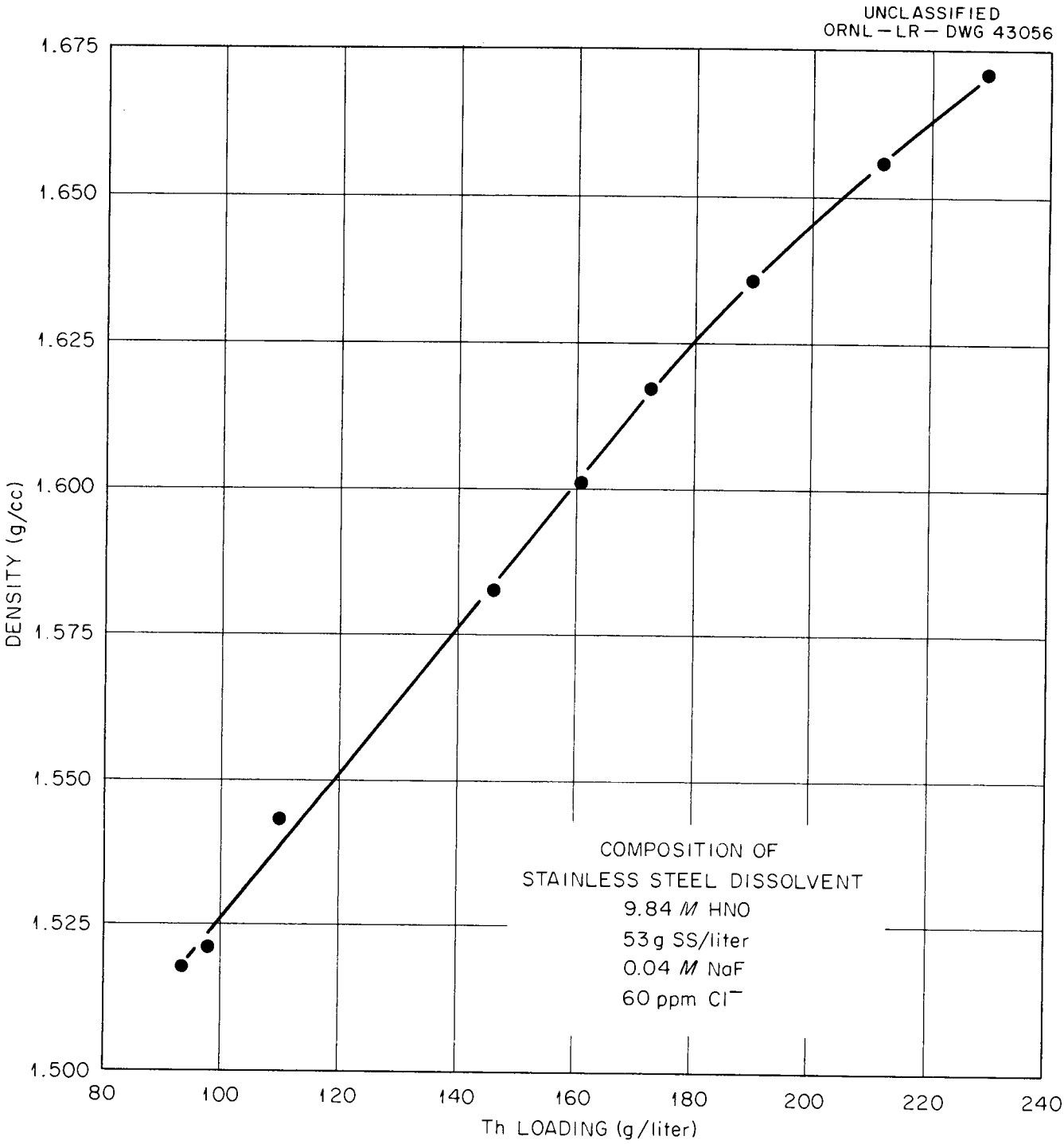

Fig. 8.2. Density as a Function of Th Loading for 95.8% ThO_2-UO_2 Pellets Dissolved in SS Dissolvent.

for only one dissolvent composition, they can be used to approximate the density corresponding to the desired loading for similar dissolvents. The densities and loadings obtained in run Th-1 were lower than the desired operating range; these results will be correlated with data for higher loadings when they are obtained.

One experiment was performed proving the feasibility of steam distilling HNO_3 from dissolver concentrate during the solvent extraction feed adjustment of mixed (SS + Th-U) dissolution product. Such data are applicable to solutions produced either by dissolving ThO_2-UO_2 in adjusted declad solution or by mixing the two solutions (clad + core) after separate dissolutions. A 1225 cc batch of solution containing 131 g Th/liter, 50 g SS/liter, 8 M HNO_3 and trace chloride and fluoride was concentrated by batch distillation to 455 cc; the 760 cc of condensate contained 10.4 M HNO_3 and was suitable for recycle. Water was then added to the 455 cc of concentrate at constant level until 350 cc of condensate (4.7 M HNO_3) had been collected. The 455 cc of concentrate remaining contained 360 g Th/liter, 137 g SS/liter and 0.15 M HNO_3. Table 8.2 shows the instantaneous compositions of both portions of the overhead. Note that the maximum temperature reached was 131°C; a batch distillation to a similar HNO_3 concentration required greater volume reduction (to 320 cc) and a maximum temperature of 143°C.

Instantaneous Thorex, ThO_2-UO_2 Dissolution Rates - J. B. Adams, T. D. Napier

Instantaneous dissolution rates of high density (ρ = 9.5) ThO_2-4% $UO_{2.3}$ pellets in fluoride-catalyzed nitric acid have been found to be highly erratic and dependent on the color produced on the surface of the pellet. In boiling 13 M HNO_3, 0.03 M fluoride, 0.1 M Al^{+++}, pellets which maintained a black surface dissolved at a rate of 0.4-0.6 mg/sq cm-min. Pellets whose surface turned partially or completely yellow in color (while remaining black beneath the surface) dissolved at rates from 1-6 mg/sq cm-min. The same phenomenon was noted in acids of different compositions.

Most of the pellets tested changed color in part. X-ray examination of samples of both black and yellow grains produced almost identical patterns, showing ThO_2 with a slightly reduced cell dimension which is indicative of a solid solution of UO_2 in ThO_2. On grinding, the black sample turned yellow, indicating that the black color was only a surface coating. The conclusion was that these pellets, although of uniformly high density, were of poor uniformity because insufficient treatment in hydrogen produced a variable grain surface coating of highly reduced uranium oxide.

The variation in dissolution rates with color was emphasized by an examination of the remains of 16 pellets used in a 4-hr semi-continuous dissolution test. Five which were still black remained essentially untouched; 3 were slightly yellowed and ~5-10% dissolved; 5 were quite yellowed and ~30-60% dissolved; and the 3 remaining pieces were completely yellow and ~80-90% dissolved.

Table 8.2. Chronological Results of Steam Distillation of Mixed Consolidated Edison Dissolution Product

1225 cc of initial solution: 8 M HNO_3, 131 g Th/liter, 50 g SS/liter

Vol HNO_3 Distilled	H^+	Temperature of the Concentrate at the end of each cut, °C
100	7.1	
100	8.4	
100	9.4	
100	10.45	
100	11.5	126.3
100	12.2	127.0
100	12.5	128.5
60	12.55	131.0
760 cc composite	10.4	

445 cc of concentrate remained.

Water was then added and the distillation was continued at constant volume.

100	8.5	129.3
100	4.4	129.0
100	2.9	~126.5
50	1.6	125.5
350 cc composite	4.7	

445 cc of final concentrate which was stable for >100 hrs at room temperature and contained: 0.15 M HNO_3, 360 g Th/liter, 137 g SS/liter. This solution can be diluted to any volume desired for solvent extraction feed and will meet the specification of 0 - 0.5 M HNO_3.

8.2 Sulfex - B. C. Finney, F. L. Rogers

Stainless steel-clad ThO_2-UO_2 and UO_2 power reactor fuel may be reprocessed by the Sulfex process. The clad metal is dissolved in boiling 4-6 M H_2SO_4; the core is dissolved in nitric acid (for UO_2) or fluoride catalyzed nitric acid (for ThO_2-UO_2 mixtures). The application of the Sulfex process to Consolidated Edison fuel is being investigated.

Six semi-continuous dissolution runs (SX-7 through 12) were made for the purpose of measuring the reaction rate (mg/sq cm-min) and dissolver product metal loading (g SS/liter) as a function of F/S (cm/min), based on initial surface area, using boiling 4 M or 6 M H_2SO_4 as the dissolvent. A summary of the run data is presented in Table 8.3. In each of these runs the fuel elements dissolved were 304L stainless steel plate assemblies consisting of 11 plates, 4.5 ft x 3-1/16-in. x 0.038-in., 1/4-in. plate spacing, 2.2 x 10^4 sq cm surface area, and weighing 7.75-8.25 kg. Two of these fuel elements were charged in each run.

Runs SX-7 and 8 were made using boiling 6 M H_2SO_4 as the dissolvent at slightly higher values of F/S (cm/min), 0.0435 and 0.0545, than in runs previously reported (Unit Operations monthly progress report, September 1959, CF 59-9-69). The corresponding reaction rates, 2.49 and 3.16 mg/sq cm-min increased as predicted. Although the times required for complete dissolution were different (2.42 hrs for Run SX-7 and 1.92 hrs for Run SX-8) the dissolver products had the same volumes (275 liters) and essentially the same metal loadings, approximately 58 g SS/liter. A loading range of 54-65 g SS/liter has been obtained in all the semi-continuous dissolution runs made using 6 M H_2SO_4 as the dissolvent (see Table 8.4).

Table 8.4. Semi-Continuous Dissolution of Stainless Steel Plate using 6 M H_2SO_4

Run No.	Time hrs	Dissolver Product Volume, liters	Dissolver Product Metal Loading g SS/liter
SX-2	3.85	238	65.0
SX-3	7.60	285	54.5
SX-4	3.50	270	58.0
SX-5	3.75	238	65.0
SX-6	2.66	174	53.7
SX-7	2.42	275	57.5
SX-8	1.92	275	58.2

Table 8.3. Summary of Semi-Continuous Sulfex Run Data

Dissolvent: Boiling 4 M or 6 M H_2SO_4 (fed continuously)

Fuel Element: 304L Stainless Steel Plate Assembly - 11 plates, 4.5 ft x 3-1/16-in. x 0.038-in. with 1/4-in. plate spacing, 2.2×10^4 sq cm surface area, 7.75 - 8.25 kg

Run No.	Time hrs	Dissolvent M	Dissolvent Flow Rate liters/min	Dissolvent Temp °C	No. of Fuel Elements	Product Volume liters	Product H_2SO_4 M	Product Metal Loading g SS/liter	Off-Gas H_2 Evolved cu ft (STP)	Off-Gas g-moles H_2 / g-mole SS	F/S cm/min	Reaction Rate mg / sq cm-min (based on complete dissolution)	Liquid Height in Dissolver ft (maximum)
SX-7	2.42	6	1.91	118	2	277	5.15	57.5	242	1.07	0.0435	2.49	~16
SX-8	1.92	6	2.40	118	2	275	5.23	58.2	260	1.14	0.0545	3.16	~19
SX-9	3.5[1]	6	0.626 for 1st hr 1.06 for 2nd hr 1.60 for 3rd hr	118	2	249	5.16	62.0	199	1.11		1.44	~16
SX-10	3.5[2]	6	1.3 for 1st hr 1.06 for 2nd hr 1.06 for 2rd hr	118	2	246	4.7	63.7	218	1.12		1.40	~16
SX-11	3.42[4]	6	(see note 3)	118	2	241	4.78	61	230	1.11		1.46	~16
SX-12	2.75[5]	4	1.42	115	2	235	2.58	75.2	284	1.13	0.0323	2.43	~18

1. Approximately 12.7 kg of fuel element dissolved in 3.0 hrs - 52 liters of dissolvent was used for heel (~3.4 kg) clean up (1/2 hr).

2. Approximately 12.9 kg of fuel element dissolved in 3.0 hrs - 40 liters of dissolvent was used for heel (~3.0 kg) clean up (1/2 hr).

3. Combination semi-continuous and batch dissolution was used. Dissolvent was fed continuously to the dissolver at an average flow rate of 2 liter/min for 15 min and then the dissolver contents were digested for 15 min. This procedure was repeated seven times.

4. Approximately 13.14 kg of fuel element dissolved in 3.25 hrs - 26 liters of dissolvent was used to batch dissolve (0.17 hrs) an additional 1.5 kg leaving a 1.2 kg heel.

5. 17.67 kg of fuel element dissolved including the 1.2 kg heel remaining from Run SX-11.

The insensitivity of the product loading to variations in feed rate is the result of a straight line relationship between reaction rate (mg/sq cm-min) and F/S (cm/min) (see Figure 8.3). The slope of the line is equal to the average loading of 58 mg/cu cm. Therefore, essentially the same dissolver product metal loading (58 g SS/liter) was obtained under conditions of complete dissolution regardless of the dissolvent flow rate (in the range investigated) when using 6 M H_2SO_4 as the dissolvent. It can be noted from Table 8.4 that there was some deviation in Runs SX-2, 5 and 6 although the difference is slight.

Runs SX-9 through 11 were made in an attempt to generate a dissolver product with a metal loading of approximately 80 g SS/liter and accomplish complete dissolution in approximately 3 hrs. A higher metal loading in the declad solution would result in a lower waste volume which has a definite economic advantage regardless of whether the waste is ultimately stored or reduced to dryness. The procedure followed in these runs was either to vary the dissolvent flow rate after a given period of time (Runs SX-7 and 8) or use a combination semi-continuous and batch dissolution (Run SX-9). None of the changes were effective, and approximately the same results were obtained as in previous runs: 245 liters of dissolver product with 60 g metal loading/liter.

Run SX-12 was made using boiling 4 M H_2SO_4 as the dissolvent: 17.67 kg of stainless steel plate (including a 1.2 kg heel from Run SX-11) was completely dissolved in 2.75 hrs. A constant flow rate of dissolvent of 1.42 liters/min resulted in a reaction rate of 2.43 mg/sq cm-min and a product loading of 75.2 g SS/liter. It can be noted from Figure 8.3 that the reaction rate for the single run with 4 M H_2SO_4 was approximately 37% higher than that for 6 M H_2SO_4 at comparable operating conditions.

A comparison of the instantaneous hydrogen evolution rate, accumulated hydrogen evolved, and product loading as a function of time for Run SX-4 and 12 are presented in Figures 8.4, 8.5 and 8.6. Although the instantaneous hydrogen evolution rate and product loading (see Figures 8.4 and 8.5) tend to be more erratic for Run SX-4 a plot of the accumulated hydrogen evolved as a function of time produces a smooth curve. This information could be incorporated in actual plant operations (decladding irradiated fuel) as an indication of the amount of the clad that had been dissolved. It can be noted in Figures 8.4 and 8.5 that there was an abrupt termination to Run SX-4 and in all probability the flow of dissolvent could have been shut off after 2.25 hrs and the metal remaining (approximately 4%) could have been batch dissolved; this procedure should have increased the product loading. Additional semi-continuous dissolution runs using 4 M H_2SO_4 will be made to determine reaction rates and product loadings.

8.3 Feed Clarification - B. A. Hannaford, G. B. Dinsmore

The purpose of the feed clarification studies is to obtain data for the design of solid-liquid separators for treatment of solvent extraction feed streams and spent dejacketing solutions.

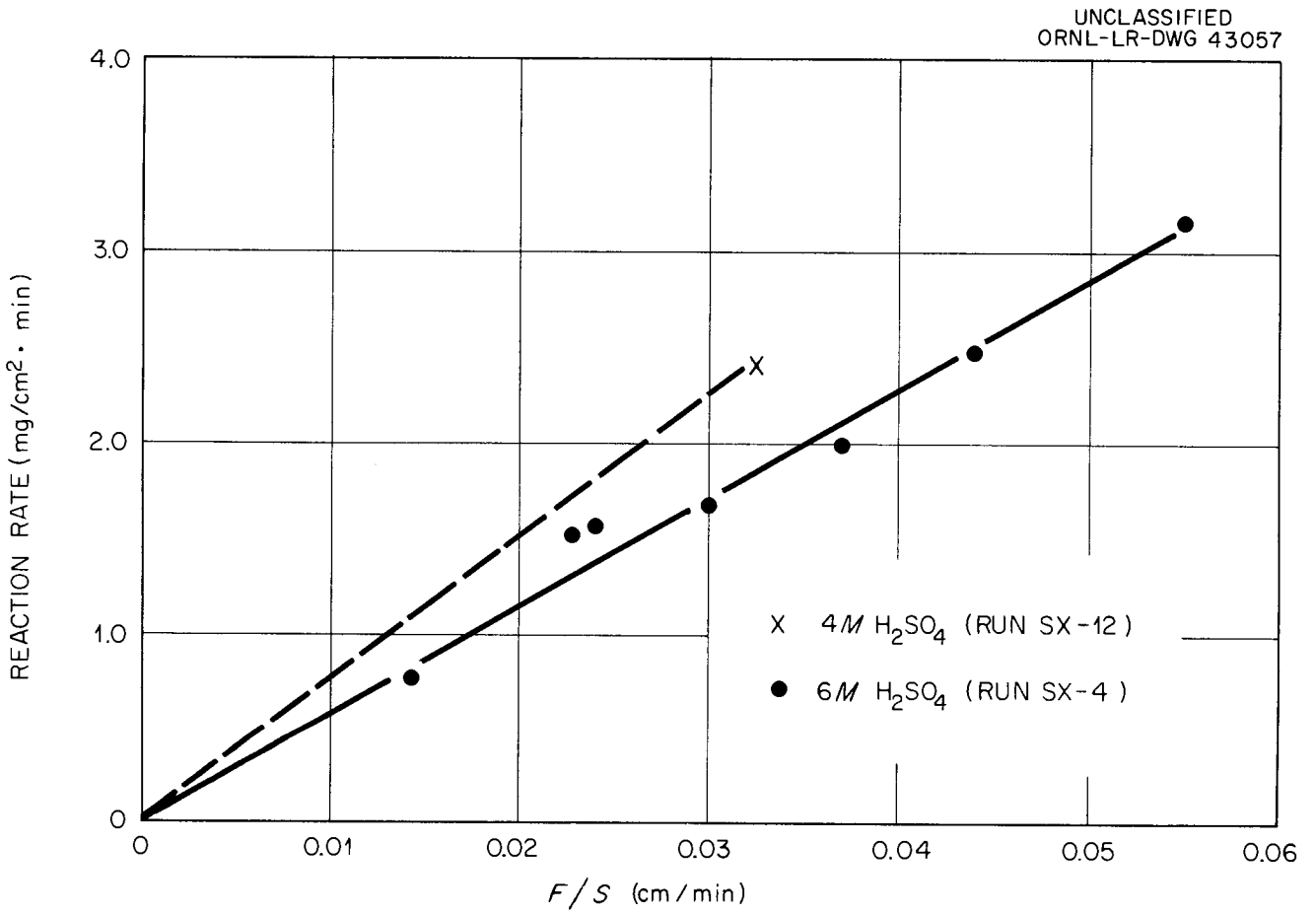

Fig. 8.3. Reaction Rate as a Function of F/S for Semi-Continious Dissolution of 304L Stainless Steel Plate Using $4M$ and $6M$ H_2SO_4 as the Dissolvent. (Based on Complete Dissolution)

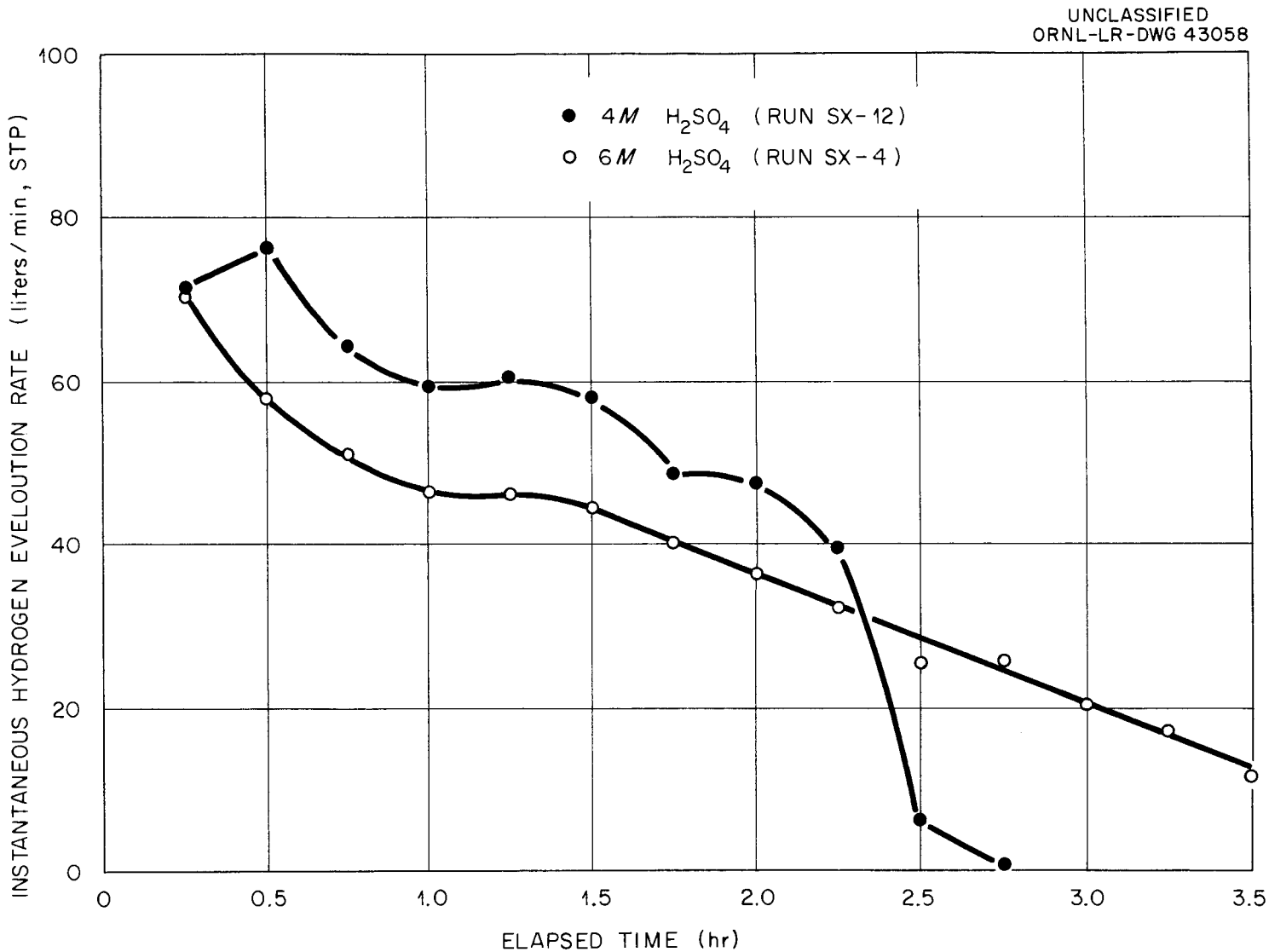

Fig. 8.4. Comparison of Instantaneous Hydrogen Evolution Rate As a Function of Elapsed Time for Semi-Continuous Dissolution of 304L Stainless Steel Plate Using 4 *M* and 6 *M* H_2SO_4 as the Dissolvent at Comparable Operating Conditions.

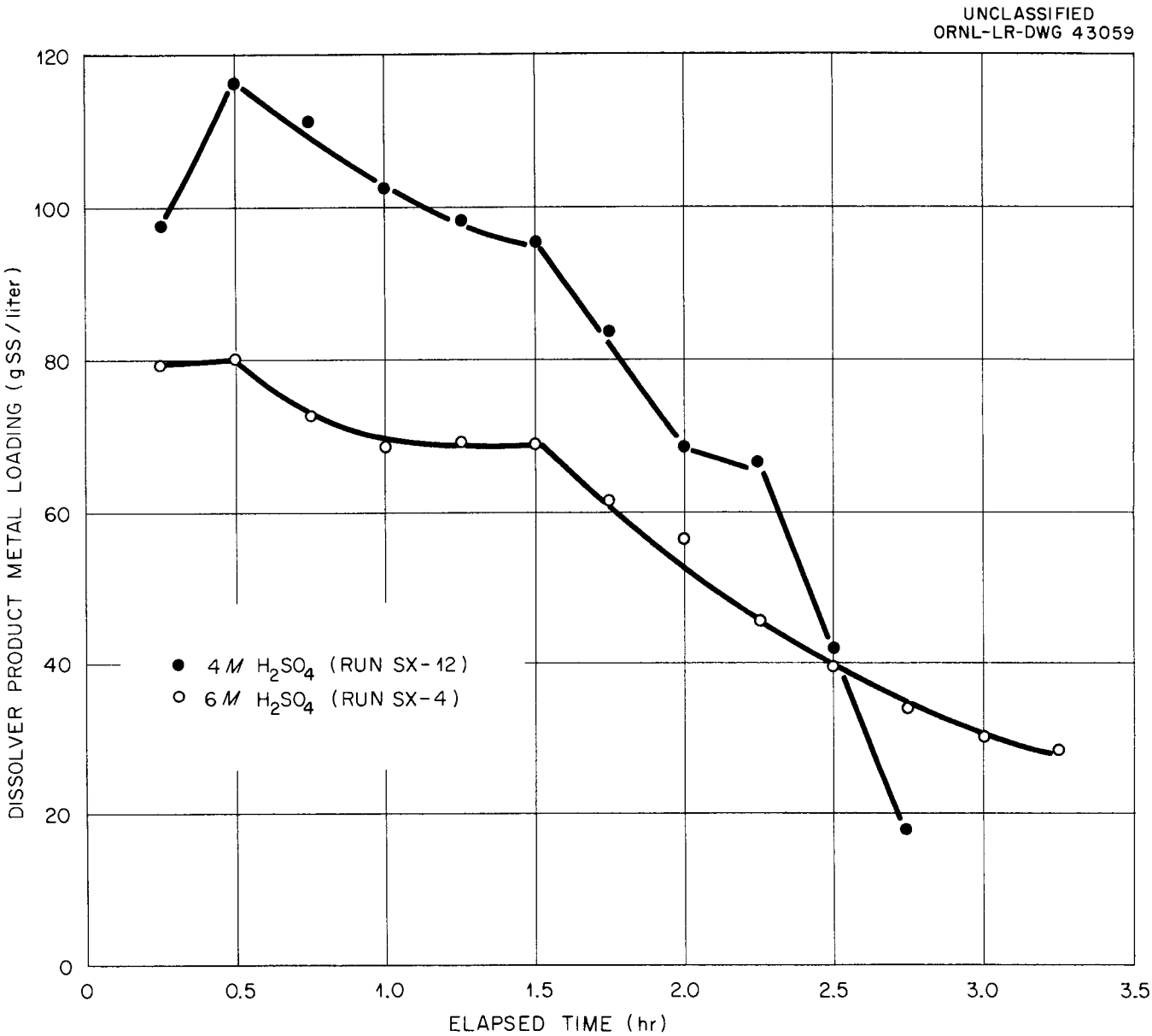

Fig. 8.5. Comparison of Dissolver Product Metal Loading As a Function of Elapsed Time for Semi-Continuous Dissolution of 304L Stainless Steel Plate Using 4 *M* and 6 *M* H_2SO_4 as the Dissolvent at Comparable Operating Conditions.

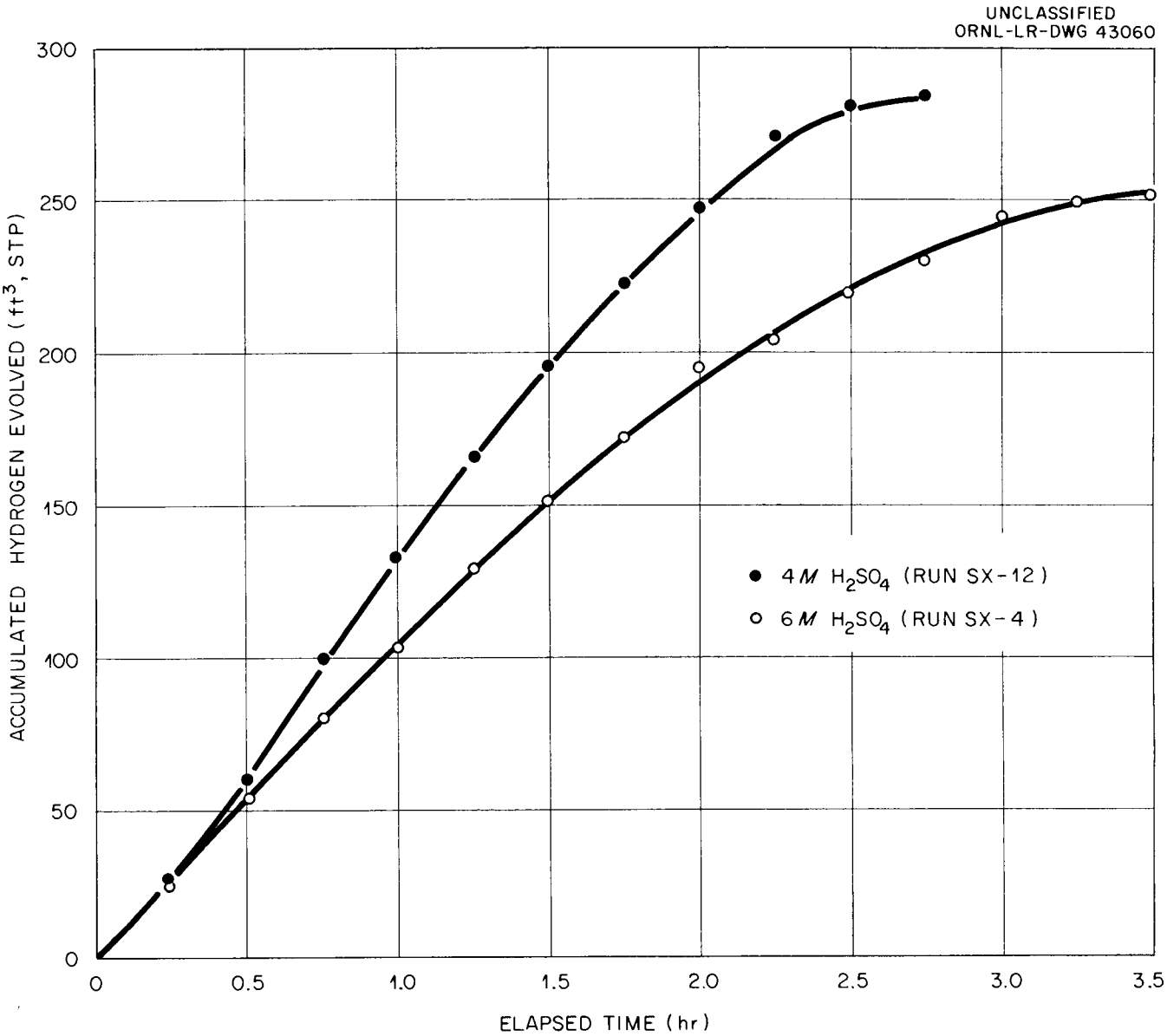

Fig. 8.6. Comparison of Accumulated Hydrogen Evolved As a Function of Elapsed Time for Semi-Continuous Dissolution of 304L Stainless Steel Plate Using 4 *M* and 6 *M* H_2SO_4 as the Dissolvent at Comparable Operating Conditions.

Centrifugation-Cake Washing. Cake washing experiments made with siliceous solids from Darex (APPR) solvent extraction feed solutions showed the uranium losses to be those predicted by simple dilution-decantation calculations, as determined by uranium analysis of centrifuge contents after n washes.

Table 8.5 summarizes data from six runs. Results of these tests, plotted in Figure 8.7, indicate that the weight of uranium remaining in the centrifuge after skimming wash n can be estimated satisfactorily by the relationship $(Y_n/Y_o) = (1-F)^{n+1}$. Three runs made in the 12-in. centrifuge gave values of (Y_n/Y_o) which were in excellent agreement with the curve predicted for F = 0.5. The somewhat scattered results obtained with the 5-in. centrifuge reflects the lower precision in reproducing volume measurements compared to work on the larger scale.

Centrifugation-Cake Dislodgment. Siliceous cake from Darex (APPR) solvent extraction feed solution, deposited on the wall of the 12-in. centrifuge at 800 gees in 1/4-3/8-in. thickness, was easily dislodged and mixed with the 0.01 M HNO_3 wash by mechanically braking the centrifuge from 2180 rpm to rest in 3-5 seconds. For the wash runs this "jogging" was repeated for a total of four times following addition of wash from a laboratory graduate. Cake was also effectively removed and slurried by addition of wash from a fan-type spray nozzle at 100 psi, with the bowl rotating at ~200 rpm, but excessive splashing of liquid from the bowl resulted. For gelatinous cake typical of Darex solvent extraction feed, wash addition by high (100 psi) pressure spray nozzles may be unnecessary.

Figure 8.8 illustrates the equipment arrangement employed in washing tests conducted in the 5-in. dia centrifuge. Figure 8.9 is a schematic of the 12-in. centrifuge installation. Feed is metered by manual control from a pump-agitated glass feed tank. Two spray headers permit flexibility in wash addition techniques.

8.4 Mechanical Processing

The purpose of the Mechanical Processing studies is to determine the feasibility of mechanical treatment of power reactor fuels for reduction in the fuel size or quantity of inert material treated by solvent extraction. The present program may be divided into two parts - the study of the decladding of a metallic core, liquid metal bonded fuel (SRE) and the determination of design criteria for a shear-and-leach facility for processing ceramic core fuels such as the Yankee or Consolidated Edison reactors.

SRE Decladding - G. A. West

Assembly of equipment for mechanically decladding SRE fuels (Figure 8.10) was completed and its operation was demonstrated by successfully decladding prototype fuels (Figure 8.11) under mineral oil. The proposed equipment layout for installation in the high level segmenting cell, Bldg. 3026, is shown in Figures 8.12 and 8.13. A new hydraulic operated wire cutter (Figure 8.14) was designed and fabricated to be positioned by Model 8 manipulators for the cutting of the 90 mil spacer wire into short lengths for scrap disposal.

Table 8.5. Summary of Data for Washing Darex (APPR) Cake

F = 0.5

Run No.	Centrifuge Diameter inches	Darex Feed Solution (+ .01% gelatin) (Run No. APPR)	Feed Batch Size liters	Centrifugal Cake Volume (approx.)(3) mls	Cake Volume + Unskimmed Supernate Volume mls	Wash(4) Volume Addition = Skim Volume mls	Number of Washes, n	Uranium Retained in Centrifuge after Skimming wash "n", mg	$\frac{Y_n}{Y_o}$(5)
103	5(1)	63-65-67	1.5	75	~150	~150	2	47.0	.022
105	5	63-65-67	1.5	75	~150	~150	4	1.9	.00074
102	5	63-65-67	1.5	75	~150	~150	6	1.1	.00046
107	12(2)	Composite	15.0	750	1200	1200	3	935.0	.0626
108	12	Composite	15.0	750	1200	1200	4	445.0	.0290
109	12	Composite	15.0	750	1200	1200	6	120.0	.00765

1. International chemical centrifuge with a solid bowl, 5-in. o.d. x 3-5/8-in. i.d. at the overflow lip x 2.7-in. deep. Maximum effective bowl volume at full speed is 315 cc. Variable speed to approximately 4000 rpm.
2. Tolhurst Laboratory centrifuge with a solid bowl separated into three compartments by two horizontal ported baffles. Bowl 12-in. o.d. x 8-1/4-in. i.d. at the overflow lip x 4-7/8-in. deep. "Dynamic" bowl volume: 4400 cc. Stepped speeds: 1500/1800/2100 rpm.
3. Obtained from centrifuged feed samples. Volume of the centrifuged cake decreases approximately 40-50% over several washes.
4. 0.01 M HNO_3.
5. $\left(\frac{\text{Weight of uranium in centrifuge after skimming wash n}}{\text{Weight of uranium in centrifuge at end of the feed cycle}}\right)$

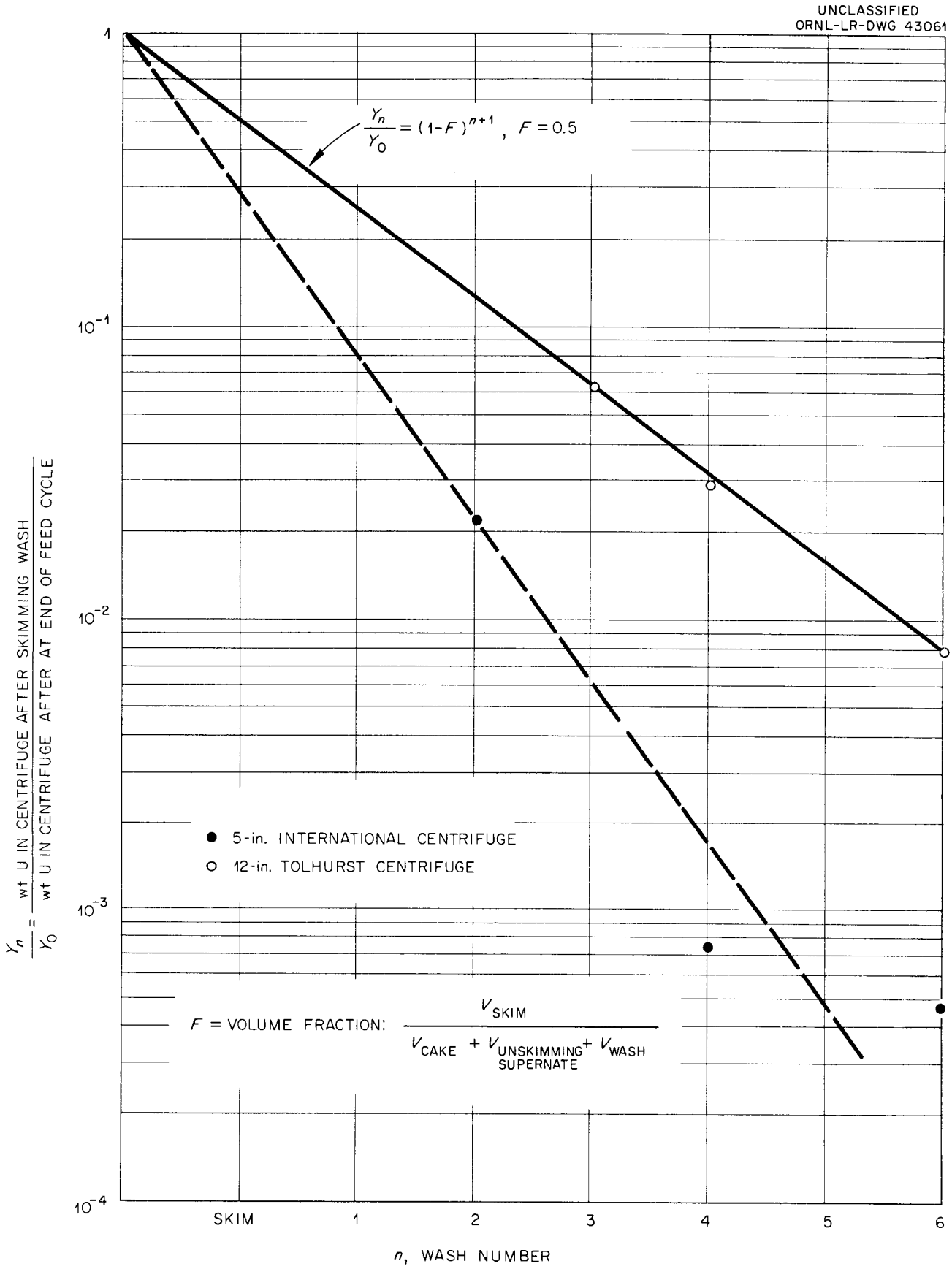

Fig. 8.7. Fraction of Uranium Retained in Centrifuge vs Number of Batch Washes.

UNCLASSIFIED
ORNL-LR-DWG 43062

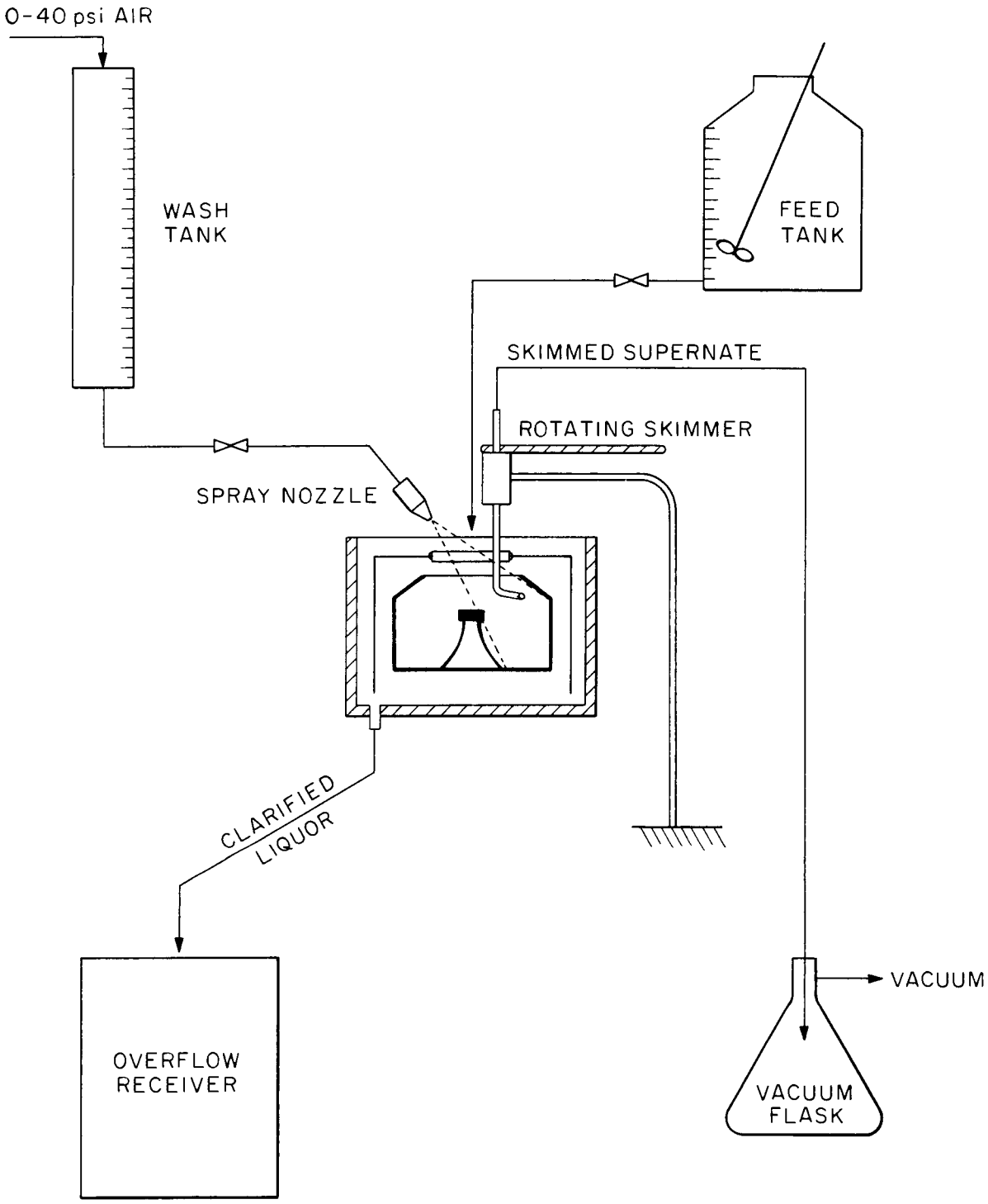

Fig. 8.8 Schematic of 5-in. Dia Centrifuge and Auxiliaries.

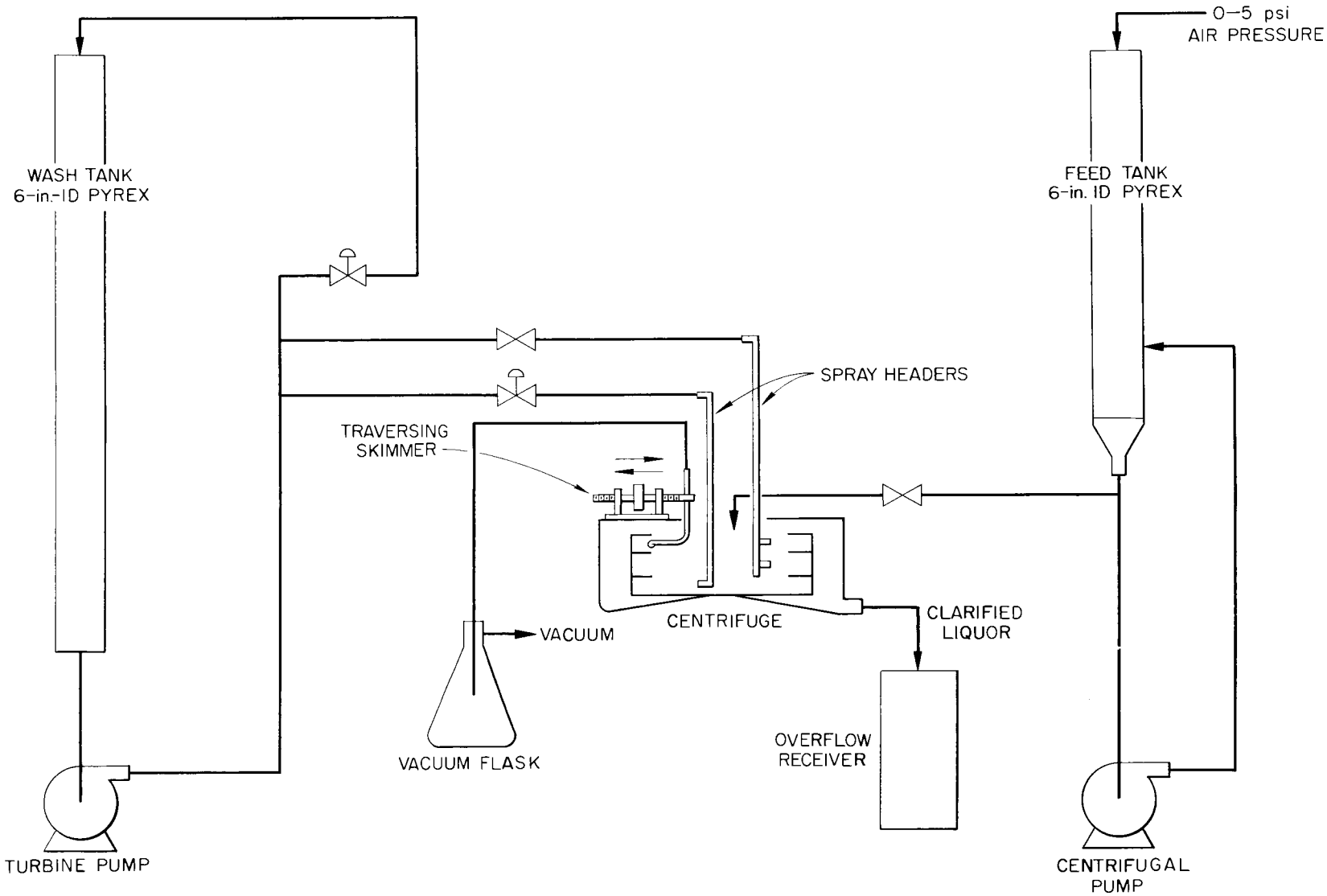

Fig. 8.9. Schematic of 12-in.-Dia Centrifuge and Auxiliaries.

UNCLASSIFIED
PHOTO 48234

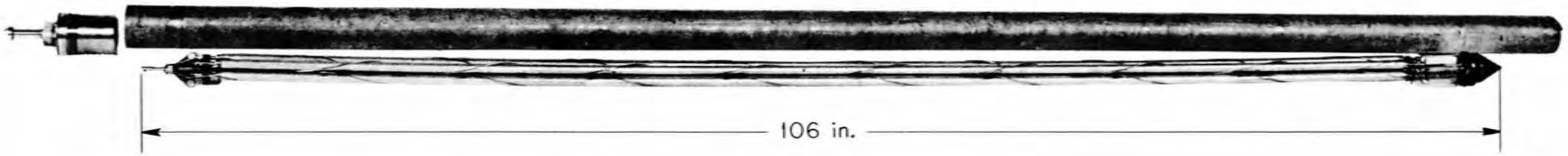

Fig. 8.10 SRE Fuel Assembly and Shipping Tube.

UNCLASSIFIED
PHOTO 48235

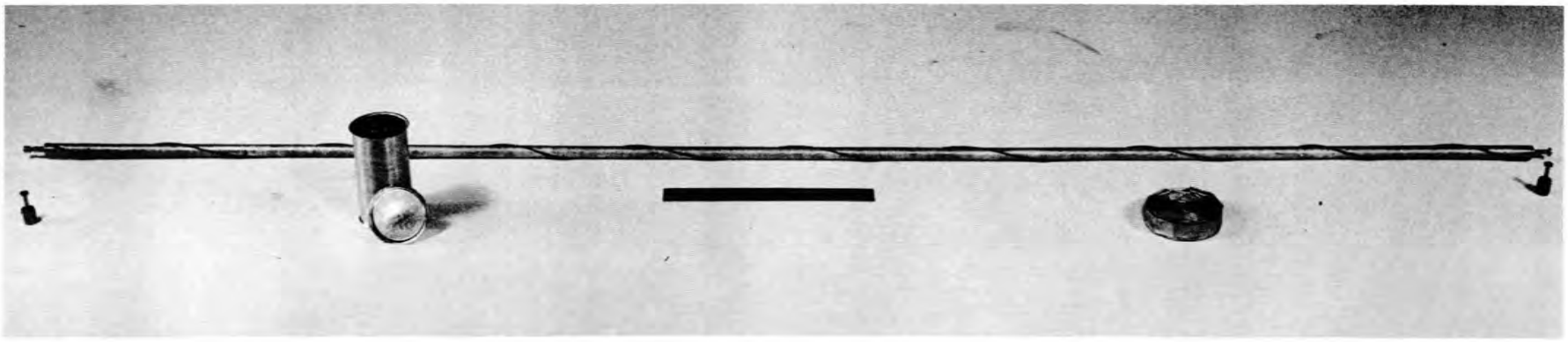

Fig. 8.11 SRE Prototype Fuel Rod Before and After Decladding.

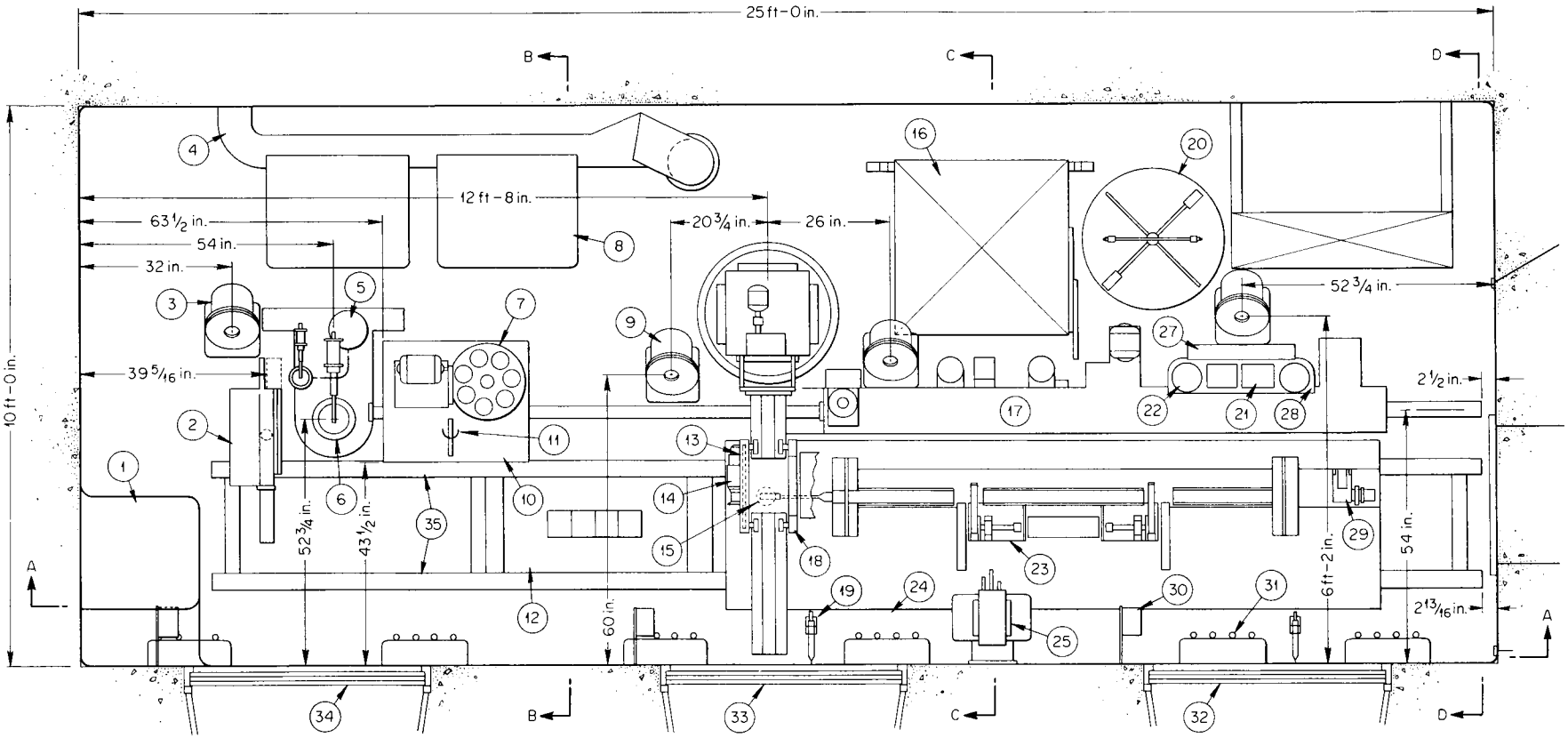

1. TRANSFER TANK
2. AUX. DECLADDER EQUIPMENT
3. SLUG WASHER STRAINER
4. OFF GAS DUCT
5. SLUG WASHER CONDENSER
6. SLUG WASHER
7. CAN STORAGE CRATE
8. FILTER
9. FINGER WASHER
10. RECANNING MACHINE
11. CAN LOADING BRACKET
12. T.V. CAMERA STORAGE CASK
13. SAW BLADE
14. WINCH
15. SRE ELEMENT GRAPPLING HOOK
16. TUNNEL HATCH COVER
17. MECHANICAL DECLADDING EQUIPMENT
18. MULTI PURPOSE SAW
19. WIRE CUTTER
20. SCRAP CONTAINER
21. SLUG BASKET
22. SLUG WASHER BASKET
23. SURGE RACK
24. TRAVERSING TABLE
25. T.V. CAMERA
26. NaK OIL DISPOSAL SYSTEM
27. TOOL RACK
28. DRAINBOARD
29. FUEL STORAGE CAP RECEIVER
30. ELECTRIC RECEPTACLE
31. SERVICE PIPING
32. WINDOW N-1
33. WINDOW N-2
34. WINDOW N-3
35. TRAVERSING TABLE TRACKS

Fig. 8.12. SRE Fuel Reprocessing Equipment Layout.

UNCLASSIFIED
ORNL-LR-DWG 41872A

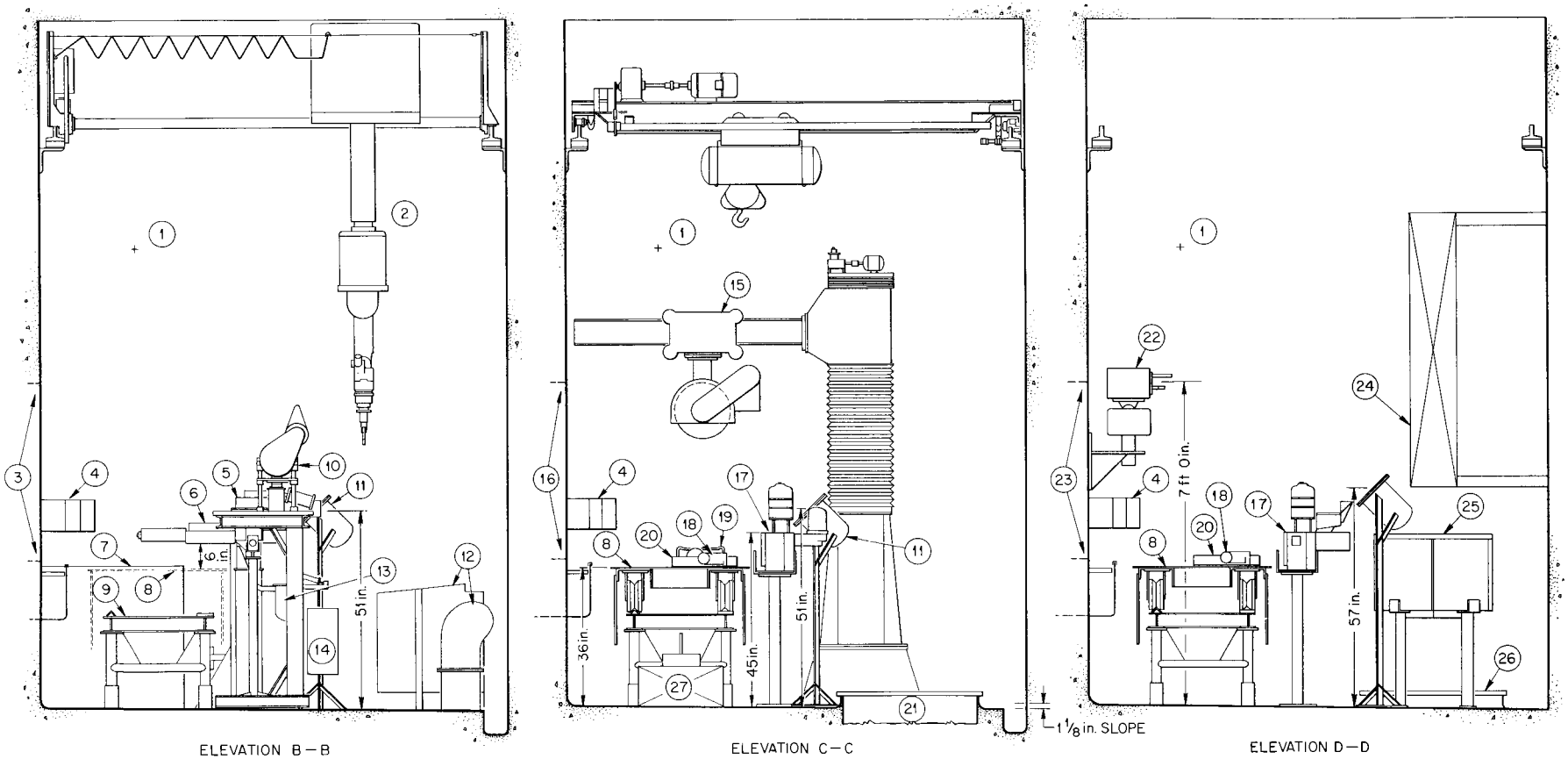

1 MODEL 8 PIVOT POINT
2 G.M. MANIPULATOR
3 VIEWING WINDOW NO. 3
4 ELECTRIC RECEPTACLE
5 SLUG WASHER
6 AUXILIARY DECLADDER
7 TRANSFER TANK
8 TRAVERSING TABLE
9 TRAVERSING TABLE RACK
10 RECANNING MACHINE AND TABLE
11 FINGER WASHER
12 EXISTING DUCT AND FILTER
13 SLUG WASHER STRAINER
14 CONDENSER
15 MULTI PURPOSE SAW
16 VIEWING WINDOW NO. 2
17 MECHANICAL DECLADDER
18 FUEL STORAGE CAP RECEIVER
19 SURGE RACK
20 SAW BOX
21 TRANSFER TUNNEL
22 TV CAMERA
23 VIEWING WINDOW NO. 1
24 NaK OIL DISPOSAL SYSTEM
25 SCRAP CONTAINER
26 TRANSFER TUNNEL HATCH
27 TV CAMERA STORAGE CASK

Fig. 8.13. Proposed Installation of SRE Fuel Element Reprocessing Equipment, Bldg. 3026, Right Side Elevations—Cell "A".

UNCLASSIFIED
PHOTO 48236

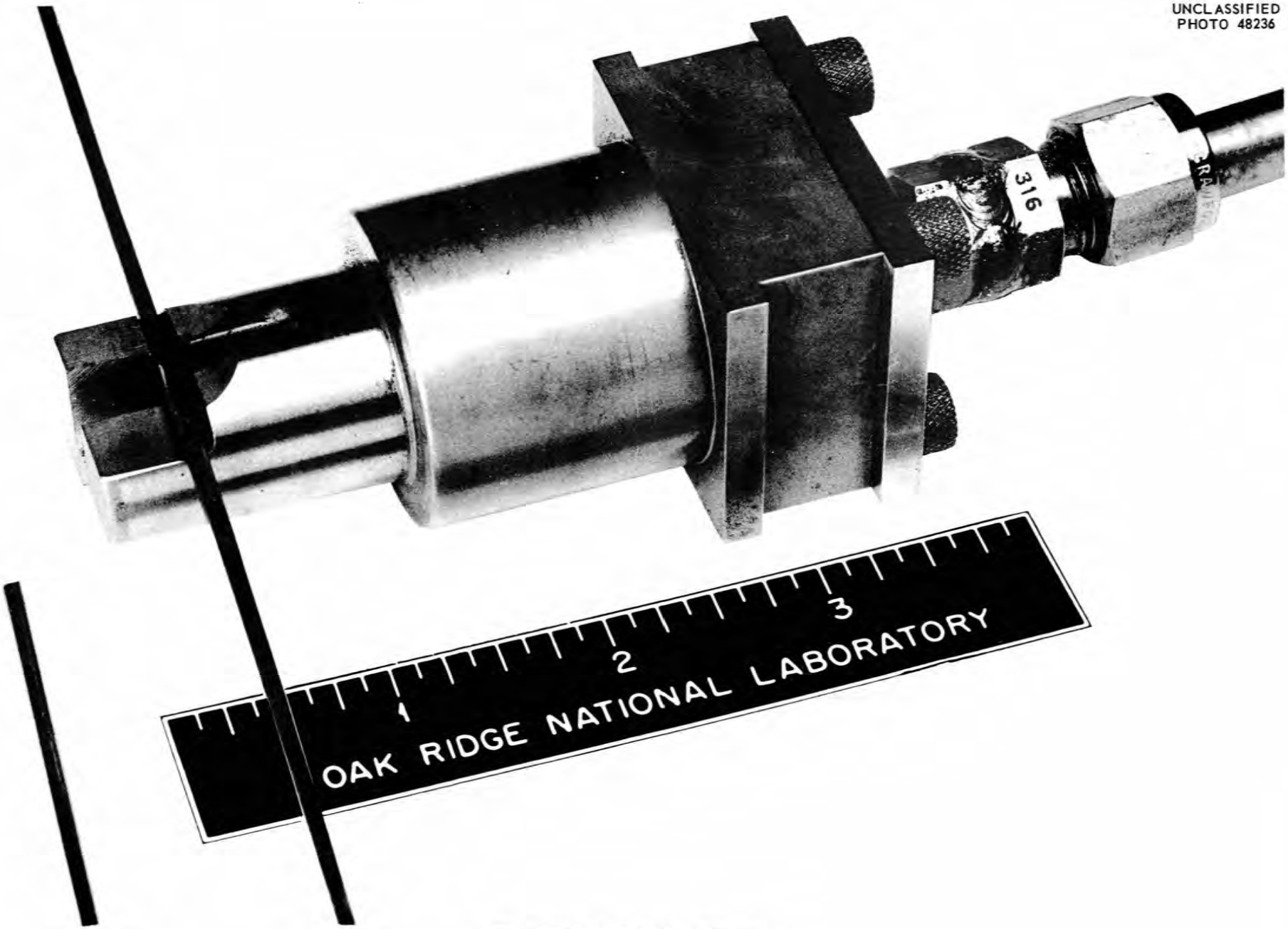

Fig. 8.14 SRE Wire Cutter.

The operational tests indicated that ~1200 psig hydraulic pressure is required to expand the 10 mil wall, 0.790-in. o.d., stainless steel tubing sufficiently to free slugs which had been cambered 1/16-in. to simulate deformed slugs. Fatigue tests on the tubing cutters used to free the end caps showed that the thin roller blade would not be satisfactory for prolonged service. A new cutting wheel was designed which changed the cutting edge from a 15 to 45° angle. Additional fatigue tests are to be made on the new cutter and the collet mechanism.

A schematic drawing of the auxiliary decladder as described in the September 1959 Unit Operations monthly report is presented in Figure 8.15.

SRE Slug Washer. A container fabricated to withstand the reaction of residual NaK and to remove mineral oil with steam (Figure 8.16) was used to demonstrate steam requirements for rotating the inner basket and time required for cleaning the slugs. The test results show that 50 psig steam pressure is the optimum pressure to start the slug basket rotating. After the rotation is started the operating steam pressure can be reduced to a minimum of 35 psig. Continuing basket rotation can not be assured at steam pressures below 35 psig. A 3.27 sq ft tube type heat exchange was adequate for condensing the steam at all operating pressures tested. The amount of condensate formed, condensate temperature and the rpm of the slug basket at various operating steam pressure is shown in Table 8.6.

Table 8.6. SRE Slug Washer Performance - The Effect of Steam Pressure on Steam Consumption and Basket Rotation

Operating Steam Pressure (psig)	Condensate Rate (gal/hr)	Condensate Temp (°C)	Slug Basket Rotation (rpm)
25	17.6	35.5	0
28	19.0	37	0 to 1000
30	20.9	37.5	0 to 1400
32	21.3	37.5	0 to 1600
34	21.6	38	0 to 1670
36	22.1	38.4	1750
38	22.9	39.5	1875
40	24.6	43.2	2450
45	26.2	45	2620

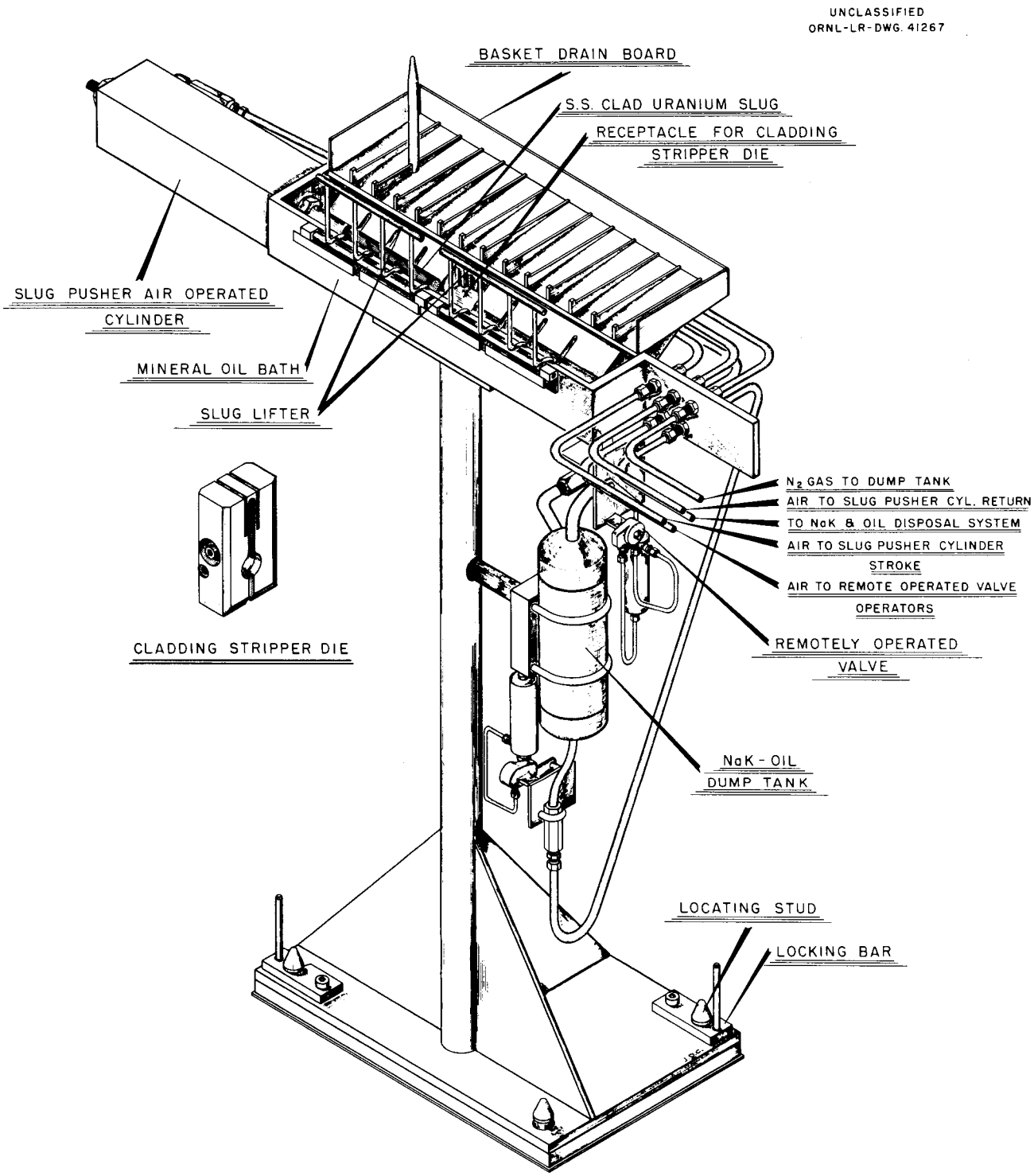

Fig. 8.15 Auxiliary Decladder-Slug.

UNCLASSIFIED
ORNL-LR-DWG 40836

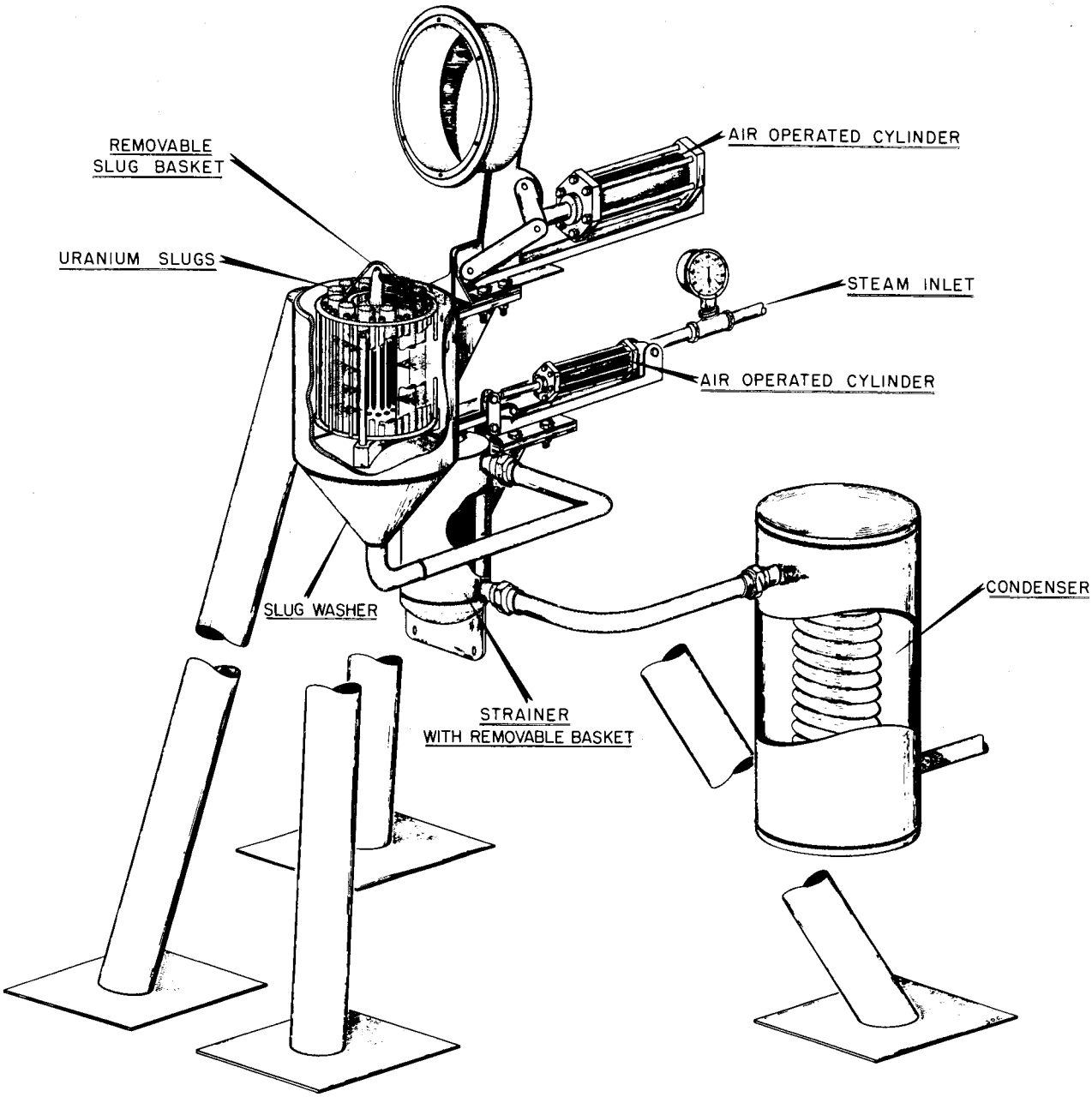

Fig. 8.16 SRE Slug Washer Installation.

SRE Canner. The twelve dejacketed and cleaned SRE slugs from each fuel rod will be recanned in aluminum containers for handling and storing prior to dissolution. A model AMS No. 131-BM Double Seamer, a home canning type machine, by the Max Ams Machine Company was assembled for remote operation. Operational tests show that the machine (Figures 8.17 and 8.18) will probably operate satisfactorily in the hot cell. The stepwise operation consists of: (1) pushing the can of 12 slugs onto the base plate using Model 8 manipulators, (2) raising the air operated base until the can lid engages with the chuck plate, (3) activating the chuck plate to rotate the can and pull a lever for automatic sealing of the can. A special lifting tong was fabricated for removing the cans and placing them in a portable storage rack. An average time of 1 min was required for loading the 12 slugs in the can, sealing and storing.

Abrasive Sawing - G. A. West

The segmenting facility in Bldg. 3026 will contain a pedestal-type multi-purpose hydraulically operated saw for use in freeing individual SRE fuel rods and to remove the inert hardware from other power reactor fuels which are to be mechanically processed. Fabrication of the saw assembly (Figure 8.19) was completed by the Ty-Sa-Man Machine Co., Knoxville, Tennessee. Hydraulic units operate the (1) saw spindle, (2) traversing head, (3) vertical movement and (4) pedestal rotation. Acceptance tests by operating the unit are to be performed at the fabricator's shop before the scheduled delivery date in October, 1959.

Shearing - G. K. Ellis

Three stainless steel-clad UO_2-filled Mark I prototype bundles will be sheared in the 125 ton Manco shear to provide 14-24 kg UO_2 batches of feed for the intermediate size glass leacher. A housing around the shear has been completed to contain the UO_2 fines produced in this operation.

Leaching - G. K. Ellis

A leaching run was made in the Cell 4A glass intermediate size leacher (Figure 8.20) leaching 4.5 kg of UO_2 sheared at 1-in. lengths from 0.4-in. dia stainless steel-clad UO_2. One fine spray fog nozzle installed in the top of the down draft condenser immediately after the leacher did not give efficient nitrogen oxides removal during the run. There appeared to be excellent liquid circulation by natural convection in this leacher simulating the full size unit (100 kg UO_2) already fabricated. The sampling system performed satisfactorily, taking five samples simultaneously from various positions in the leacher. Quantitative information on leacher performance will be reported after analytical results are available.

A valve may be required between the shear and leacher to isolate the shear from the leaching operation. Two full opening valves, a Gemco and a Red Cap, were tested for this application by dumping batches of sheared 1-in. lengths of a Mark I through each valve from a full 2-ft tall section of 4-in. dia Sch 40 pipe on top of this valve. The Red Cap air operated

UNCLASSIFIED
ORNL-LR-DWG NO. 41069

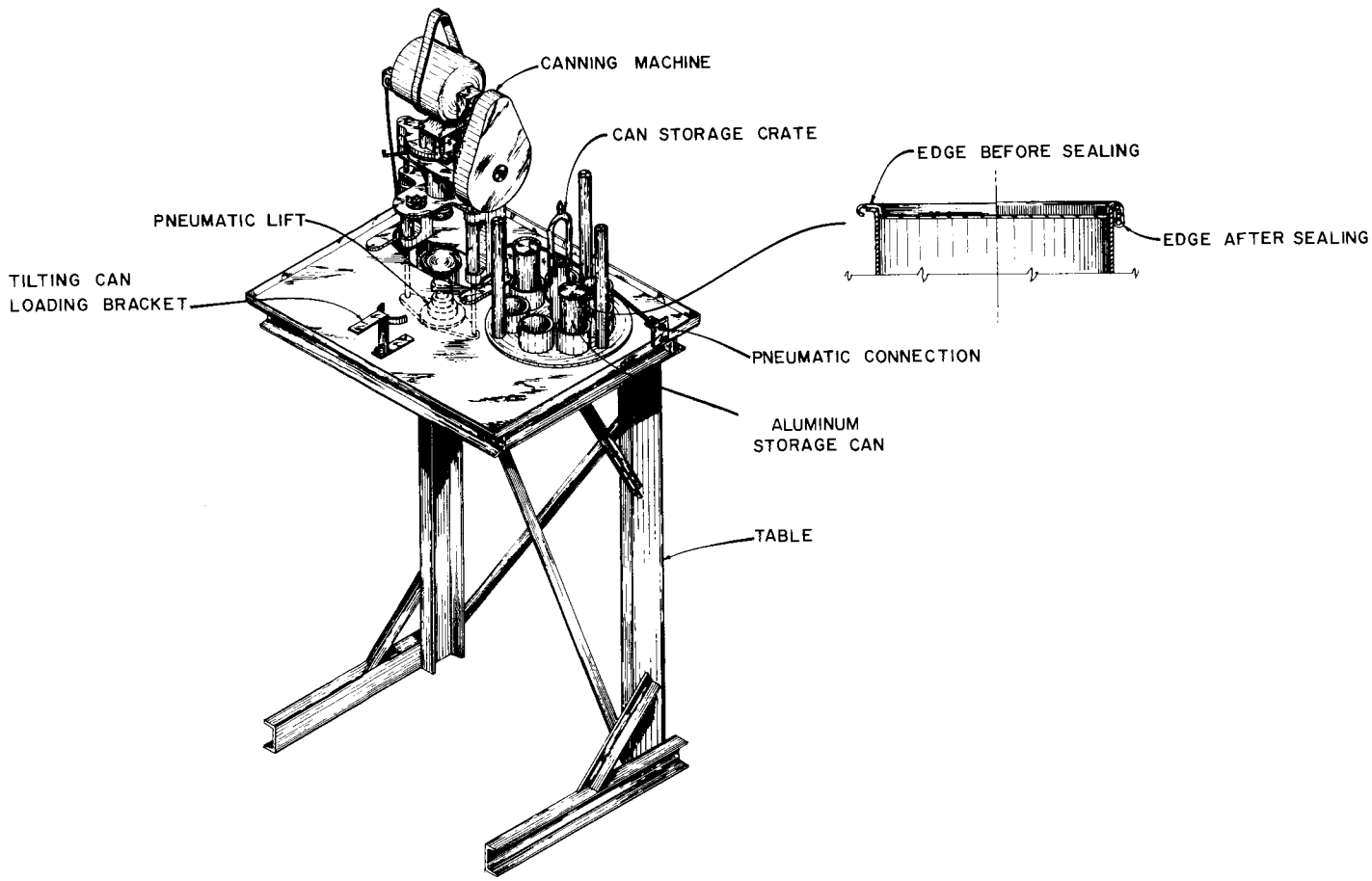

Fig. 8.17 Canning Operation.

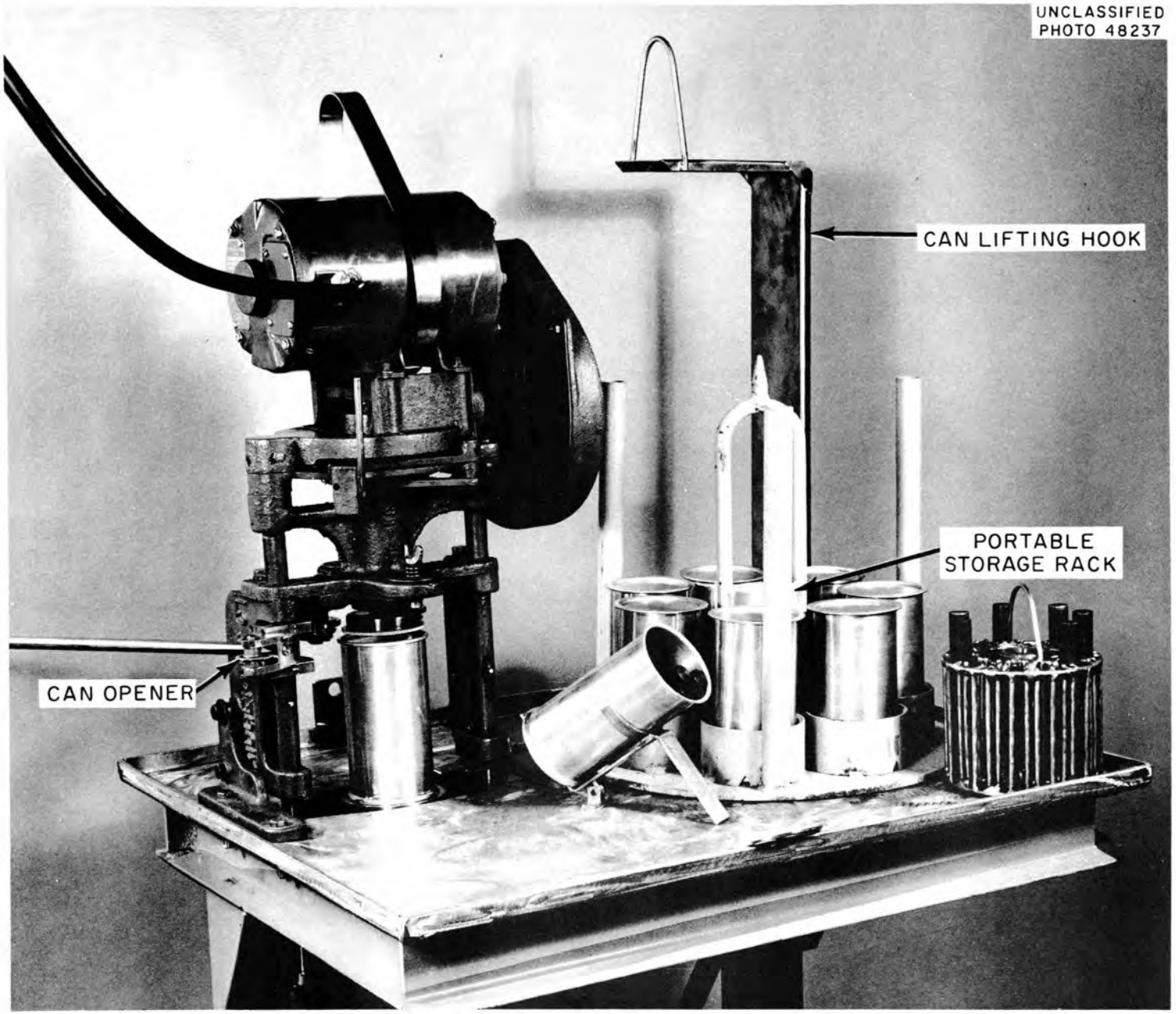

Fig. 8.18 Slug Canning.

UNCLASSIFIED
ORNL-LR-DWG 40798

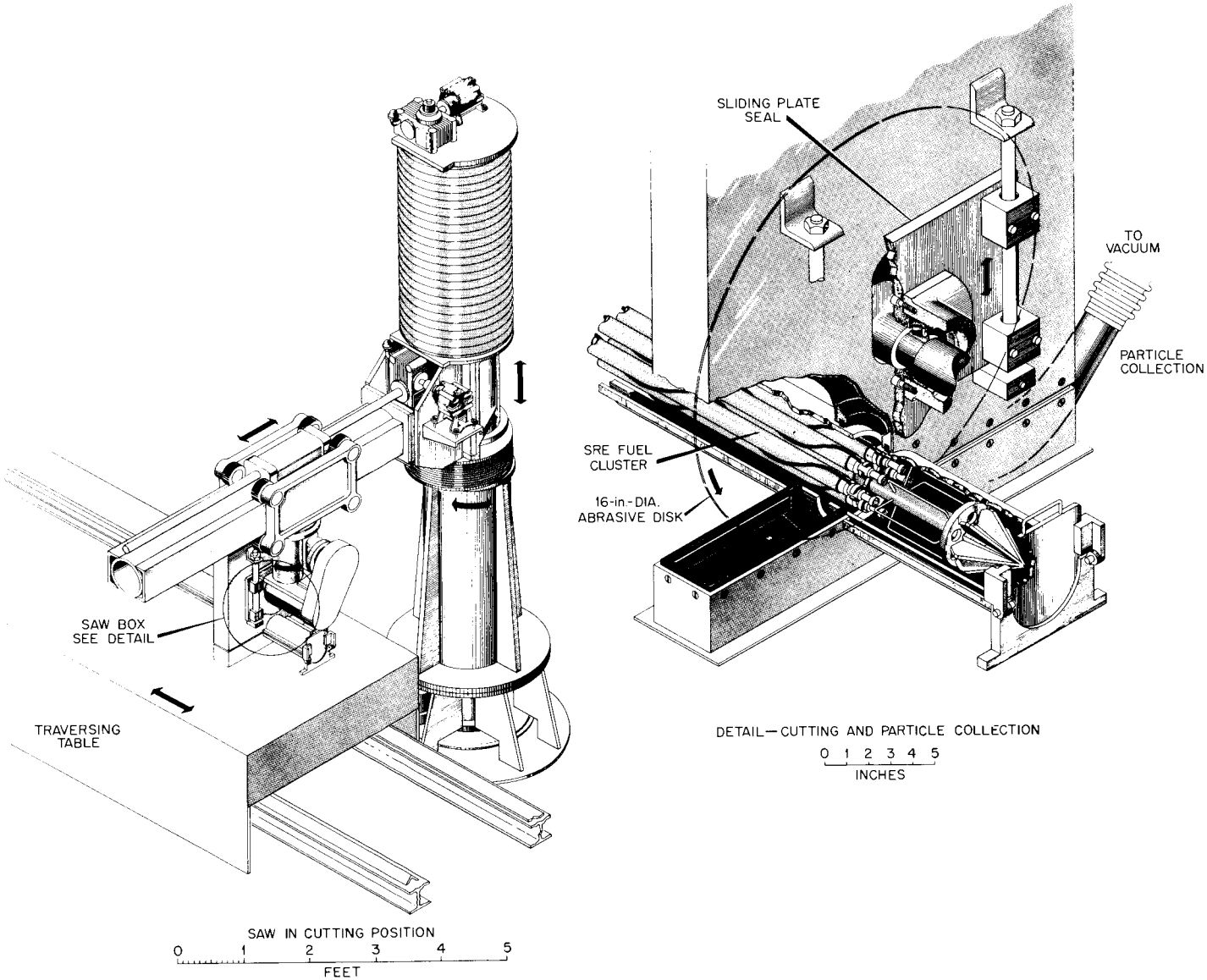

Fig. 8.19 Multi-Purpose Hydraulic Disassembly Saw.

UNCLASSIFIED
PHOTO 48193

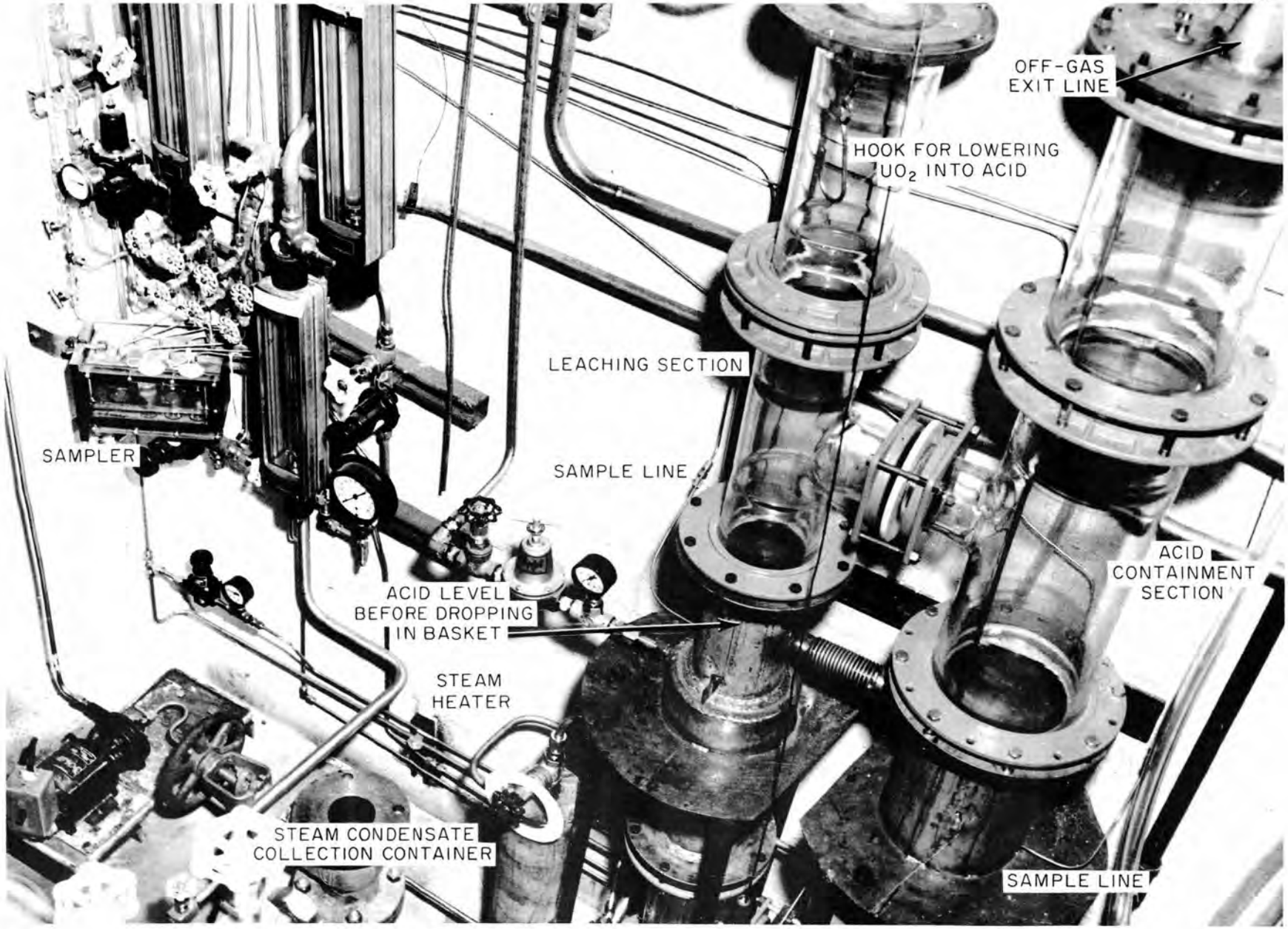

Fig. 8.20 Batch Leacher-24 kg UO_2 Size for Leaching Stainless Clad Sections of Ceramic Fuel.

neoprene flex-type valve did not jam during 25 tests in which the neoprene liner was opened (depressurized) by a quick opening solenoid valve. The Gemco valve was found to be unsuitable after the first several tests because its closure piece jammed on the sheared pieces.

8.5 Radiation Damage - G. A. West

Hydraulic fluids, greases, oils, formica formulations and paint specimens are being irradiated by a cobalt-60 source at 2.0 x 10^8r/hr and an ambient temperature of 157°F to determine acceptable materials for use in the Segmenting Facility and the PRFP pilot plant.

Fire-resistant hydraulic fluids are to be used to operate the multipurpose disassembly saw. Three ethylene glycol-water types with different additives were irradiated. Two fluids (1) "UCON" Hydrolube 150-CP and (2) "Gargoyle Nyvac" No. 20 remained serviceable after 10^8r, γ, exposure, but both failed (became rubbery insoluble gels) when the exposure was increased to 3.465 x 10^8r, γ. The pH and the per cent water did not vary significantly in samples exposed to 10^8r, γ, in tests conducted by the Linde Co. Laboratory (Table 8.7).

A third hydraulic fluid, "UCON" Hydrolube AC, an ethylene glycol-water type with a ployglycol-type thickener and aromatic starter, failed at 4 x 10^8r, γ. This fluid was serviceable after an exposure of 3 x 10^8r, γ, but the increased exposure resulted in separation into two phases, a light syrupy phase and a denser phase which remained quite fluid. It is estimated that the "UCON" Hydrolube AC would be serviceable for a minimum time of 1000 hrs exposure to radiation from spent SRE fuel.

Two lubricants, (1) type APL grease by the Shell Oil Co., and (2) Bemol No. 3 grease with MoS_2 by Bemol, Inc. have exhibited the best radiation resistance at 6 x 10^8r,γ, exposure of several lubricants being irradiated. Exposures are to continue to 3 x 10^9r, γ. The results from visual observation of the lubricants exposed to 6 x 10^8r, γ, are as follows:

a. APL grease, Shell Oil Co. Slight color change to a darker purple. Lubricating qualities were relatively unchanged.

b. Andox No. 275 grease, Standard Oil Co. About 30% less fluid; however, it would probably remain serviceable for low rpm bearing use.

c. Type "A" liquid molykote, The Alpha Corp. Material was still homogeneous with no noticeable physical change.

d. Type "3-A" liquid with MoS_2, Bemol, Inc. Material was less viscous, indicating a separation of the MoS_2 and oil.

e. Type No. 50 MoS_2 paste, Bemol, Inc. The paste became liquified by the separation of the MoS_2 from the oil.

Table 8.7. Identification and Results of Examination of Irradiated Hydrolube Samples

Irradiation Dose at Oak Ridge National Laboratory, Roentgens	Assigned Tonawanda Identification No.	Appearance	pH	Alkaline Content(1)	Water %	Viscosity SUS at 100°F
A. "UCON" Hydrolube 150-CP Series						
None (control)	E9-90	Pale straw liquid	9.5	163	47	160
10^6	E9-84	Very pale straw liquid	9.6	159	46	153
10^7	E9-86	Deep straw liquid	9.9	159	46	132
10^8	E9-88	Amber liquid	9.9	160	43	164
$3x465 \times 10^8$	E9-92	Dark amber, rubbery gel	-	-	28(a)	-
B. "Gargoyle Nyvac" No. 20 Series						
None (control)	E9-89	Light red liquid	9.4	164	35	202
10^6	E9-83	Pale straw liquid	9.5	156	36	198
10^7	E9-85	Straw liquid	9.7	162	37	176
10^8	E9-87	Deep amber liquid	9.4	136	37	156
3.465×10^8	E9-91	Dark amber, rubbery gel	-	-	34	-

(1) Alkaline Content = ml 0.1N HCl to neutralize 100 ml to pH 5.5

(a) Gelled "Ucon" Hydrolube 150-CP was exceedingly difficult to disperse in solvent, which complicated and threw some doubt on the water content determination. The values on the whole are, however, regarded as suitable for comparative purposes.

f. Type "3" grease with MoS_2, Bemol, Inc. Material was slightly more viscous; however, its lubricating qualities were not significantly changed.

The irradiation of the paints will continue to 3×10^9r,γ, exposure. Results after 1×10^9 exposure in both air and water are as follows:

a. Acti-Thane HC-100, Saran Protective Coatings Co. Failed at 1.5×10^8r, γ, (exposure in water) by blistering. Coating was satisfactory in air after 10^9r, γ, exposure.

b. Acti-Thane HC-100 over HC-244 primer, Saran Protective Coatings Co. Same results as (a) above.

c. Phenoline No. 300, a modified phenolic coating, Carboline Co. Satisfactory in both air and water after 10^9r,γ, exposure.

d. Phenoline No. 305, a modified phenolic vehicle and alkaline catalyst coating, Carboline Co. Satisfactory in both air and water after 10^9r, γ, exposure.

e. Polyclad 933-1 DG, a vinyl system coating, Carboline Co. Failed in water after 1.5×10^8r,γ, exposure by blistering. Sample in air remains satisfactory after 10^9r,γ, exposure.

f. Amercoat No. 74 Surfacer Seal on concrete with a glass fabric layer between coats, an epoxy coating, Amercoat Corp. Satisfactory after 10^9r, γ, exposure in water.

g. Amercoat No. 74 Surfacer Seal as in (f) above but without the glass fabric. Failed at 1.5×10^8r, γ, exposure in water by the seal coat separating from the body coat.

h. Amercoat No. 66, an epoxy, Amercoat Corp. Remained satisfactory after 10^9r, γ, exposure in both air and water.

i. Amercoat No. 1680 over Dimetcoat No. 3, Amercoat Corp. Remained satisfactory after 10^9r, γ, exposure in water.

A total of 5 Formica formulations are undergoing irradiation to 3×10^9r, γ, to determine their use for shear blade guides as required in the 267 ton Birdsboro shear proposed for the segmenting cell.

9.0 SOLVENT EXTRACTION STUDIES

A. D. Ryon

The purpose of the solvent extraction studies is to assist in the adaption of TBP processes to the reprocessing of various power reactor fuels by obtaining pulse column performance data necessary for the design and operation of the pilot plant. Towards this objective column capacities and HETS's for several pulse column cartridge designs are being determined using chemical flowsheets developed by Chemical Development Section B.

Three extraction and two stripping columns were erected for the studies of column performance. The extraction columns consist of 24 ft x 2-in. dia precision bore glass pipe with 2 ft x 4-in. dia glass pipe as disengaging section at each end of the column. Feed and sample points were provided at various points along the columns as shown in Figures 9.1 and 9.2 and specifications for the different cartridges used in each column are listed in Table 9.1. Pulsing is supplied by a positive displacement piston pulser, and interface control for either aqueous continuous (top interface) or organic continuous (bottom interface) operation is provided by differential pressure cells.

A 24 ft x 2-in. dia concatenated strip column equipped with sieve plates (0.125-in. dia holes, 23% free area, 2-in. spacing) is piped so that it may be run either as a concatenated column (B-1) or as a 12 ft section of sieve plate column (Figures 9.3 and 9.4). The second stripping column (B-2) consists of 12 ft of 2-in. dia pipe with 2 ft sections of 4-in. dia pipe as disengaging sections at each end equipped with nozzle plate cartridge (0.125-in. holes, 10% free area, 2-in. spacing). Pulsing and interface control are supplied by units similar to those used on the extraction column.

Pulse Column Performance - F. L. Daley, R. S. Lowrie

Several of the proposed power reactor fuel reprocessing flowsheets are sufficiently advanced to warrant obtaining pulse column performance data to aid in pilot plant design. At the present time, column performance tests are scheduled for the Yankee Atomic, Consolidated Edison, and FRR flowsheets in that order and evaluation of the Yankee Atomic flowsheet is underway. The results reported this month were obtained in sieve plate columns using the experimental conditions shown in Table 9.2.

The A-1 column, was operated as a compound extraction-scrub column with a 13 ft extraction and a 11 ft scrub section. Stripping tests were carried out in the top 12 ft section of the B-1 column.

Flooding Rates - Aqueous Continuous Operation

The method used to determine pulse column flooding rates for aqueous continuous (top interface) operation has been reported previously.[1] The criteria used were deviation from the linear plot of steady state solvent hold up vs. throughput plus visual observation. Flooding always occurred

1. ORNL CF 56-4-210.

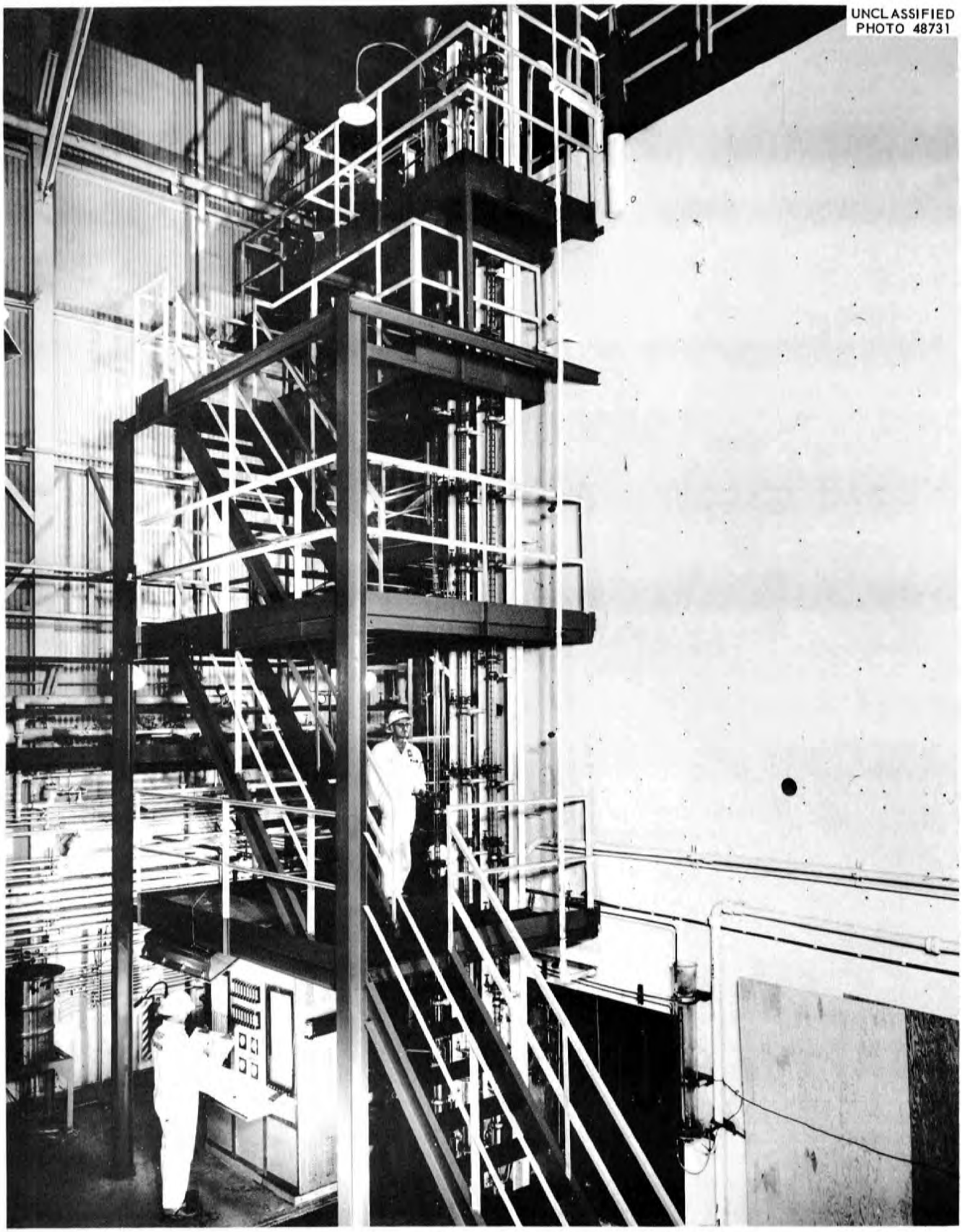

Fig. 9.1 View of Unit Operations Extraction Columns.

UNCLASSIFIED
ORNL-LR-DWG 43069

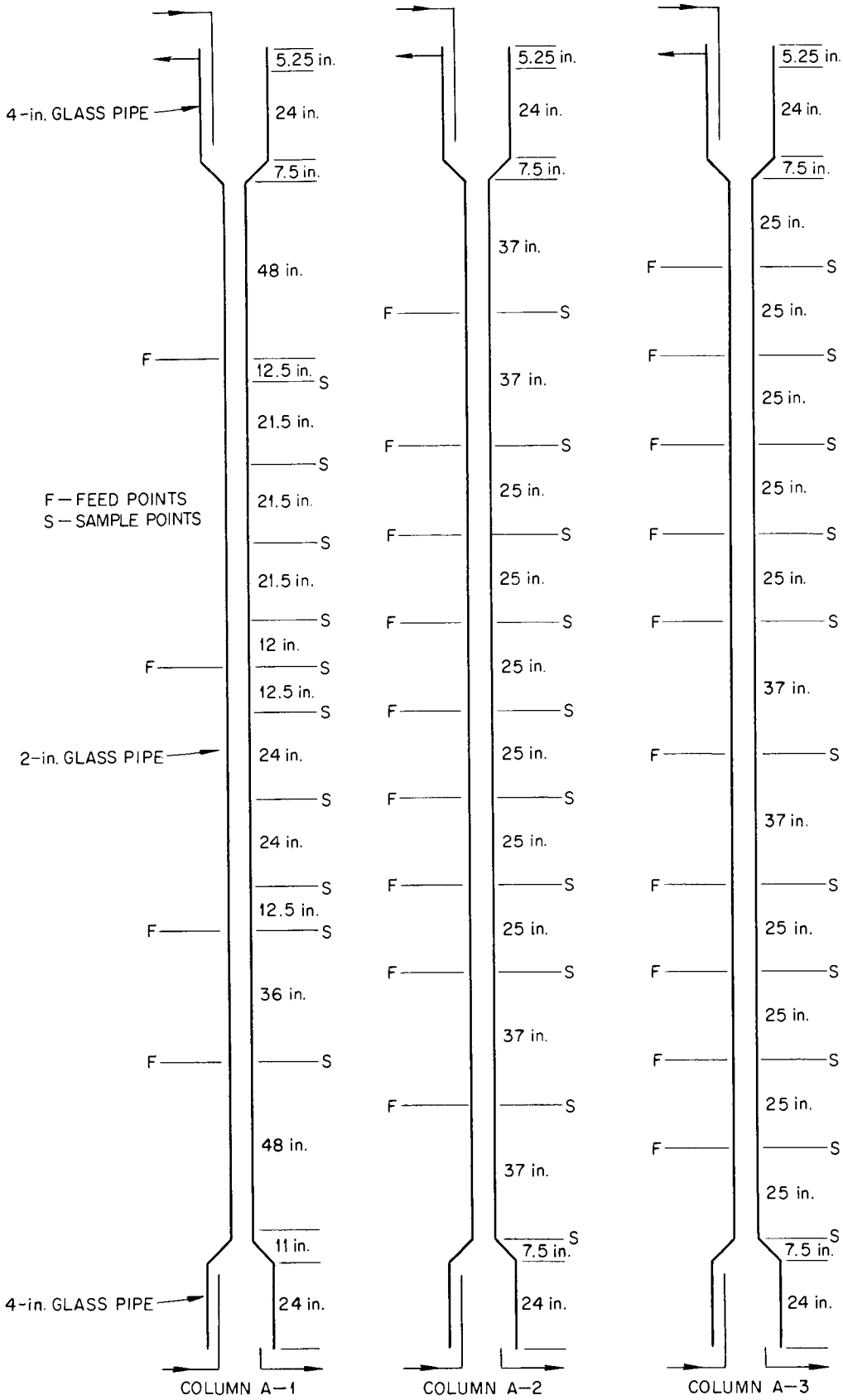

Fig. 9.2. Schematic Diagram; Experimental Extraction Pulse Columns (ORNL Bldg 3503)

Table 9.1. Extraction Column Cartridges

Column No.	Extraction Section	Scrub Section
A-1	13 ft stainless steel sieve plates 0.125-in. holes 23% free area, spacing 2-in.	11 ft stainless steel sieve plates 0.125-in. 23% free area, spacing 2-in.
A-2	12 ft stainless steel nozzle plates 0.188-in. holes, 23% free area, nozzle depth 0.06-in., spacing 2-in.	12 ft Zebra cartridges 2-polyethylene sieve plates 0.188-in. holes, 23% free area 4-stainless steel sieve plates 0.085-in. holes, 21% free area spacing 1-in.
A-3	12 ft stainless steel nozzle plates, 0.125-in. holes, 10% free area, nozzle depth 0.06, spacing 2-in.	same as extraction section

Table 9.2. Experimental Conditions - Yankee Atomic Flowsheet[1]

Stream	Relative Flow	Uranium g/liter	HNO_3 M	Other
Feed	100	321.4	2.0	0.03 M in $NaNO_2$
Scrub	66	-	2.3	-
Solvent	367	-	-	30% TBP in Amsco diluent
Strip	666	-	0.01	-

1. Data taken from ORNL CF 59-7-24, "Solvent Extraction for Power Reactor Fuel Reprocessing Program: A Preliminary Review," A. R. Irvine, A. C. Schaffer, Jr., July 1, 1959.

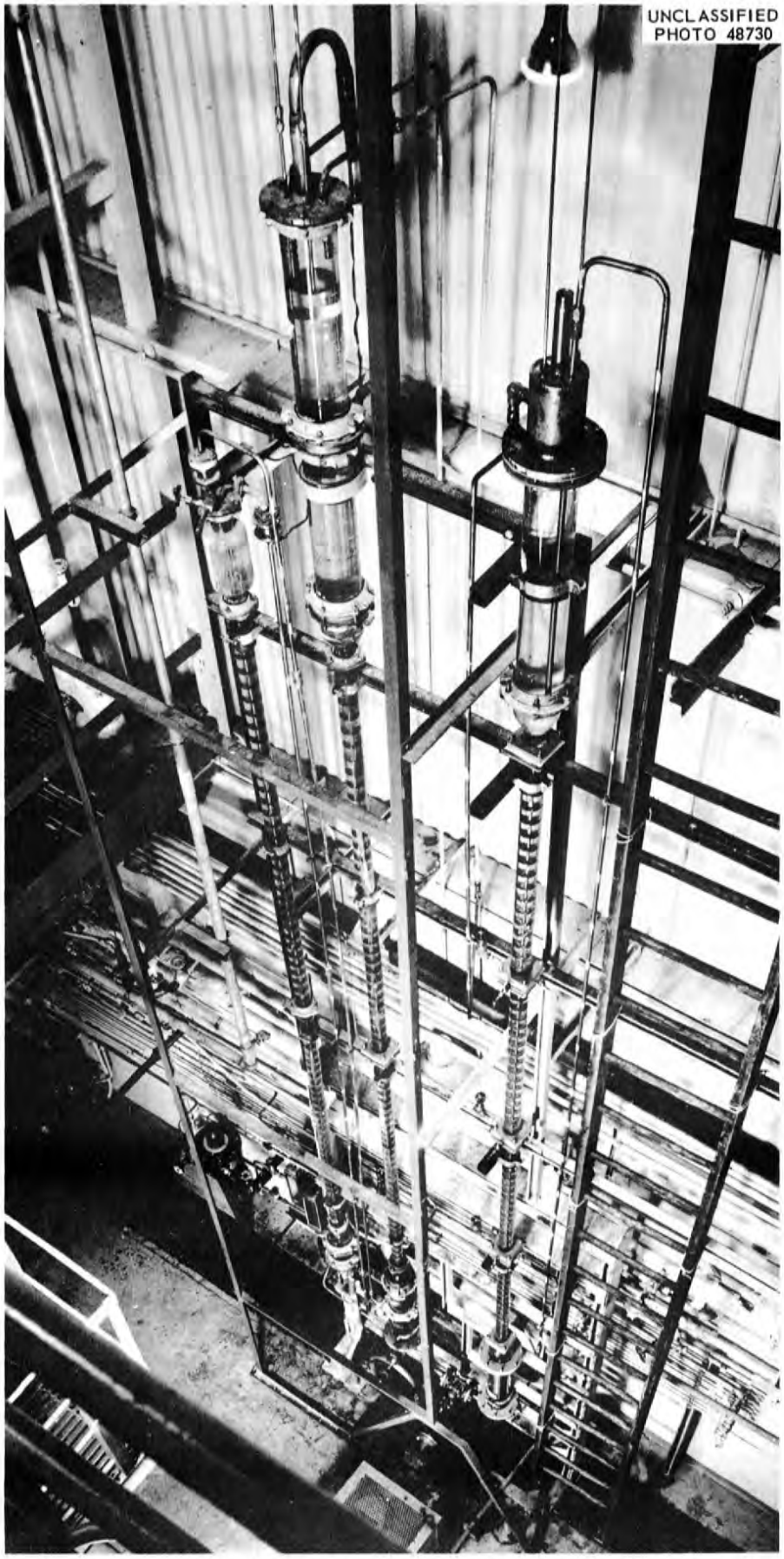

Fig. 9.3 View of Unit Operations Stripping Columns.

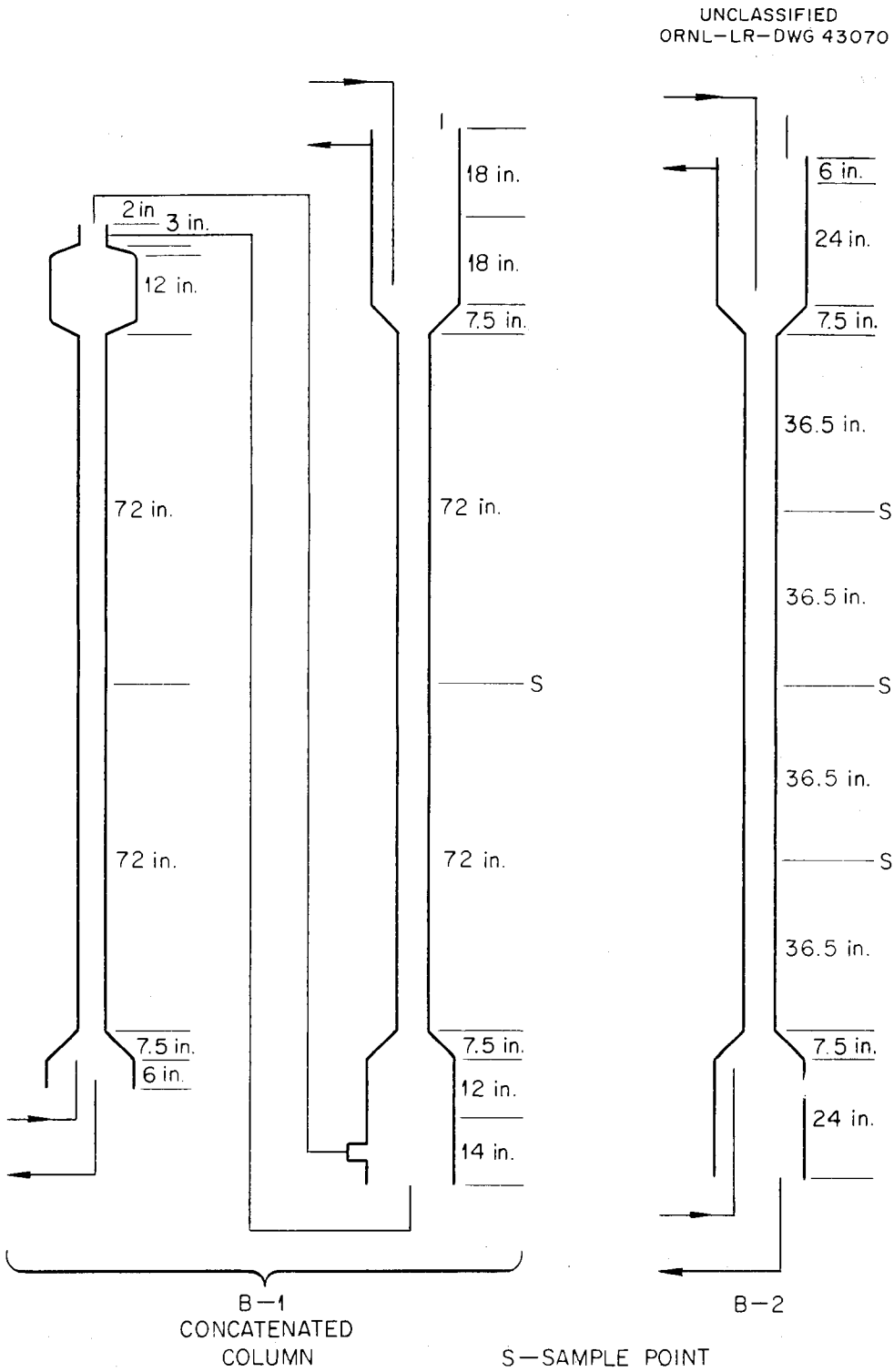

Fig. 9.4. Schematic Diagram; Experimental Strip Pulse Columns (ORNL Bldg 3503)

in the scrub section of the extraction column and the top few feet of the stripping column. Flooding rates (measured in the scrub section) increased from 380 to 730 GSFH as pulse frequency decreased from 70 to 30 cpm in the extraction column, and increased from 720 to 1100 GSFH as pulse frequency decreased from 70 to 25 cpm in the stripping column (Table 9.3, Figure 9.5). Changing the pulse amplitude from 1-in. to 0.5-in. in the stripping column did not markedly affect the flooding rate for the same pulsed volume (amplitude times frequency).

Table 9.3. Sieve Plate Pulse Column Flooding Rates

Aqueous Continuous Operation

Pulse Frequency cpm	Pulse Amplitude inches	Flooding Rate GSFH
Extraction Column		
70	1	380
50	1	640
30	1	730
90	1	< 350
Stripping Column		
70	1	720
50	1	720
35	1	920
25	1	1100
100	0.5	720
70	0.5	1100
50	0.5	1100

Flooding Rate - Organic Continuous Operation

Visual observation of the columns operating with the organic phase continuous indicated that two regions of steady state operation existed. Region I, characterized by a film of aqueous solution flowing down the column wall and sieve plate support rod, occurred at relatively low flow rates. Region II, characterized by the inversion of the scrub section of the extraction column or the top few feet of the strip column to an aqueous

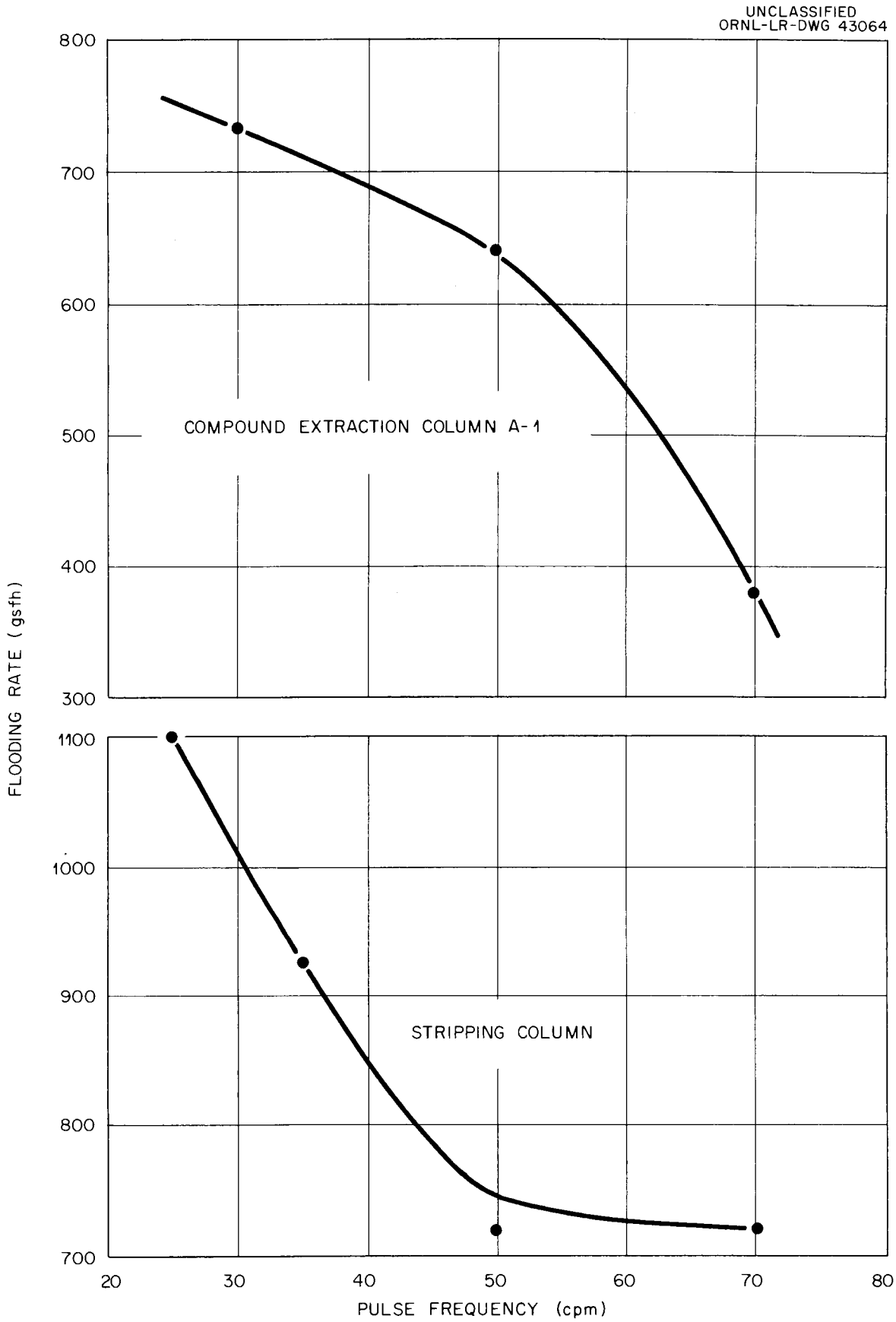

Fig. 9.5. Column Flooding Rates for Aqueous Continuous Operation.

continuous dispersion (a film of aqueous with the bulk of the liquid organic), occurred at higher flow rates and required several hours to reach steady state. Aqueous phase hold up increased linearly with increasing flow rates in each region of operation although the slopes of the two lines differed (see Figure 9.6). Flooding occurred when the aqueous dispersion band rose into the top disengaging section. The width of the band of aqueous dispersion remained constant during steady state operation (duration of longest run was 8 hours) and was readily reproducible when the column was again run at the same conditions. The flow rate at which Region I (film flow) changed to Region II (aqueous continuous dispersion) operation increased from 130 to 300 GSFH as pulse frequency decreased from 70 to 30 cpm for the extraction column.

Practical flooding rates for the two columns, based on steady state operation in Region II, increased from 690 to 1200 GSFG as pulse frequency decreased from 70 to 30 for the extraction column and increased from 720 to 1100 GSFG as the pulse frequency decreased from 70 to 25 for the stripping column (Table 9.4, Figure 9.7).

Table 9.4. Sieve Plate Pulse Column Flooding Rates - Organic Continuous Operation

Pulse Column Frequency cpm	Flooding Rate GSFH
Extraction Column	
70	690
50	790
30	1200
Strip Column	
70	720
50	920
35	1100
25	1100

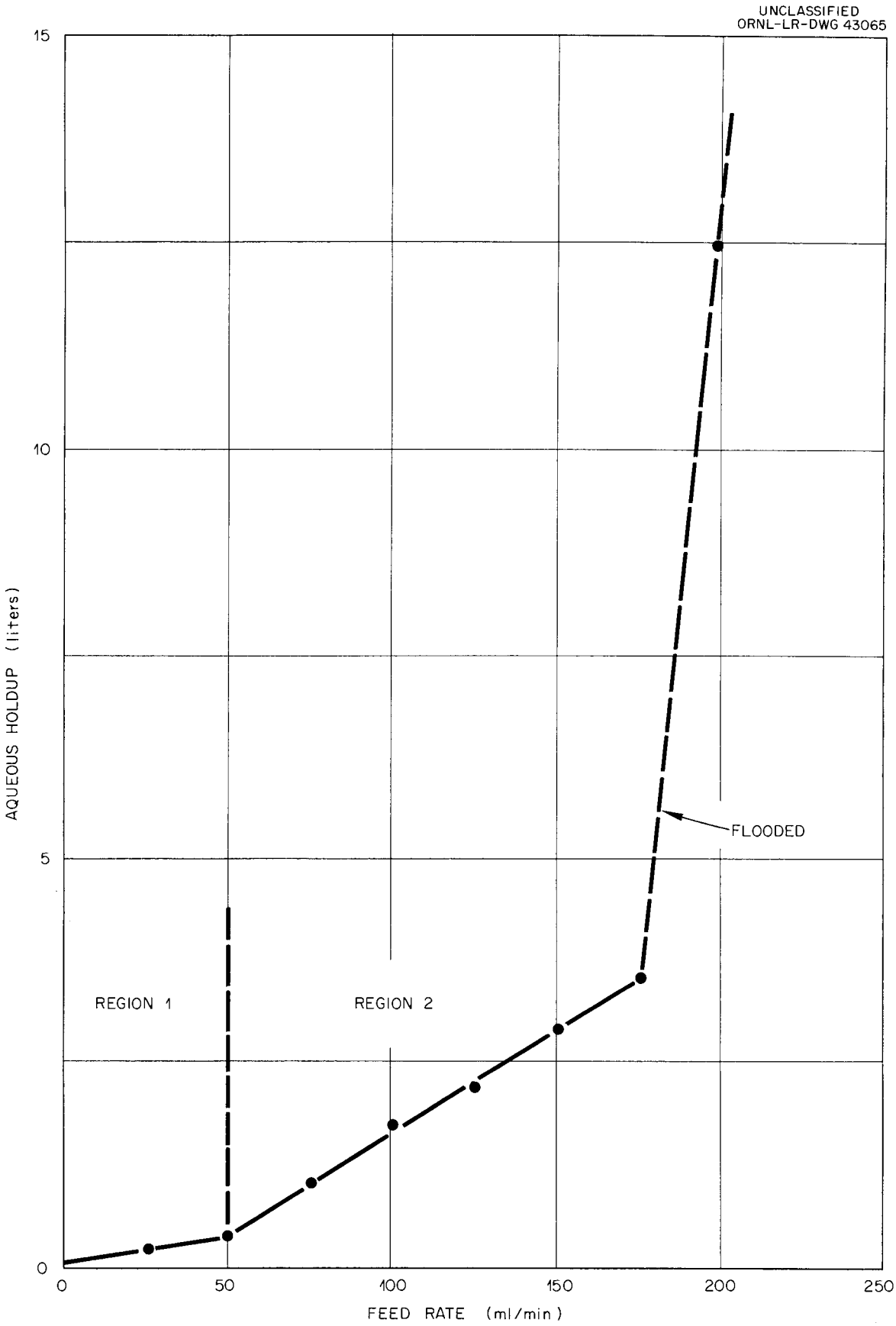

Fig. 9.6. Aqueous Holdup in A-1 Column, Organic Continuous Operation.

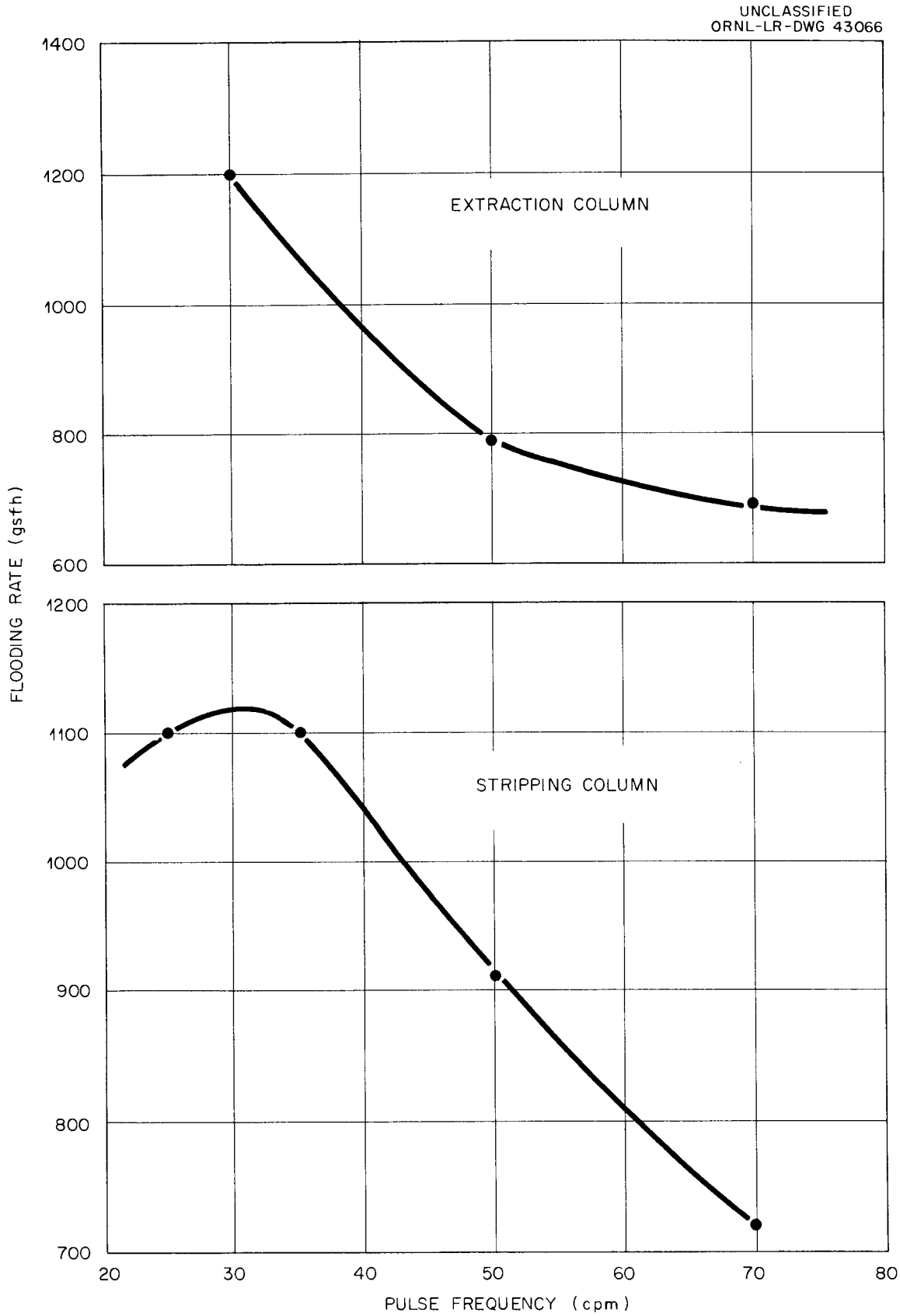

Fig. 9.7 Column Flooding Rates; Organic Continuous Operation.

10.0 VOLATILITY

R. W. Horton

The Volatility Process is a proposed method for the recovery of highly enriched, irradiated uranium from heterogeneous zirconium-based fuel elements. The process steps are fuel element hydrofluorination in a molten salt bath with an HF sparge, liberation of UF_6 from the salt with a F_2 sparge, and final UF_6 decontamination by NaF sorption-desorption.

Solids Formation During Hydrofluorination of Zircaloy-2 - L. E. McNeese

Solids formation during the hydrofluorination step has been observed during previous studies (September Unit Operations monthly report, CF 59-9-69), when it was concluded that the solids resulted from the reduction by Zr metal of fluoride impurities of metals less active than Zr.

In the previous studies, impurity concentrations higher than expected in process operation were used to magnify the effect of the reduction reaction in order to better understand the mechanism of formation, deposition, and removal to the dissolver off-gas as well as the effect of impurities on dissolution rate. The experimental work reported here (Run N-4) is an extension of studies on solids formation under expected hydrofluorination conditions.

The experimental equipment used for this run was identical to that described in detail in CF 59-9-69. All dissolver surfaces contacted by molten salt were made of copper and were cleaned free of fluoride scale prior to the run. A 2513 g Zircaloy-2 dummy fuel element constructed of 10 plates measuring 2.5-in. x 6-in. x 0.125-in. and 18 spacers measuring 0.25-in. x 6-in. x 0.125-in. was dissolved completely with a 1.82 lb/hr anhydrous HF sparge in 10.08 hrs in a bath of 24.5 lbs of 43 mole % NaF-57 mole % LiF. The bath contained the impurities noted in Table 10.1. The total metallic impurities in the feed salt were < 0.14 wt %.

An argon sparge of 5 SCFH removed gases from the system during the heat up period. The dissolution temperature, 700°C, was determined by a 0.25-in. dia copper thermowell in the salt outside the draft tube 0.5-in. from the bottom of the dissolver. The run was interrupted three times for sampling of the solids in the dissolver off-gas line when a pressure buildup was noted. Analyses of these samples and one taken at the conclusion of the run are found in Table 10.1. The weight and time at which each sample was taken is noted in Table 10.2.

Hydrogen off-gas rate, HF utilization, and dissolution rate, based on original element surface is shown in Figure 10.1. The dissolution rate for run N-4 was essentially that observed in run N-3 where the initial impurity concentration was < 0.25 wt %. For run N-4, the average dissolution rate was 2.21 mg/(min)(sq cm); the average HF utilization was 26.5%.

Table 10.1. Samples and Analyses from Run N-4

Sample	Na wt %	Li wt %	F wt %	Fe ppm	Ni wt %	Cr wt %	Mo ppm	Cu wt %	Zr wt %	Sn wt %	S ppm	HF wt %	NH_4^+ wt %	NO_3^- wt %	Totals wt %	Loss on Ignition 110°C wt %	Loss on Ignition 300°C wt %
Feed Salt	29.31	11.92	56.57	515	315 ppm	320 ppm	22	129 ppm	0.3	<100 ppm	15	-	-	-	98.23	-	-
Product Salt	20.40	7.95	52.39	465	125 ppm	0.08	<50	0.10	17.5	740 ppm	<10	-	-	-	98.55	-	-
Freeze-out Salt	16.18	13.78	57.18	195	4.18	0.04	<50	0.15	8.7	220 ppm	800	-	-	-	100.34	-	-
Metal Foil	8.98	3.19	34.43	160	1.77	0.10	<50	53.43	8.1	0.23	1200	-	-	-	110.38	-	-
Solids from inside draft tube	14.12	5.88	23.20	400	0.88	0.06	<50	34.77	7.5	1.21	525	-	-	-	87.72	-	-
Solids from flange	21.67	8.05	53.61	725	0.13	0.12	<50	0.42	14.2	1.34	-	0.467	0.03	0.77	100.89	-	-
Off-gas Solids No.1	14.05	4.89	51.70	0.97%	0.56	0.48	390	2.64	1.45	450 ppm	-	6.94	0.04	1.03	84.84	-	-
Off-gas Solids No.2	13.17	5.32	57.01	0.68%	0.16	0.25	145	1.30	3.20	0.57	800	8.07	4.03*	0.36	94.21	12.9	10.0
Off-gas Solids No.3	14.11	5.37	52.96	0.47%	0.25	0.32	168	6.84	5.6	0.62	0.95%	2.08	0.29	0.74	90.62	-	-
Off-gas Solids No.4	14.78	5.40	53.85	0.19%	0.18	0.22	<50	1.97	10.1	2.97	-	2.38	0.35	0.60	93.00	-	-

* Sample exposed to NH_3

Table 10.2. Off-gas Sample Data

Sample No.	Weight, g	Time, hrs
1	22.8	0.91
2	10.4	2.91
3	2.8	4.91
4	4.9	10.1

Table 10.3. Contribution of Metals to System by Element and Salt During Run N-4

Metal	Wt in Salt g	Wt % by Salt	Wt in Element g	Wt % by Element	Total g	Wt % of Total Metals
Fe	5.72	57.4	4.26	42.6	9.98	15.820
Ni	3.50	95.1	0.179	4.9	3.679	5.840
Cr	3.58	50.5	3.51	49.5	7.09	11.230
Mo	0.244	100.0	0.0	0.0	0.244	0.386
Sn	0.555	1.5	41.5	98.5	42.055	66.700
Totals	13.599	21.6	49.449	78.3	63.048	99.976

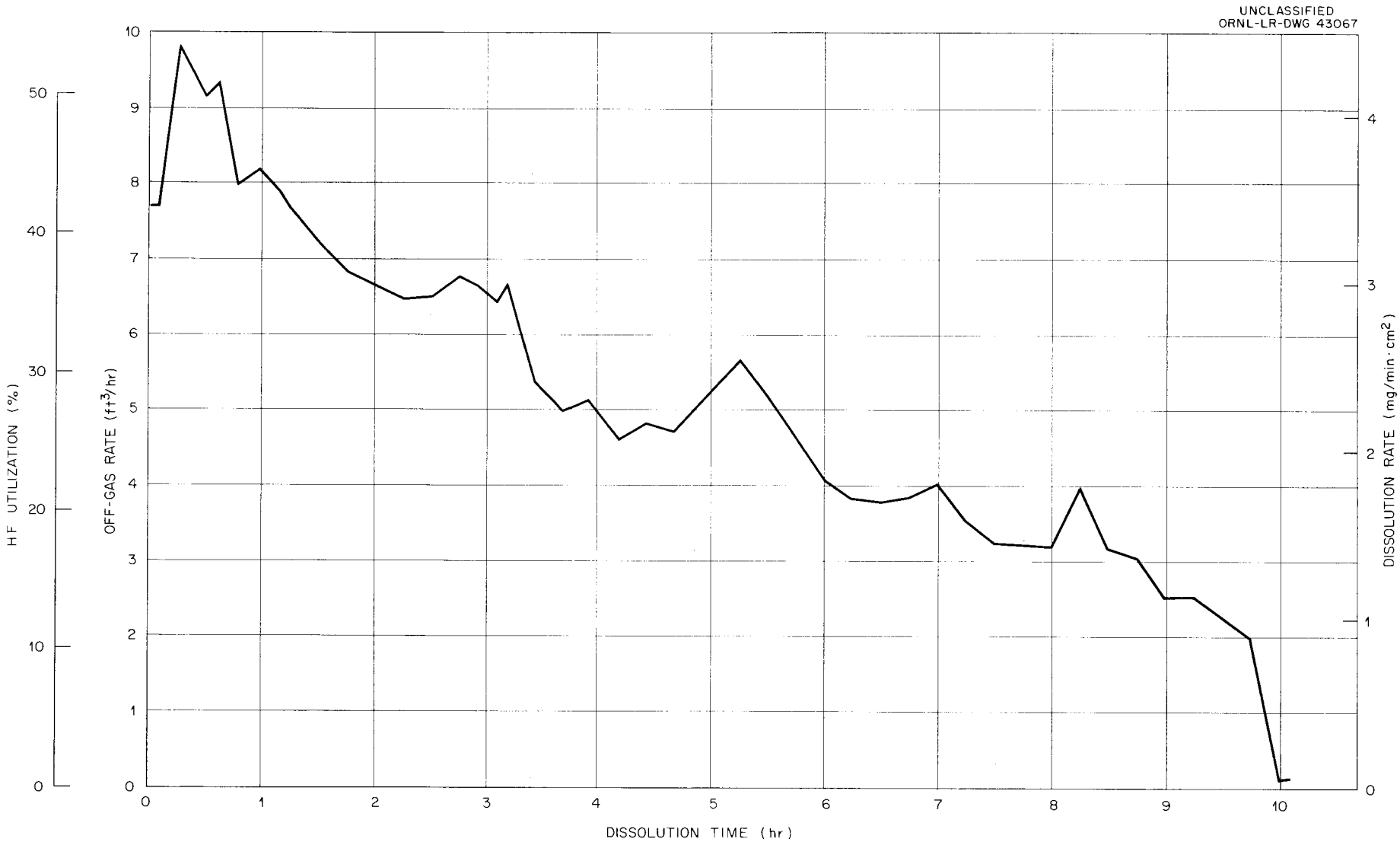

Fig. 10.1 Change in Dissolution Rate as Dissolution Progressed in Run N-4.

After the run a slight deposition of solids was noted on all surfaces submerged in salt with a heavy deposition on the inside draft tube surface as shown in Figure 10.2. As shown in Table 10.1, this material was 34.77 wt % copper with lesser quantities of other metals.

Solids deposition in the form of 5-10 mil thick metallic foil was also observed on the draft tube outer surface (Figure 10.3) and on the vessel wall. A view of this material is shown in Figure 10.4. The solids were 53.43 wt % copper (Table 10.1).

The contribution of metals less active than Zr to the system by the feed salt and by the element is shown in Table 10.3. It should be noted that the salt contributed essentially all the Mo and Ni and the element, essentially all the Sn. The two sources were equally responsible for the metals Fe and Cr. It should also be noted that the element contributed approximately 63 wt % of the metals, the bulk of this being Sn. Copper was not included in the table since the corrosion rate of the vessel was undetermined.

The off-gas solids analyses were corrected for S, NH_4, HF, NO_3, and H_2O content and the metals contents were plotted (exclusive of Na, Li, and Cu), in Figures 10.5 and 10.6. The off-gas concentration of metals contributed largely by the element (Sn and Zr) steadily increased while the concentration of those metals contributed approximately 50% or more by the salt decreased approximately exponentially.

Also presented in Figure 10.5 is the time variation of Sn and Zr content of the melt for comparison purposes. The curve for Zr was calculated from H_2 off-gas rate; that for Sn from a knowledge of the initial and final melt composition and the shape of the dissolution curve.

Based on initial and final melt compositions from Table 10.1 and the data from Figures 10.5 and 10.6, the ratios of off-gas composition to melt composition were calculated for the beginning and end of the run. As may be noted in Table 10.4, the ratio varied between 3.19 and 46 for the metals less active than Zr, and between 0.575 and 0.733 for Zr.

Based on a material balance for the individual elements, using the initial and final melt compositions, the per cent of each element removed from the salt by deposition and the off-gas can be calculated (Table 10.5). As may be observed, 70% of the major impurity, Sn, and smaller percentages of Fe and Ni, were removed from the salt. The distribution for Mo could not be calculated since the concentrations were below analytical background; also, a satisfactory material balance for Cr could not be made.

From these data, one may conclude that under dissolution conditions, an appreciable fraction of the major impurity, Sn, was deposited or removed in the dissolver off-gas. The dissolution rate from run N-4 substantiates that for run N-3 which occurred under similar conditions. The value of copper as a material of construction for vessel liners is questionable at this time in view of the behavior reported.

UNCLASSIFIED
PHOTO 48256

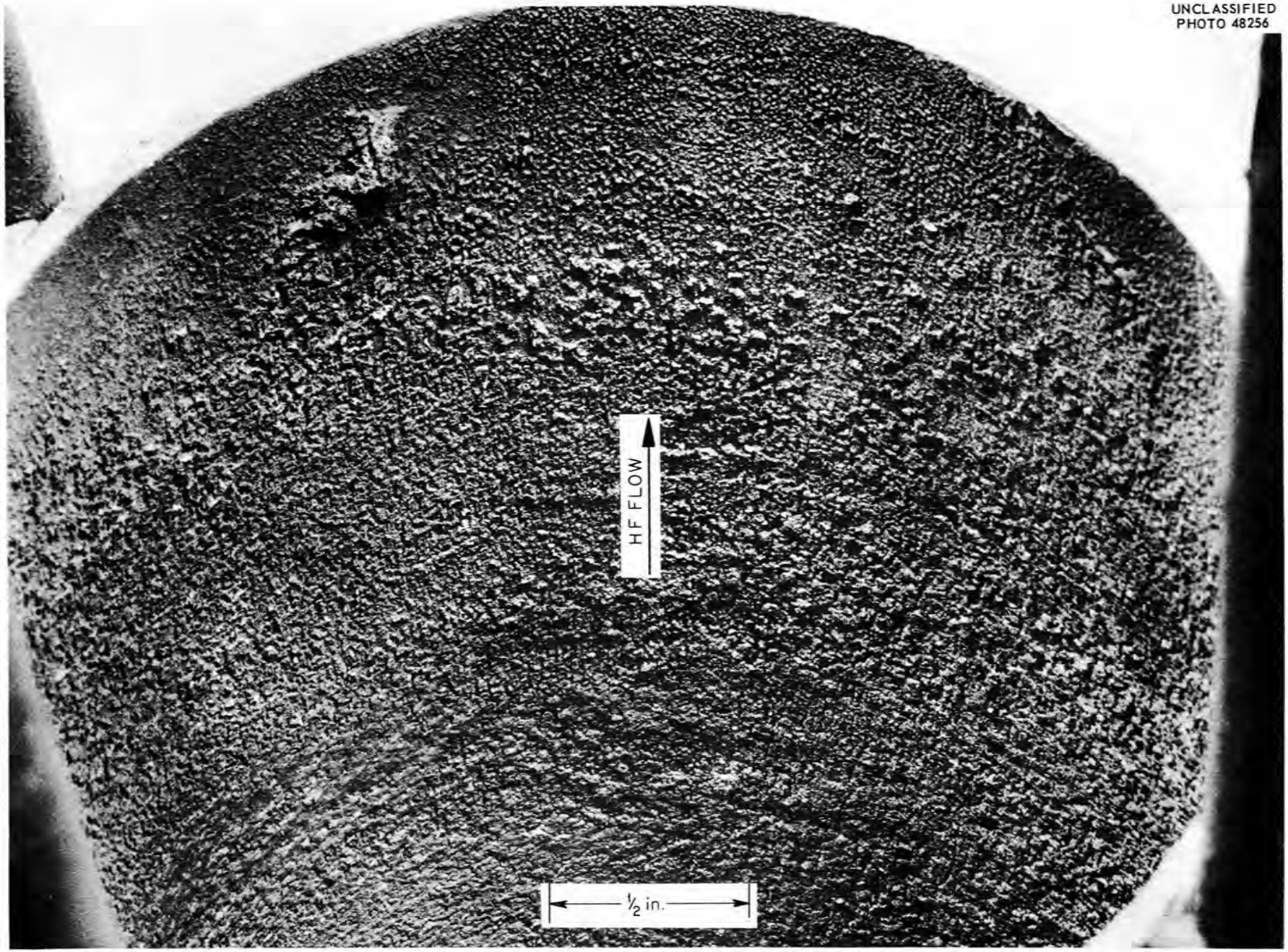

Fig. 10.2. Solids Deposition on Inside Draft Tube Surface.

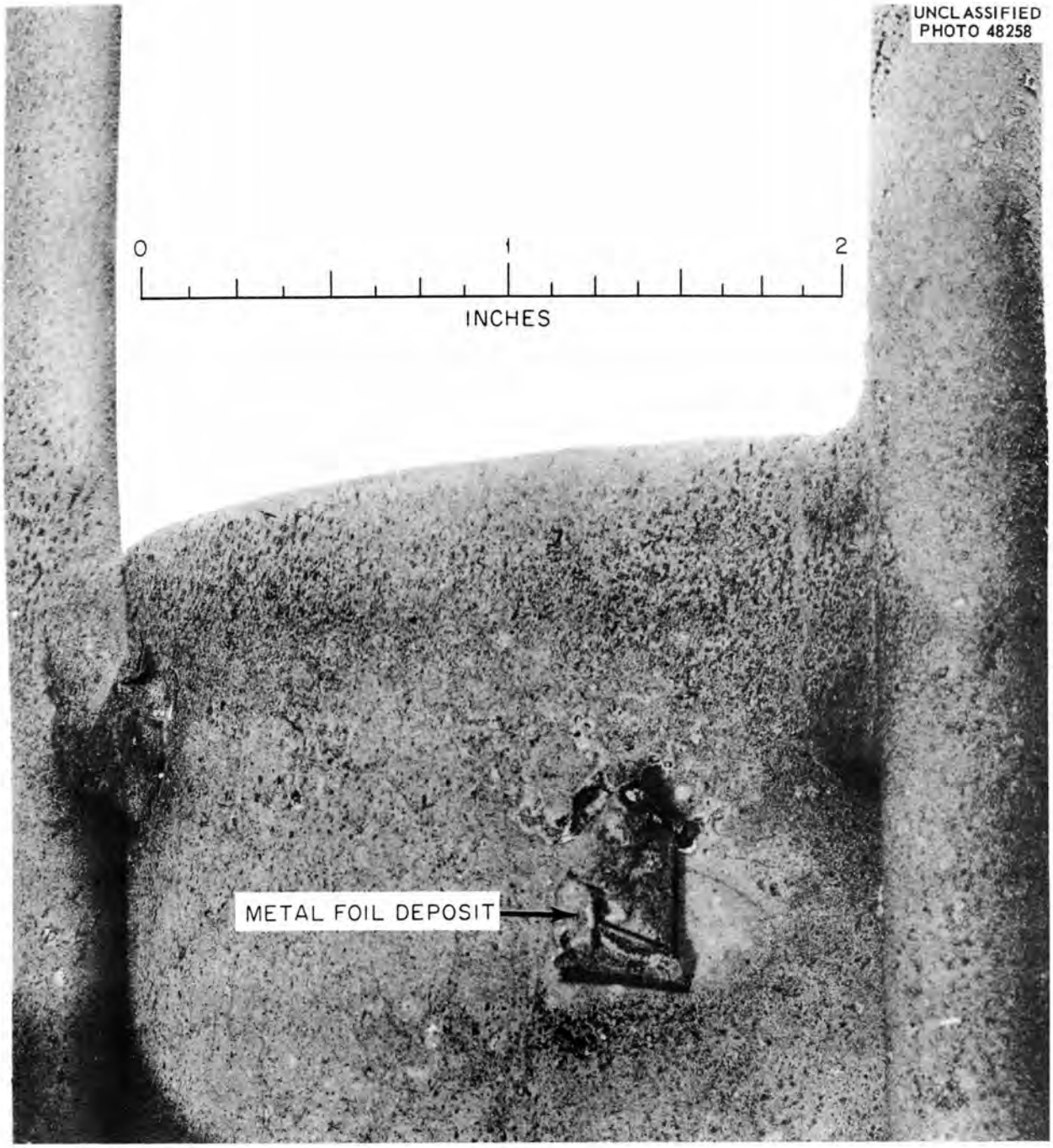

Fig. 10.3 Metallic Foil Deposit On Outside Draft Tube Surface.

UNCLASSIFIED
PHOTO 48257

Fig. 10.4 Metal Foil Deposits.

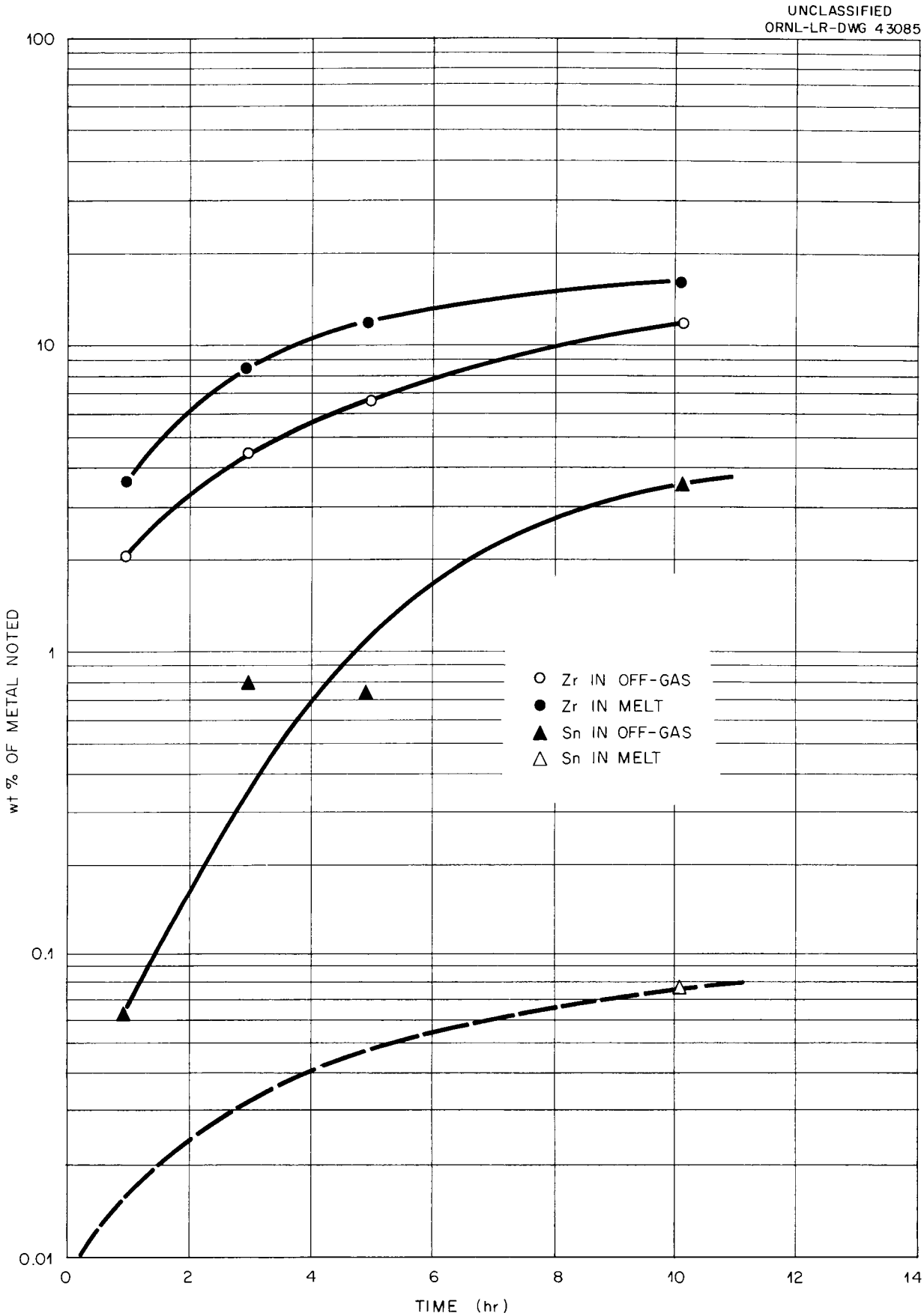

Fig. 10.5 Time Variation of Zr and Sn Content of Melt and Off-Gas.

UNCLASSIFIED
ORNL-LR-DWG 43068

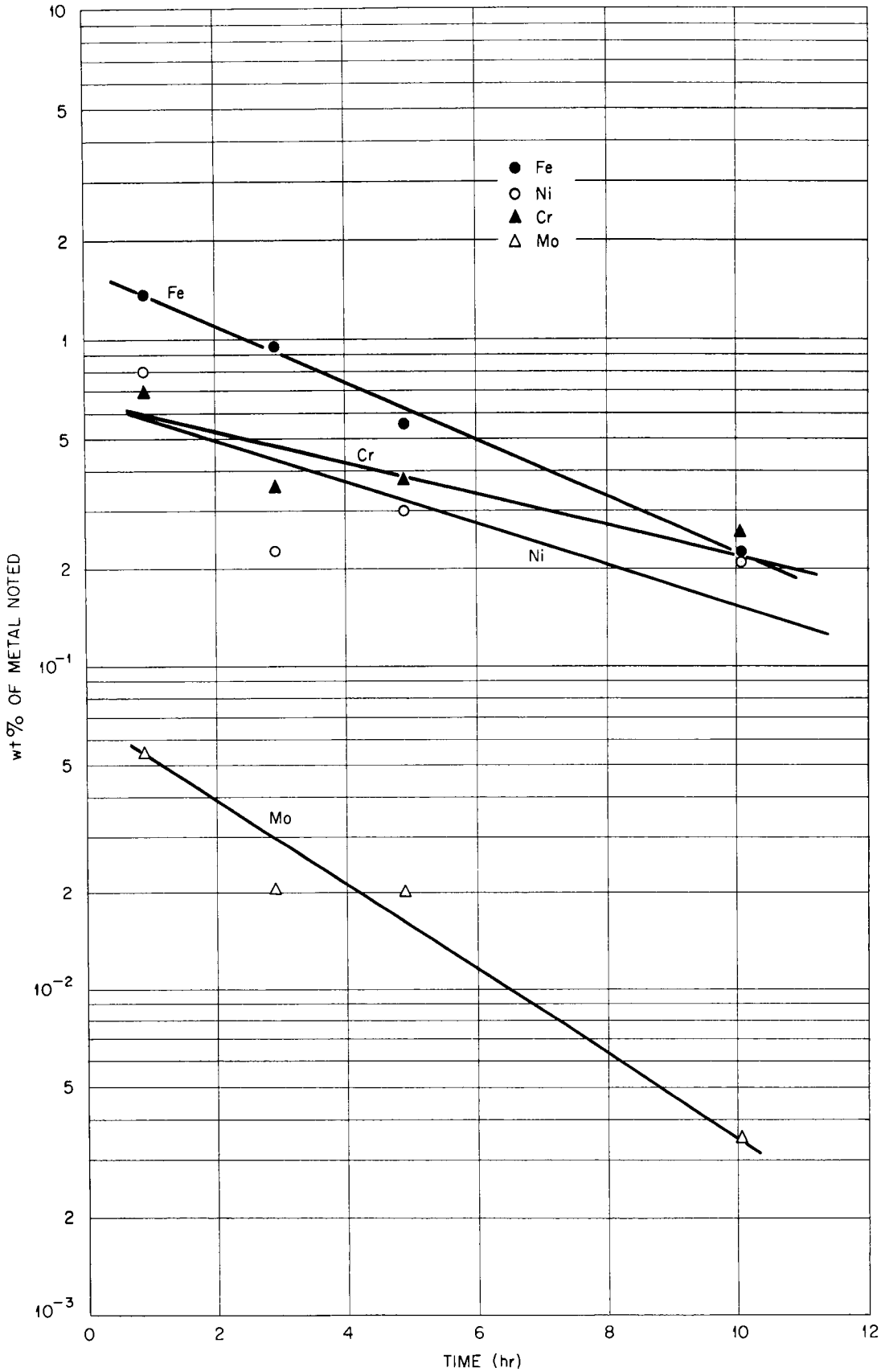

Fig. 10.6. Time Variation of Fe, Ni, Cr, Mo Content of off-gas.

Table 10.4. Comparison of Off-gas to Melt Compositions

Element	Ratio, $\frac{\text{off-gas composition}}{\text{melt composition}}$	
	beginning of run	end of run
Fe	31.0	4.73
Ni	21.0	12.18
Cr	12.5	3.19
Mo	31.6	-
Sn	4.0	46.0
Zr	0.575	0.733

Table 10.5. Per Cent of Metals Removed from Salt by Deposition and Off-gas

Metal	Wt % Removed
Fe	20.8
Ni	42.3
Sn	70.0

11.0 WASTE PROCESSING

J. O. Blomeke

The purpose of the waste processing program is to provide engineering data for the design of a pilot plant for reduction of high-level radioactive waste to solids for permanent disposal. This report describes the two most recent calcination tests and summarizes the results of the six tests made to date with evaporated Darex waste. In addition, the initial performance tests with the distillation tower operating as an aerosol attenuator are described.

11.1 Calcination - C. W. Hancher, J. J. Perona, J. S. Taylor, J. C. Rose

Two calcination tests (R-20 and R-21) were carried out during this report period in the 8-in. dia by 48-in. long calciner for the purpose of determining the effects of increasing the feed rate. The tests were performed in the equipment described in the August Unit Operations monthly report (CF 59-8-76) except that the primary off-gas line from the calciner pot to the condenser was increased in size from 1/2-in. tubing to 1-in. pipe.

A secondary 1-in. off-gas line to a seal-pot vented to the atmosphere through a 20-ft head of water was installed as a safety precaution in case the primary line plugged. In both runs, the equipment functioned properly and the secondary line was not used. The operating conditions and results are compared with the previous runs of this series in Table 11.1.

In test R-20, synthetic Darex waste, evaporated to an iron concentration of 157 g/liter, was fed to the calciner at a rate of 5.6 liter/hr. The overall rate, based on the time required for feeding and calcining was 3.1 liter/hr. The volumetric ratio of non-condensable off-gas to feed was 4.6 cu ft/liter, representing about a 30% increase over the ratios obtained during the previous tests at feed rates near 3 liter/hr. The amount of iron entrained in the off-gas and the characteristics of the final cake were not significantly different than found in the previous runs.

The evaporated Darex waste used for test R-21 had an iron content of 137 g/liter and was fed to the calciner at a rate of 10.6 liter/hr. The overall rate for the test was 3.1 liter/hr. Compared to the previous runs, the ratio of off-gas to feed volume increased to 7.1 cu ft/liter; the iron entrainment decreased to 0.012% of the iron in the feed; and the final cake possessed a desirably higher bulk density, and a lower water and nitrate content than previously.

Although this series of Darex calcination tests has not been concluded as yet, it appears that Darex waste can be successfully calcined at estimated overall rates of at least 3 to 5 liters per hour in an 8-in. pot. This rate would correspond to a capacity of about 15 to 20 liters per hour of raw (unevaporated) waste, equivalent to the volume produced by reprocessing 200-500 g/day of U-235 in APPR-type reactor fuel.

Table 11.1. Calcination of Darex Evaporated Waste

Test	Conc. Fe in Feed	Vol. Feed	Rate Feed	Total Time	Overall Rate	Furnace Temp.	Ratio Off-gas Vol. to Feed Vol.	Per cent Fe in Feed Recovered in Condensate	Characteristics of Cake				
									Vol.	Bulk Density	Fe Content	H_2O Content	NO_3^- Content
	g/liter	liters	liters/hr	hours	liters/hr	°C	cu ft/liter		liters	g/cc	wt. %	wt. %	wt. %
R-16	170	95	2.8	43	2.2	900	-	-	34	0.95	47.8	0.46	0.22
R-17	160	80	2.8	38	2.1	900	3.0	0.098	35	0.80	50.1	0.06	0.03
R-18	154	63	3.5	-	-	900	Pot ruptured as reported in ORNL CF 59-9-69						
R-19	131	73	3.1	33	2.2	900	3.9	0.080	31.6	0.64	50.7	0.90	0.05
R-20	157	73	5.6	23	3.1	800	4.6	0.073	38.0	0.64	48.0	1.00	0.11
R-21	137	74	10.6	23	3.1	800	7.1	0.012	30.0	0.80	48.5	0.29	0.005

11.2 Particulate Attenuation of a Packed Distillation Tower - J. J. Perona, C. W. Hancher

The effectiveness of a distillation tower as an aerosol attenuator is being studied as a function of tower operating variables and aerosol properties. Two runs were made in which an air stream bearing an aerosol of $Cr(NO_3)_3 \cdot 9H_2O$ containing Cr-51 as a tracer was fed into the bottom of a packed distillation tower operating with water at a total reflux (Table 11.2). The apparatus is described in the September Unit Operations monthly report (ORNL CF 59-9-69).

During the first run the entire non-condensable stream leaving the distillation tower was passed through a Millipore filter, resulting in an upset of the tower operation each time a sample was taken due to the pressure drop across the filter. Thus, while a decontamination factor of up to 1.2×10^3 was obtained during the first two hours of the run, the continual perturbation of the tower is believed to be responsible for the poor decontamination during the latter part of the run (Table 11.3).

An isokinetic sampler was installed in the off-gas line prior to run 2. With this device about 20 per cent of the flowing gas stream was diverted out through a Millipore filter, care being taken that the velocity of the air stream within the sampler tube was the same as that in the main gas stream. An isokinetic sampler was also used on the gas stream entering the tower. Good decontamination was obtained throughout the second run, with the activity of the off-gas stream only 0.8 to 1.6 per cent above background during the last three hours of the five hour run. The off-gas samples and background were counted a sufficient length of time to give a standard deviation of $\pm$ 3.0% for each sample, which results in $\pm$ 4.2% for the difference between sample and background. Impractically long counting times would be required to improve the precision appreciably.

Liquid samples from the tower condenser showed a general trend of increased activity as the run progressed, and the condenser sample activities were generally lower than corresponding reboiler samples. Quantitative comparison of liquid activities is not possible due to poor counting statistics.

Particle size distribution of the aerosols has not yet been determined. Comparison of activities collected in Millipore AA and HA filters, which have pore sizes of 0.80μ $\pm$ 0.05μ and 0.45μ $\pm$ 0.02μ, respectively, revealed that the weight fraction below 0.80μ was insignificant.

Table 11.2. Run Conditions for Particulate Attenuation Runs

Variable	Run 1	Run 2
water boil up rate, lb/hr	5.1	5.1
reflux ratio, L/D	∞	∞
air rate, cu ft/min (STP)	3.16	1.02
ΔP across packing, inches H_2O	16	5
tracer nuclide	Cr-51	Cr-51
aqueous carrier solution	2% $Cr(NO_3)_3 \cdot 9H_2O$	2% $Cr(NO_3)_3 \cdot 9H_2O$
aerosol generation rate cc/liquid phase/min	0.091	0.032

Table 11.3. Activities of Process Streams above Background for Runs 1 and 2

Sample	Time, hours				
	1	2	3	4	5
Run 1:					
Gas in, counts/min-cu ft	390	-	385*	440	-
Gas out, counts/min-cu ft	0.45	0.33	33.7	77.2	-
Distillate counts/min cc	1.0	0.0	2.2	8.5	4.9
Reboiler Liquid, c/min cc	6.7	4.1	3.8	3.3	7.2
Run 2:					
Gas in c/min-cu ft	244	210	187*	174	98
Gas out c/min-cu ft	1.87	0.47	0.14*	0.28	0.25
Distillate c/min cc	1.0	0.2	0.0	3.5	2.6
Reboiler Liquid, c/min cc	5.0	0.4	3.4	2.6	3.5

* Millipore HA filter paper used on these samples. Millipore AA used on all other gas samples.

DISTRIBUTION

1. E. L. Anderson (AEC Washington)
2. F. P. Baranowski (AEC Washington)
3. W. G. Belter (AEC Washington)
4. R. E. Blanco
5. J. O. Blomeke
6-35. J. C. Bresee
36. K. B. Brown
37. F. R. Bruce
38. L. P. Bupp (HAPO)
39. G. I. Cathers
40. J. T. Christy (HOO)
41. W. E. Clark
42. V. R. Cooper
43. K. E. Cowser
44. F. E. Crokton (Goodyear Atomic Corp.)
45. F. L. Culler, Jr.
46. D. C. Davis (AEC ORO)
47. W. Davis, Jr.
48. O. C. Dean
49. W. K. Eister
50. D. E. Ferguson
51. L. M. Ferris
52. R. J. Flanary
53. M. J. Fortenbery (Y-12)
54. E. R. Gilliland (Consultant MIT)
55. H. E. Goeller
56. M. J. Googin (Y-12)
57. A. T. Gresky
58. P. A. Haas
59. M. K. Harmon (HAPO)
60. L. P. Hatch (BNL)
61. O. F. Hill (HAPO)
62. J. M. Holmes
63. R. W. Horton
64. A. R. Irvine
65. George Jasny (Y-12)
66. H. F. Johnson
67. W. H. Jordan
68. S. H. Jury
69. K. K. Kennedy (IDO)
70. F. Kerze (AEC Washington)
71. L. J. King
72. B. B. Klima
73. E. Lamb
74. D. M. Lang (ORGDP)
75. S. Lawroski (ANL)
76. R. E. Leuze
77. J. A. Lieberman (AEC Washington)
78. R. B. Lindauer
79. A. P. Litman
80. J. T. Long
81. B. Manowitz (BNL)
82. J. P. McBride
83. R. A. McNees
84. R. P. Milford
85. J. W. Morris (SRP)
86. D. M. Paige (ICPP)
87. F. S. Patton, Jr. (Y-12)
88. Harry Pearlman (AI)
89. R. H. Rainey
90. J. T. Roberts
91. C. A. Rohrmann (HAPO)
92. O. T. Roth (AEC Washington)
93. A. D. Ryon
94. W. F. Schaffer
95. C. H. Secoy
96-98. E. M. Shank
99. M. J. Skinner
100. C. M. Slansky (ICPP)
101. S. H. Smiley (ORGDP)
102. C. E. Stevenson (ICPP)
103. E. G. Struxness
104. J. A. Swartout
105. V. R. Thayer (duPont, Wilmington, Del.)
106. W. E. Unger
107. J. Vanderryn (AEC ORO)
108. F. M. Warzel (ICPP)
109. C. D. Watson
110. M. E. Whatley
111. G. C. Williams
112. C. E. Winters
113. R. G. Wymer
114-115. Central Research Library
116-119. Laboratory Records
120. Laboratory Records (RC)
121. Document Reference Section